Identification of the Molecular Mechanism in Scar Regeneration by Studying the Cellular Crosstalk between Adipocytes and Connective Tissue

Inaugural-Dissertation

to obtain the academic degree

Doctor rerum naturalium (Dr. rer. nat.)

submitted to the Department of Biology, Chemistry and Pharmacy

of Freie Universität Berlin

by

Katharina Hörst

from Münster

2019

This thesis and all associated experiments were prepared and performed from August 2015 to February 2019 at the Institute of Pharmacy, Department of Pharmacology & Toxicology, Freie Universität Berlin under the supervision of Prof. Dr. Sarah Hedtrich (Faculty of Pharmaceutical Sciences, University of British Columbia, Vancouver, Canada).

1st Reviewer	Prof. Dr. Sarah Hedtrich University of British Columbia Faculty of Pharmaceutical Sciences 2405 Wesbrook Mall Vancouver, BC V6T 1Z3, Canada
2nd Reviewer	Prof. Dr. Matthias F. Melzig Freie Universität Berlin Institut für Pharmazie Königin-Luise-Straße 2+4 14195 Berlin, Deutschland
Date of Disputation	19.08.2019

She decided to free herself, dance into the wind, create a new language. And birds fluttered around her, writing “yes” in the sky.

Monique Duval

Part of this thesis has already been published:

Hoerst, K., Van Den Broek, L., Erdmann, G., Klein, O., Von Fritschen, U., Gibbs, S. & Hedtrich, S. 2019. Regenerative potential of adipocytes in hypertrophic scars is mediated by myofibroblast reprogramming. *Journal of Molecular Medicine***,** 97(6):761-775.

All figures and text passages based on this publication were marked with the specific source. Experimental work and other contributions of co-authors were also clearly indicated.

SUMMARY

Abnormal scarring and its accompanying cosmetic, functional and psychological burden is a major challenge in modern medicine. Pathological scars such as hypertrophic scars or keloids present cutaneous conditions characterized by excessive collagen deposition which can be itchy and painful, causing serious functional and aesthetical disabilities. The crucial role of myofibroblasts and transforming growth factor-beta (TGF-β) signaling in the pathogenesis of fibrosis and, thus, scarring, is widely accepted. Nevertheless, effective preventive or therapeutic strategies are still not available despite extensive research. Autologous fat grafting is a novel approach leading to partly significant improvements of scar tissue regarding functionality and appearance. Here, fat is harvested from body deposits and re-injected into areas with scarred tissue. Since adipose tissue does not only contain adipocytes but is a source for adipose-derived stem cells (ASCs) and even more cell types, various origins for the observed scar regeneration are conceivable. Regenerative effects from adipocytes or ASCs are discussed, however, the underlying mechanism is still unknown. Aiming to unravel the regenerative potential of adipose tissue, paracrine effects of ASCs and adipocytes on *in vitro* differentiated myofibroblasts and fibroblasts from hypertrophic scars were investigated. Interestingly, following incubation with adipocyte-conditioned medium, the expression of the myofibroblast marker α-smooth muscle actin and the extracellular matrix components collagen 1 and 3 decreased significantly indicating a myofibroblast reprogramming. Secretome analysis, ELISA, Western blot and high throughput protein analysis indicate a pivotal role of BMP-4 secreted by adipocytes in the cellular reprogramming. In addition, direct as well as indirect activation of peroxisome proliferator-activated receptor (PPAR)γ signaling was shown after application of conditioned medium from adipocytes. Remarkably, speculations about a reciprocal, antagonistic relationship between PPARɣ and TGF-β do exist which might indicate anti-fibrotic effects on the part of PPARɣ. Although a myofibroblast-to-adipocyte transition was hypothesised, myofibroblasts trans-differentiation, however, was not observed.

Overall, adipocytes induce myofibroblast reprogramming via BMP-4 secretion and by direct as well as indirect activation of PPARγ signaling. These findings highlight the regenerative potential of adipocytes on scar tissue and may pave the way for novel therapeutic strategies in the prevention or treatment of hypertrophic scars.

ZUSAMMENFASSUNG

Eine überschießende Wundreaktion und eine damit einhergehende Narbenbildung stellt betroffene Patienten nicht nur vor ästhetische Herausforderungen, sondern bedingt meist auch schmerzhafte, funktionelle Einschränkungen. Zugrundeliegende Mechanismen weisen auf eine zentrale Rolle von Myofibroblasten sowie des *transforming growth factor-beta* (TGF-β) Signalwegs hin. Zur Behandlung von hypertrophen Narben und Keloiden existieren eine Vielzahl invasiver als auch non-invasiver Methoden; jedoch liefert bisher keine dieser Behandlungsmöglichkeiten zufriedenstellende und ausreichend wirkungsvolle Ergebnisse. Eigenfetttransplantationen bieten eine neue Alternative und zeigen vielversprechende Verbesserungen des Narbengewebes hinsichtlich Histologie und Funktionalität. Die zugrundeliegenden Mechanismen dieser Effekte sind bislang weitestgehend unbekannt, obwohl den Fettgewebsstammzellen (*adipose-derived stem cells*, ASCs) und Adipozyten ein regeneratives Potenzial attestiert wird. Um dieses Potenzial hinsichtlich einer Narbenregeneration näher herauszustellen, wurden parakrine Effekte von beiden Zelltypen auf Myofibroblasten sowie auf Fibroblasten aus hypertrophem Narbengewebe untersucht. Dabei zeigte sich interessanterweise, dass der Myofibroblastenmarker *α-smooth muscle actin* (α-SMA) und die extrazellulären Matrixproteine Kollagen 1 und 3 signifikant reduziert waren, nachdem die Zellen zu konditioniertem Medium von Adipozyten exponiert wurden. Weitere Analysen inklusive einer Sekretomanalyse, Western Blot, ELISA sowie einer *high-throughput*-Proteinanalyse ergaben eine Schlüsselrolle des *bone morphogenetic proteins* (BMP)-4, welches von Adipozyten sezerniert wird, und entscheidend für die beobachtete Umprogrammierung der Myofibroblasten zu sein scheint. Zusätzlich kristallisierte sich der Peroxisom-Proliferator-aktivierte Rezeptor gamma (PPARγ) als wichtig heraus, dessen vermehrte Expression ebenfalls durch Zugabe von konditioniertem Adipozyten-Medium beobachtet wurde. Bemerkenswert ist, dass zwischen PPARγ und TGF-β Signalwegen eine reziproke, antagonistische Beziehung zu bestehen scheint, welche auf anti-fibrotische Effekte seitens PPARγ deutet.

Insgesamt induzierten Adipozyten eine Umprogrammierung von Myofibroblasten, welche durch BMP-4-Sekretion sowie PPARγ-Aktivierung erfolgte. Diese Ergebnisse heben die entscheidende Rolle von Adipozyten in der Narbenregeneration hervor und könnten für zukünftige Therapieansätze in der Prävention bzw. Behandlung hypertropher Narben nützlich sein.

LIST OF ABBREVIATIONS

15d-PGJ2	15-Deoxy-Delta-12,14-prostaglandin J2
2D	two-dimensional
3D	three-dimensional
ALK	activin receptor-like kinase
APS	ammonium persulfate
ASC	adipose-derived stem cell
α-SMA	alpha-smooth muscle actin
BAT	brown adipose tissue
BMP	bone morphogenic protein
BMPR	BMP receptor
BSA	bovine serum albumin
CAL	cell-assisted lipotransfer
cAMP	cyclic adenosine monophosphate
CEBPα	CAAT enhancer binding protein alpha
CITED2	cbp/p300-interacting transactivator 2
CM	conditioned medium
DAPI	4′,6-diamidino-2-phenylindole
DKK-1	Dickkopf-related protein-1
DMEM	Dulbecco’s modified eagle medium
ECM	extracellular matrix
EDTA	ethylenediaminetetraacetic acid
EMT	epithelial-mesenchymal transition
ERK	extracellular-regulated kinase
FABP4	fatty acid binding protein 4
FBS	fetal bovine serum
FFA	free fatty acids
FGM	fibroblast growth medium
FSP1	fibroblast-specific protein-1
GDF	growth differentiation factor
GPDH	glycerol-3-phosphate dehydrogenase
HBSS	hank’s balanced salt solution
HS	hypertrophic scar
HSC	hemopoietic stem cell
JNK	c-Jun N-terminal kinases
KLF	Krueppel-like factor
LAP	latency-associated protein

LLC	large latent complex
MAPK	mitogen-activated protein kinase
miR	microRNA
MMP	matrix metalloproteinase
MSC	mesenchymal stem cell
PAI	Plasminogen activator-inhibitor 1
PBS	phosphate buffered saline
PFA	paraformaldehyde
PPARɣ	peroxisome-proliferator activated receptor
PTEN	phosphatase and tensin homolog
RXR	retinoid X receptor
SBE	Smad binding element
SREBP1	Sterol regulatory element-binding protein-1
SSc	Systemic Sclerosis
SVF	stromal vascular fraction
TGF	transforming growth factor
TIMP	tissue inhibitor of metalloproteinase
TZD	thiazolidinedione
UCP-1	uncoupling protein 1
VEGF	vascular endothelial growth factor
WAT	white adipose tissue
Wnt	wingless/integrated
Zfp	zinc finger protein

TABLE OF CONTENT

INTRODUCTION

1.1. Skin Fibrosis

Fibrosis is the process of excessive connective tissue formation affecting a plethora of tissues and organs thereby disrupting their normal organ architecture, eventually leading to organ failure. Fibrotic processes can be caused by multi-system diseases such as systemic sclerosis (SSc) or nephrogenic systemic fibrosis but also affect specific organs including the lung, kidney, liver, heart or bladder. Although the underlying mechanisms are quite diverse, they all have distinct characteristics in common. Virtually every organ in the human body can be affected by physiological or pathological fibrotic processes (Wynn, 2008). Especially the human skin represents an organ where normal and abnormal fibrotic responses lie very close together. As the primary barrier, the skin protects the human body against physical injuries, pathogens or other potential hazards. Therefore, the skin is an intricate structure comprising various layers, each with multiple functions. In the epidermis, the upper layer, keratinocytes are the major residing cell type. Its barrier function and the protection against trans-epidermal water loss are the most important epidermal attributes. The layer below, the dermis, provides nutrients to the non-vascularized epidermis. Here, fibroblasts alongside with collagenous and elastic fibers are found, ensuring skin elasticity and strength. In addition to the dermis and epidermis, which together form the cutis, there is a subcutaneous layer where fat depots are located for energy storage and thermal insulation. Moreover, this highly vascularized structure provides oxygen and nutrient supply to the upper skin layers. When injured, the skin must repair itself rapidly to sustain cutaneous integrity. Therefore, the skin presents a fascinating cascade of repair responses (Gurtner et al., 2008). However, these mechanisms are prone to aberrations and may lead to skin fibrosis, and abnormal scars such as hypertrophic scars and keloids can occur.

1st1st1st Hypertrophic Scars and Keloids: Appearance and Treatment

Abnormal scarring and its accompanying cosmetic, functional and psychological burden is a major challenge in modern medicine. Up to 30% of elective surgeries are followed by aberrations in physiological wound healing, resulting in hypertrophic scarring or keloid formation (Mokos et al., 2017, Hoerst et al., 2019). Typically, tissue repair, beginning after a skin injury, ultimately results in a scar which never obtains the flexibility or strength of the original tissue. Therefore, scars are considered as the end point of mammalian tissue repair (Bayat et al., 2003). Ideally, tissue repair would result in total regeneration with the repaired tissue having the same structural and functional characteristics as the uninjured skin. So far, scarless healing is only observed in mammalian embryos as well as in lower vertebrates, including fish (Zebrafish) or amphibia (axolotl and *Xenopus*), and invertebrates

(Suzuki et al., 2005, Brockes and Kumar, 2002). For axolotl and *Xenopus* froglets it is known that their entire skin, including secretory appendages, regenerates after a full-thickness injury. Even the skin pigmentation pattern can be restored. In contrast, adult mammalian wound healing processes challenge to obtain such regeneration (Gurtner et al., 2008). Scars are often considered as trivial but in fact, scars can place a high burden on patients and potentially come along with disfiguring and aesthetical issues. Indeed, scars can cause severe itching, tenderness, pain, sleep disturbance, anxiety, depression, and disruption of daily activities. Together with other psychological liabilities such as post-traumatic stress reactions or loss of self esteem, scarring may lead to a reduced quality of life (Bayat et al., 2003).

Skin tissue repair results in a broad range of scar types. Five main types of scars can be divided, starting with a 'normal' fine line and continuing with widespread and atrophic scars, scar contractures and raised scars. All these scars have a different clinical appearance, etiology and pathogenesis, therefore requiring different therapeutic approaches (Bayat et al., 2003). Raised scars are caused by excessive extracellular matrix (ECM) deposition and can be further classified into hypertrophic scars and keloids. Although there are similarities between both types of scars, there are also some clinical, histological and epidemiological differences (**Fig. 1**). Hypertrophic scars are raised scars that remain within the boundaries of the original lesion. They occur 4 to 8 weeks after dermal injury, have a rapid growth phase of up to 6 months and eventually regress with time (Wheeland, 1996). These scars are often red, firm, itchy and painful. Typically, hypertrophic scars occur after extensive trauma such as deep burns or even standard surgeries. Commonly, hypertrophic scarring develops in areas with high tension such as shoulders, neck, prosternum or ankles (Gauglitz et al., 2011).

Different to hypertrophic scars, keloids are raised scars that spread beyond the margins of the original wound. They invade the surrounding normal skin and often continuously grow. Keloids may appear years after a minor injury or even develop spontaneously. Keloids are very site specific with examples of the ear lobe or cheeks, and it happens that they invariably reoccur after excision (Rockwell et al., 1989). Usually, keloids do not regress spontaneously after time and are unique to humans (Leventhal et al., 2006). Keloids appear to be inflamed, itchy and painful, especially when they are in the growing phase.

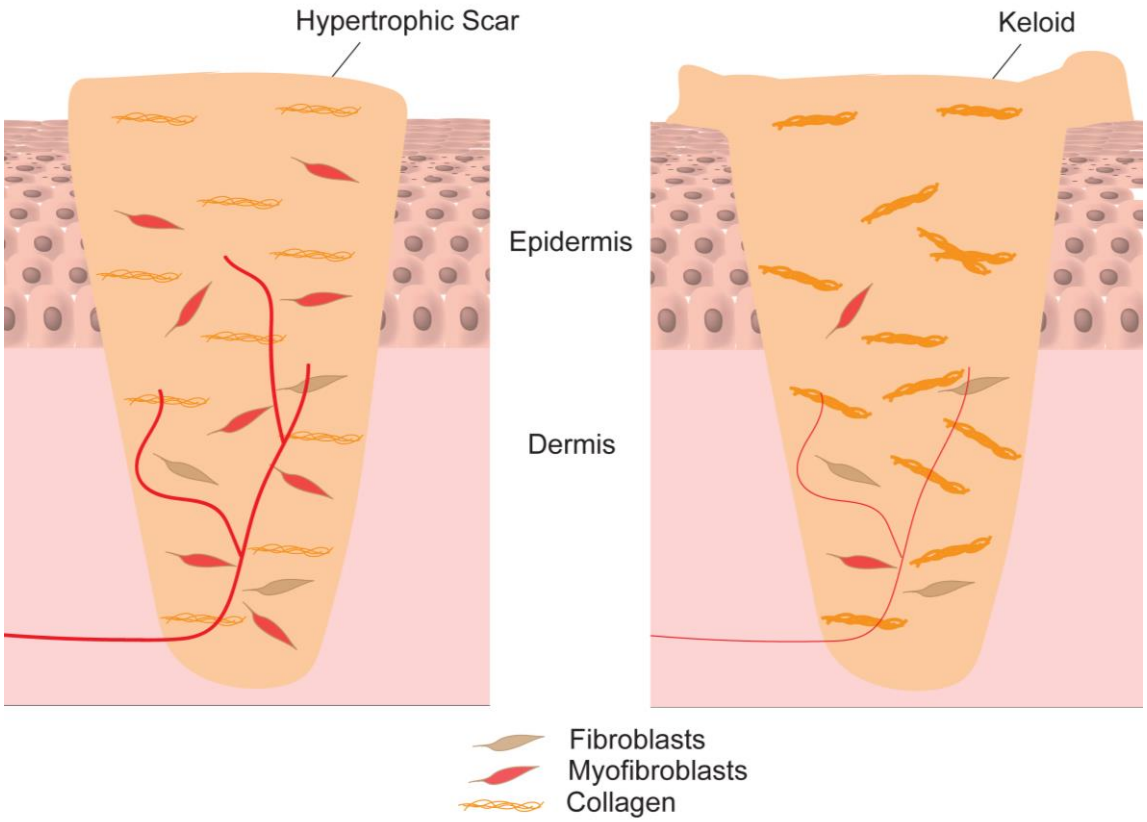

Fig. 1: Morphological differences between hypertrophic scars and keloids.
Hypertrophic scars show excessive collagen deposition and numerous myofibroblasts. In contrast, keloids extent beyond the boundaries of the original lesion and contain thick, disorganized collagen bundles. Myofibroblasts are only rarely seen in keloids and blood vessels are occluded. Modified from a template kindly provided by Anna Löwa.

In addition to that, there are also histological differences between hypertrophic and keloid scars. Both scar types contain an overabundance of dermal collagen, but hypertrophic scars contain primarily collagen 3 which is organized in bundles parallel to the epidermis (Gauglitz et al., 2011). Characteristic for hypertrophic scars, abundant nodules containing myofibroblasts are being observed. Contrary to hypertrophic scars, keloids are composed of disorganized collagen 1 and 3 without nodules of myofibroblasts (Slemp and Kirschner, 2006). The presence of myofibroblasts, specialized fibroblasts which are alpha-smooth muscle actin (α-SMA)-positive, in hypertrophic scars would explain the observed contraction seen in hypertrophic scars but not in keloids (Junker et al., 2008). However, using myofibroblasts and its marker to distinguish between both scar types is currently re-discussed as this protein seems to be expressed under both conditions (Lee et al., 2004).

Both hypertrophic and keloid scars have an equal sex distribution and predominantly occur in the second to third decade of patient's life. The incidence for hypertrophic scars is with up to 91% highest after burn injuries followed by incidence rates of 40 to 70% after injuries, always depending on the depth of the wound (Bombaro et al., 2003). Keloids are being

observed in all races with dark-skinned individuals being more prone to keloid formation (incidence of 6 to 16% in African populations) (Cosman et al., 1961). A genetic predisposition for keloid occurrence is being discussed since patients with keloids often describe a positive family history in contrast to those with hypertrophic scars (Gauglitz et al., 2011).

Both scar types are major therapeutic challenges for surgeons and dermatologists. Although there exists a wide range of treatment options, none of these is efficient and optimal (Marshall et al., 2018). In general, non-invasive and invasive procedures need to be distinguished. Non-invasive therapies include the use of compression therapy such as pressure garments with or without gel sheeting (O'Brien and Jones, 2013). Also, acrylic casts, masks and clips or various oils, lotions and creams are applied. In addition, silicone sheeting is a popular option (Fulton Jr, 1995). More invasive treatments include surgical excision or intralesional corticosteroid injection. Other treatments with variable results involve injections of fluorouracil, bleomycin or interferon gamma, radiotherapy, laser therapy and cryosurgery (Rabello et al., 2014). One option is also the leave alone management. Occasionally, scars are best left undisturbed especially after invasive treatment. This can take up to one year until further treatment options can be considered by the scar's appearance (Bayat et al., 2003). Therapeutics based on molecular targets have not yet been beyond clinical trial but are expected longingly (Friedman 2013).

1.1.2. Wound Repair Mechanisms

Much of the research focus on pathological scarring includes the attempt for a better understanding of the cellular and molecular processes involved in wound healing processes. These repair mechanisms include a series of dynamic and physiological processes involving various cell types, matrix molecules, cytokines and mediators (Gurtner et al., 2008). In general, wound healing is divided into three overlapping phases: inflammation, proliferation and remodeling/maturation (**Fig. 2**).

Triggered by a deep tissue injury or damage, the inflammatory response phase is initiated. Platelet aggregation forms a hemostatic plug and blood coagulation provides a first provisional matrix (Baum and Arpey, 2005). This matrix, mainly composed of fibrin and fibronectin, fills the tissue defect and enables effector cell influx as well as cell migration by acting as a scaffold. Platelets release multiple cytokines thereby recruiting inflammatory cells: at the early stage of an acute inflammation granulocytes are the predominant infiltrating leucocytes, later replaced by monocyte infiltration (Werner and Grose, 2003). Monocytes differentiate into phagocytic macrophages ensuring debris removal. Following activation, macrophages also release a broad spectrum of biologically active mediators.

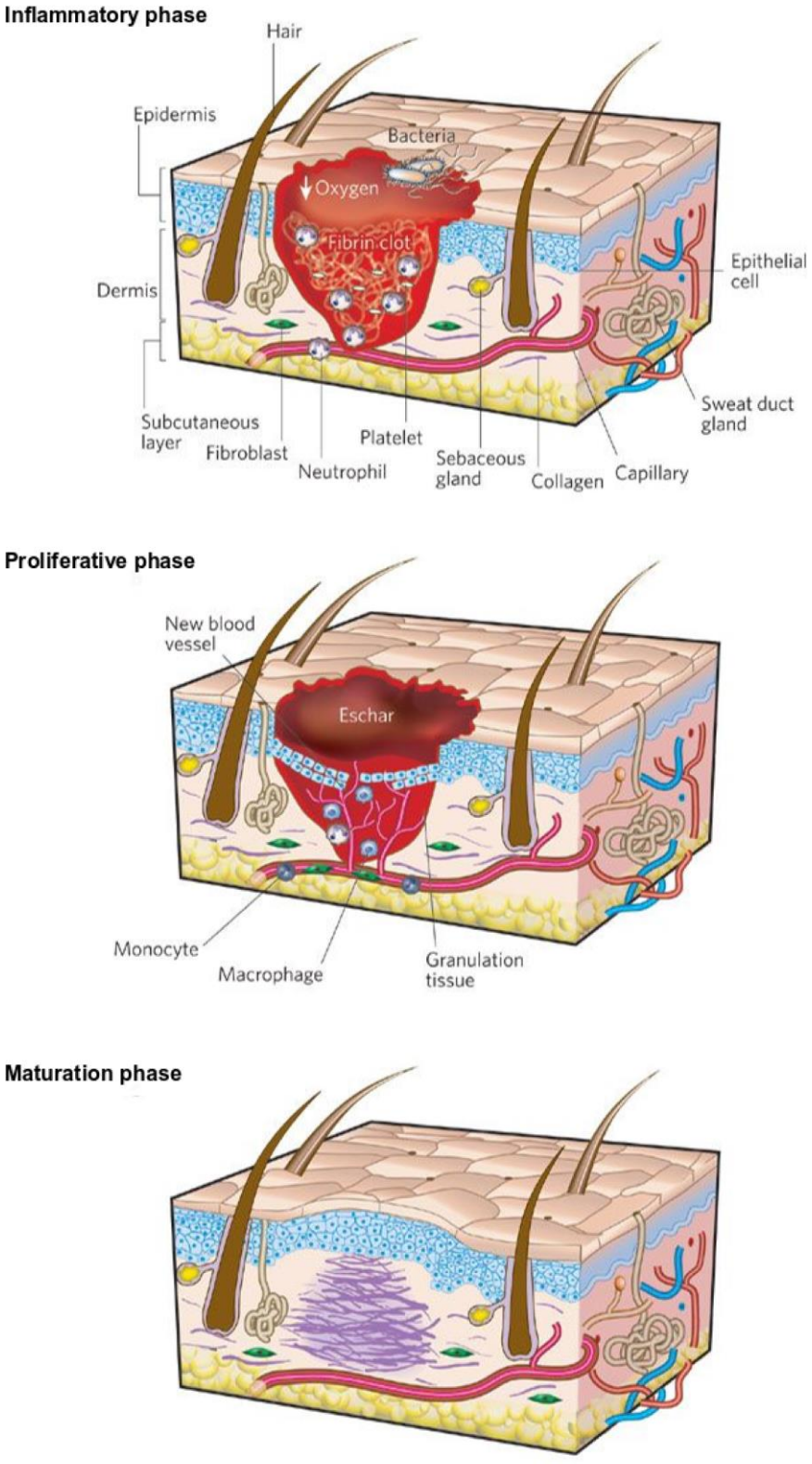

Fig. 2: The three classical stages of wound healing.

Inflammatory phase: wound after 24h to 48h of injury. The wound bed is characterized by a fibrin clot with abundant bacteria, neutrophils and platelets. Proliferative phase: depicted is a wound 5-10 days after injury where an eschar (scab) has been formed on the wound surface. New blood vessels now appear, and keratinocytes migrate under the eschar. Granulation tissue has replaced the fibrin clot. Maturation phase: this phase can last up to one year or longer. Disorganized collagen has been laid down by fibroblasts. The re-epithelialized wound is slightly higher than the surrounding skin and contains no skin appendages. Modified from (Gurtner et al., 2008).

These include proteases and oxygen derived free radicals for tissue destruction, cytokines and chemokines for chemotaxis, thromboxane A2 and prostaglandins involved in vascular hemodynamics plus a plethora of growth factors as well as matrix metalloproteinases (MMPs) responsible for fibrogenesis (Singer, 1999, Werner and Grose, 2003). Therefore, the inflammatory phase serves, besides the removal of bacteria and debris, to prepare the wound bed for repair. Usually 72h after injury, the inflammatory response diminishes, and the wound healing process shifts towards the proliferative phase (Gurtner et al., 2008).

The proliferative phase takes place on day 2 to 10 after injury with the major attempt to generate granulation tissue which replaces the provisional matrix. This phase includes several processes that partially cross and work together, which are namely re-epithelization, angiogenesis and fibrogenesis for granulation tissue development. The process of re-epithelialization begins just hours after injury and continues during inflammatory and proliferative phase. Keratinocytes begin to migrate from the wound edge and local hair follicles, and advance across the wound surface until they reach keratinocytes from the other wound site (Raja et al., 2007). Especially in larger wounds, proliferation of keratinocytes is important as well, in order to close the wound defect sufficiently (Coulombe, 2003, Baum and Arpey, 2005). In addition, keratinocytes secrete a variety of growths factors stimulating fibrogenesis and angiogenesis in the parts below, these include transforming growth factor-beta (TGF-β), vascular endothelial growth factor (VEGF), epidermal growth factor (EGF) and keratinocyte growth factor (KGF) (Werner and Grose, 2003). Another critical factor in the ongoing wound healing process is angiogenesis. Adequate blood supply is important for the granulation tissue being formed providing nutrient delivery and support for fibroblast migration. Endothelial cells in local uninjured capillaries migrate into the wound bed and form tubules that mature into new capillaries (Li et al., 2003). A wide range of pro-angiogenetic factors is being released at the site of injury facilitating this new vascularisation with TGF-β1, angiopoietin and VEGF representing one of the most important factors (Li et al., 2003). Primary responsible for the development of granulation tissue are fibroblasts, representing the key cell type in this wound healing phase. Fibroblasts move into the provisional matrix as a basis for fibrogenesis, serving as the main source for ECM proteins such as collagens, glycosaminoglycans or proteoglycans (Bainbridge, 2013). These ECM proteins constitute the newly formed granulation tissue thereby providing structural integrity to the wound. In addition to ECM deposition, fibroblasts differentiate into so-called myofibroblasts which provide force for wound contraction, thereby contributing to wound closure (Hinz, 2007). Also, they secrete MMPs and their inhibitors (tissue inhibitor of metalloproteinases, TIMPs) and hence, are in involved in granulation tissue remodeling (Sarrazy et al., 2011).

Up to 2 to 3 weeks after injury, the tissue defect has been closed by granulation tissue and is covered with new epithelial cells. The wound area is now comprised of a widely acellular mass with disorganized collagen fibers and other ECM proteins. There are no dermal appendages such as hair follicles or sweat glands. The wound surface contracted, which is the reason for the wound base to be wider than the surface (Marshall et al., 2018). Most of the cells that entered the wound bed initially, like fibroblast, macrophages and endothelial cells, disappear via apoptosis or move away from the wound area (Gurtner et al., 2008). On this occasion, a process called remodeling or maturation begins and eventually lasts for months to years. During this phase, the collagen matrix is subject to a continuous remodeling especially by MMPs and TIMPs. Progressively, collagen 3, the main component of granulation tissue, is replaced by collagen 1, the major ECM protein found in the dermis (Monaco and Lawrence, 2003). This new collagen is more oriented and reorganized into a structurally sound lattice based on glycosaminoglycans and proteoglycans. Elastin, usually absent in granulation tissue, appears again and contributes to skin elasticity (Gurtner et al., 2008). The resulting scar reaches a maximum tensile strength up to 80% of the original skin and often manifests less pigmented due to lacking hair follicles containing melanocyte stem cells (Levenson et al., 1965, Baum and Arpey, 2005).

Even if the wound healing process includes a highly coordinated succession of events, however, it is prone to aberrations and may escape the controlled regulatory system. These abnormal repair mechanisms result in impaired remodelling of the granulation tissue leading for example to hypertrophic scarring in cutaneous repair or to fibrosis of internal organs such as lung, liver and kidney. During these fibrotic conditions, an excessive, uncontrolled accumulation of ECM proteins is observed with functional tissue being replaced by non-functional fibrotic tissue (Wynn, 2008). At the cellular level, the continued presence of myofibroblasts in fibrotic tissues is broadly accepted as the main effector of fibrosis (Biernacka et al., 2011). Myofibroblasts removal or loss by apoptosis is normally considered as the transition between granulation tissue and healing or normal scar formation (Desmouliere et al., 1995). However, these cells persist in fibrotic lesions and are believed to be relevant for excessive collagen production leading to alterations of tissue architecture (Hinz, 2016).

1.1.3. Myofibroblast Formation and Function

Although the mechanisms of wound healing are not completely understood so far, it has become clear that fibroblasts and myofibroblasts play a critical role during this process. Especially the highly coordinated contraction of myofibroblasts is believed to be responsible for wound contraction and therefore wound closure. However, since excessive

myofibroblast activity is believed to cause abnormal scar formation, insights into myofibroblasts generation and their characterization is essential (Desmoulière et al., 2005).

Phenotypically, myofibroblasts are an intermediate cell type between fibroblasts and smooth muscle cells. They exhibit ultrastructural features of fibroblasts with a spindle shape, prominent cytoplasmic projections and an abundant rough endoplasmic reticulum. Like smooth muscle cells, myofibroblasts have longitudinal cytoplasmic bundles of microfilaments and multiple nuclear membrane folds (Serini and Gabbiani, 1999).

Due to the high demand for contractile cells in wound healing processes, myofibroblasts can originate from various cell types. In skin repair, myofibroblasts are believed to originate mainly from local dermal fibroblasts but pericytes and vascular smooth muscle cells are also potential sources, especially during vascular wound healing (Rajkumar et al., 2005). In addition, there is evidence that myofibroblasts come from tubular epithelial cells through epithelial-mesenchymal transition (EMT) (Krenning et al., 2010). More recently, it came up that a similar process is possible with endothelial cells, termed endothelial-mesenchymal transition (EndMT) (Zeisberg et al., 2007). Also, the recruitment of fibroblast precursor cells (fibrocytes) from the bone marrow is seen as a potential source for myofibroblasts (Abe et al., 2001). The classical view of myofibroblasts originating from local quiescent fibroblasts, which is still believed to be the major myofibroblast source, was the object of several studies which revealed the transformation as a two-step process (Desmoulière et al., 2005, Tomasek et al., 2002) (**Fig. 3**).

First, fibroblasts evolve into proto-myofibroblast in early granulation tissue 2-4 days after wounding. Such cells exert tractional force and may be induced by mechanical stress. The proto-myofibroblast is characterized by stress fibers which only contain β- and ɣ-cytoplasmic actins as well as by the expression of cellular fibronectin including the splice variant ED-A (Tomasek et al., 2002). The switch from the proto-myofibroblast to the differentiated myofibroblast has been connected to the production of TGF-β by inflammatory cells, the most accepted stimulator of myofibroblast differentiation. The action of TGF-β is related to the local presence of ED-A fibronectin (Tomasek et al., 2002). Therefore, myofibroblast differentiation depends both on a cell product and an ECM component. The transition into myofibroblasts is characterized by *de novo* expression of α-smooth muscle actin (α-SMA) (Hinz, 2007). Incorporation of α-SMA into stress fibers enhances the contractile activity of myofibroblasts thereby providing the cell's most important characteristic (Hinz et al., 2001).

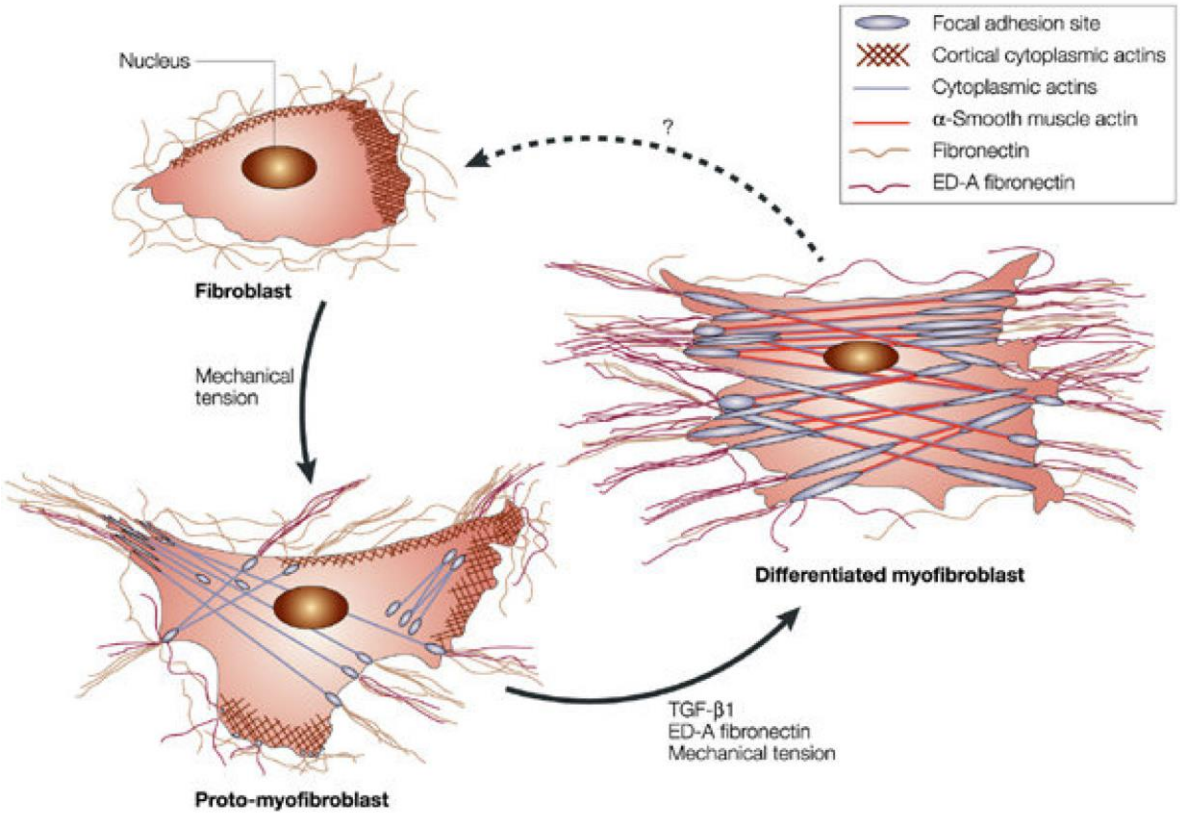

Fig. 3: Myofibroblast differentiation as a 2-step process.
First, fibroblasts differentiate into proto-myofibroblasts characterized by stress fibers which contain β- and γ- cytoplasmic actins. Due to the presence of TGF-β1 and the splice variant ED-A fibronectin, proto-myofibroblasts convert into differentiated myofibroblasts known for their alpha-smooth muscle actin (α-SMA expression). If a reversion of myofibroblasts back into fibroblasts is possible, is speculated. (Hinz 2008)

Besides α-SMA, the most reliable myofibroblast marker, other distinctive and unique factors for myofibroblasts are difficult to name. One promising target is the expression of specific cadherins, cell-cell adhesion proteins linked to the intracellular actin skeleton. Proto-myofibroblast in the early granulation tissue do express N-cadherin which makes them easily distinguishable from cadherin-negative dermal fibroblasts. In differentiated myofibroblasts, N-cadherin becomes replaced by OB-cadherin, playing an important role in coordination of contraction. However, since OB-cadherin is expressed in a variety of cell types with mesenchymal origin, it can not be considered as a unique marker for myofibroblasts (Hinz et al., 2004, Hinz, 2007). Desmin, an intermediate filament protein normally expressed in muscle cells, has been taken into account as a negative marker for myofibroblasts. Even so, in some pathological conditions of scarring, myofibroblast were found to be desmin-positive (Skalli et al., 1989). Other markers tested as myofibroblasts characteristic were not reliable as to inconsistent staining results such as for the fibroblast-specific protein (FSP-1) (Eddy, 2013). Therefore, it is difficult to distinguish myofibroblasts

from other cell types with similar cytoskeletal features, especially smooth muscle cells and pericytes (Hinz, 2007).

The contraction, myofibroblasts are known for, is based on a contractile apparatus known as the fibronexus. The fibronexus is a specialized adhesion complex which links bundles of actin to extracellular fibronectin domains via integrins. This linkage enables the fibronexus as a mechano-transduction system transmitting the force generated by stress fibers to the surrounding ECM (Tomasek et al., 2002, Hinz, 2007). In addition to its contractile features, myofibroblasts synthesise ECM proteins, notably collagen types I-VI, glycoproteins and proteoglycans (Schűrch et al., 2006). Also, myofibroblasts secrete many other matrix molecules such as laminin and thrombospondin as well as MMPs and TIMPs (Powell et al., 1999).

For many years, myofibroblasts were considered as terminally differentiated cells and that they would, most likely via apoptosis, disappear after wound contraction and closure was performed in physiological wound healing (Desmouliere et al., 1995, Hinz, 2007). However, more and more evidence come up that myofibroblasts become deactivated or revert to a more normal phenotype in designated situations (Hecker et al., 2011, Wettlaufer et al., 2016). The question of the reversibility of myofibroblast differentiation is essential, particularly for fibrotic conditions where myofibroblast are involved. Given that myofibroblast appearance and dysfunction has severe consequences, knowledge about their development, function and survival is crucial (Hoerst et al., 2019). By this, not only myofibroblasts are in the research focus but also TGF-β signaling with its pivotal role in myofibroblast generation.

1st1st4th TGF-β as a Profibrotic Mediator

The TGF-β superfamily is composed of several growth factors that play major roles in physiological and pathological processes including cellular development and differentiation, embryogenesis, inflammatory response mechanisms and tissue repair (Shi and Massagué, 2003, Ten Dijke et al., 2002). Indeed, the TGF-βs are one of the most pleiotropic and multifunctional growth factors known so far. The superfamily can be divided into the TGF/Activin/Nodal subfamily and the bone morphogenetic protein (BMP)/growth differentiation factor (GDF) subfamily with both subgroups activating distinct intrinsic pathways. There exist three isoforms of TGF-β in mammals, namely TGF-β1, TGF-β2 and TGF-β3, encoded by three different genes. Although the expression of the different isoforms is greatly tissue specific, all three function through the same cell surface receptor and affect similar cellular targets. TGF-β1 is the most common isoform with a ubiquitous expression in all mammalian tissue structures (Biernacka et al., 2011). In contrast to TGF-β1, the other

isoforms are more tissue specific and limited to defined areas. Even if all three isoforms are involved in fibrotic processes, the main impact on fibrosis is attributed to TGF-β1 (Biernacka et al., 2011). Usually, TGF-β1 is an inactive latent complex with a C-terminal mature peptide and a N-terminal latency-associated peptide (LAP) (Munger et al., 1997). While LAP is bound to the mature peptide, the binding to its receptor is not possible. Before TGF-β1 is secreted by cells, the LAP is cleaved (Yang et al., 2007b). However, the mature peptide remains inactive since the LAP remains attached by a large latent complex (LLC). This complex still shields TGF-β1's active epitope and prevents the interaction to its receptor. In connective tissue, the LLC is bound to ECM proteins such as elastin fibrils. Therefore, there are typically significant amounts of latent TGF-β1 stored in the matrix waiting to be activated if TGF-β1 signaling needs to be initiated (Todorovic et al., 2005). For activation of TGF-β1 signaling, the LLC must be deliberated from the matrix by several proteases including plasmin, mast cell chymase and thrombin (Annes et al., 2003). Also, the interaction between TGF-β1 and LLC needs to be disrupted, a process that is so far poorly understood but believed to be protease-dependent (Biernacka et al., 2011).

Active TGF-β1 binds to and phosphorylates the transmembrane TGF receptor type II (**Fig. 4**). Upon ligand binding, type I receptor is recruited and forms a heterodimeric complex with the type II receptor, thus enabling a serine/threonine kinase activity. In mammals, there are seven different type I receptors termed ALK 1-7 (activin receptor-like) with ALK-5 being the most important one regarding fibrotic processes (Rahimi and Leof, 2007). The canonical TGF-β1 signaling pathway involves the Smad family of transcriptional activators. The eight Smad proteins can be divided into three functional groups: the receptor activated Smads (1, 2, 3, 5, 8), the common mediator Smad4 and inhibitory Smads (6, 7). It is generally accepted that the TGF-β/Activin/Nodal subfamily activates Smad2 and 3, whereas the BMP/GDF subfamily signals through Smad1, 5 and 8 (ten Dijke and Hill, 2004). Smad activation is conducted through phosphorylation by the specific type I receptor depending on the cell type. For instance, Smad2 and 3 are usually triggered by ALK-5. Activated Smads form a complex with Smad4, translocate into the nucleus and induce the expression of specific target genes by cooperating with DNA transcription factors (Feng and Derynck, 2005). Alternatively, gene expression can be regulated Smad independently via the non-canonical signaling pathway (**Fig. 4**). Here, members of the mitogen-activated protein kinase (MAPK) family possess serine/threonine kinases and respond to external stimuli by activating a signaling cascade inducing differentiation, cell survival or apoptosis (Gaestel, 2016). All three known MAPK pathways may be triggered by TGF-β1: extracellular signal-regulated kinase (ERK), p38 MAPK and c-Jun-N-terminal kinase (JNK). Signaling through those pathways may also regulate Smad proteins but rather exert Smad independent effects (ten Dijke and Hill, 2004).

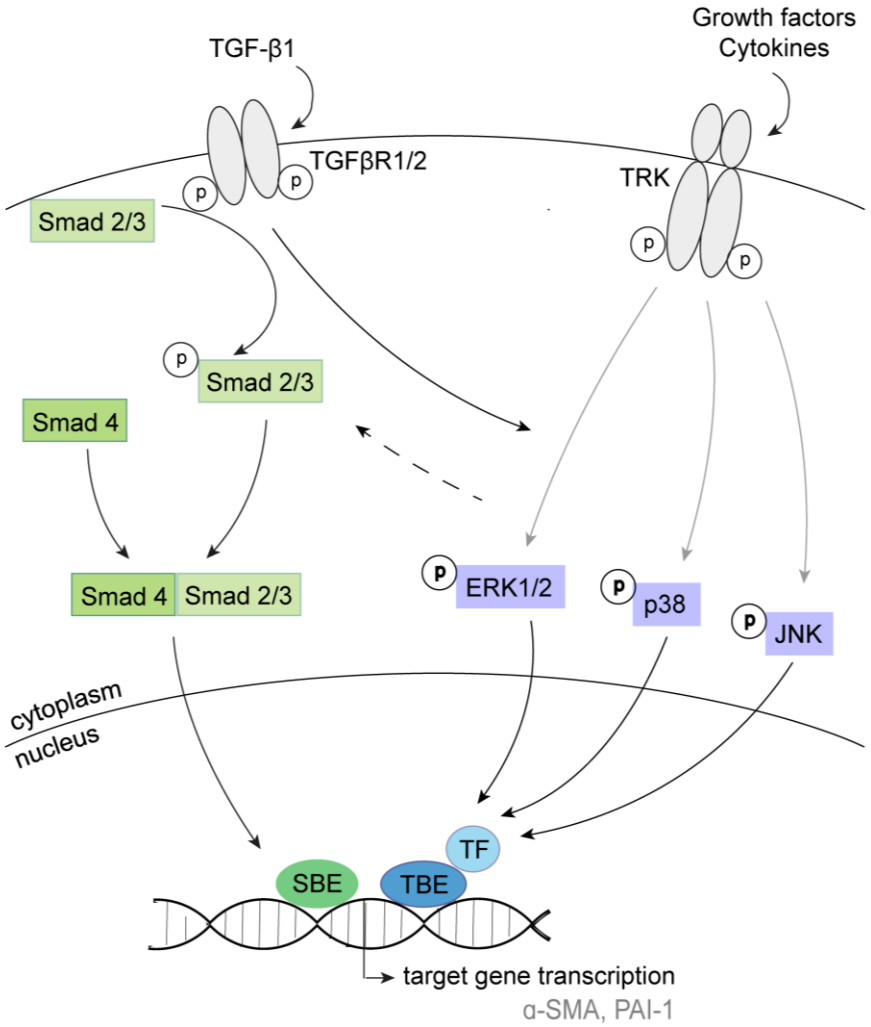

Fig. 4: Canonical and non-canonical TGF-β signaling.
Upon TGF- binding, the receptor type I and II (TGFR1/2) become phosphorylated. Subsequent Smad 2/3 activation leads to a complex formation with Smad 4, translocation into the nucleus and target gene induction (α-SMA, PAI-1). TGF exerts its functions also Smad independent by activating the mitogen-activated protein kinase (MAPK) signaling pathways ERK1/2, p38 and JNK. α-SMA = alpha-smooth muscle actin, PAI-1 = plasminogen activator inhibitor-1, TGF = transforming growth factor, TRK = tyrosine receptor kinase, SBE = Smad binding element, TF = transcription factor.

The crucial role of TGF-β1 as a regulator of fibroblast differentiation has brought the focus on α-SMA induction and other fibrotic targets by TGF-β signaling. Extensive research revealed the important role of the TGF-β/Smad3 signaling pathway involved in the pathogenesis of fibrosis in many tissues. Transcription of α-SMA mediated by Smad3 is linked to the binding of Smad3 to the Smad binding element 1 which is upstream of the α-SMA core promoter element (Hu et al., 2003, Uemura et al., 2005). Interestingly, Smad3 null mice exhibit attenuated fibrosis in a wide range of experimental models (Bujak et al., 2007, Dobaczewski et al., 2010). Indeed, a resistance was shown for bleomycin-induced pulmonary fibrosis or dermal fibrosis following irradiation (Zhao et al., 2002). However, α-SMA expression has been proven in Smad3-deficient hepatic stellate cells indicating that

Smad3 is not solely responsible for myofibroblast differentiation (Schnabl et al., 2001). Although its key role in TGF-β1 mediated fibrosis is widely accepted, increasing evidence considers non-canonical signaling as an additional pivotal point (Biernacka et al., 2011). Indeed, it was shown that a TGF-β mediated fibrogenic program was initiated by the ERK pathway in SSc fibroblasts (Pannu et al., 2007). Another study highlighted the essential role of the p38 MAPK pathway in a model of renal fibrosis (Stambe et al., 2004). The relevance of both canonical and non-canonical TGF-β signaling regarding fibrosis, as well as potential interactions between pathways, remains poorly understood (Biernacka et al., 2011). Although TGF-β mediated myofibroblast activation is pivotal for a normally proceeding wound healing process, it should not be forgotten that persistent myofibroblasts activity seems to be responsible for abnormal scarring. Since myofibroblast activity is inseparable from TGF-β signaling, these signaling pathways are most likely involved in fibrotic conditions such as hypertrophic scars or keloids.

Although many fundamental findings about myofibroblasts and their TGF-β mediated formation were accumulated in the past years, many aspects of abnormal scar growth and persistence are still questioned or unknown. This lack of knowledge contributes, indeed, to non-optimal or improvable treatment options for hypertrophic scars and keloids as described in 1st1st1st. Remarkably, one outstanding scar treatment emerged in recent years, which is the use of autologous fat grafting. Here, fat depots are harvested from body deposits and re-injected into scar tissue with promising outcome. This technique, and adipose tissue as a new, auspicious research field will be introduced in the next chapter.

1.2. Multiple Functions of Adipose Tissue

Adipose tissue is a complex organ that revealed surprising characteristics once it was studied in more detail. The traditional role, adipose tissue is attributed to, is energy storage. Often, adipose tissue is associated with obesity and is therefore connected with undesirable effects (Trayhurn and Beattie, 2001). However, what is many times not mentioned or known is the actual complexity of this tissue with its different subgroups of white, brown and beige/brite adipose tissue as well as its variety of cell types residing in this tissue, thereby enabling adipose tissue as an endocrine organ (Kershaw and Flier, 2004, Nedergaard et al., 2007). Indeed, fat mediates a plethora of beneficial effects to the human body including wound healing processes (Scherer, 2006).

Adipose tissue is a special loose connective tissue composed of lipid-laden adipocytes. Those fat cells are held together by reticular fibers which are characterized by lobule formation and are usually found in a capillary and innervation network. Notably, adipocytes are not the sole cell type in adipose tissue even if they are the most prominent cell type by volume. But, in fact, adipocytes make up only up to 40% of the total cell mass of a fat pad with macrophages, fibroblasts, endothelial cells, mesenchymal stem cells, pericytes, blood cells and immune cells coming along (Rosen and Spiegelman, 2014). This multicellularity provides a first indication for the complex functions adipose tissue holds.

When talking about the classical role of adipose tissue in the human body, it is usually the white adipose tissue (WAT) that is referred to. Contradictory to a classic organ localization, WAT distributes in single fat pads dispersed throughout the body. It is usually subcategorized into subcutaneous and internal depots. Subcutaneous fat layers are typically found beneath the skin in a region called hypodermis located between the dermis and the muscle. Internal depots are mainly composed of visceral fat that covers internal organs such as the heart or liver but also consist of non-visceral fat with intramuscular fat as an example (Rosen and Spiegelman, 2006). White adipocytes have a characteristic spherical form that vary greatly in size, ranging from 20 to 200 µm in diameter. Mature white fat cells contain a single large lipid droplet that takes about 90% of the cell volume (Rosen and Spiegelman, 2014). Interestingly, adipocytes possess the characteristic of changing their cell volume according to the current demand such as an increased lipid load. Therefore, a diameter increase up to 20-fold has been reported as well as a several 1000-fold increased cell volume (Frühbeck, 2008). Described as unilocular, the lipid droplet is mainly made up by a mixture of triglycerides, neutral fats, phospholipids, fatty acids and glycerol (Rosen and Spiegelman, 2006). Notably, triglycerides in brown adipocytes are stored in multilocular fat droplets in contrast to white adipocytes with one large lipid vacuole. Interestingly, brown adipocytes are rich of mitochondria thereby explaining their brownish

appearance. Recently, a third type of adipose tissue was discovered called beige or brite adipose tissue (Wu et al., 2012). Those adipocytes are found in white adipose tissue but show characteristics of brown adipocytes. An overview of the three different classes of adipocytes is shown in **Fig. 5**.

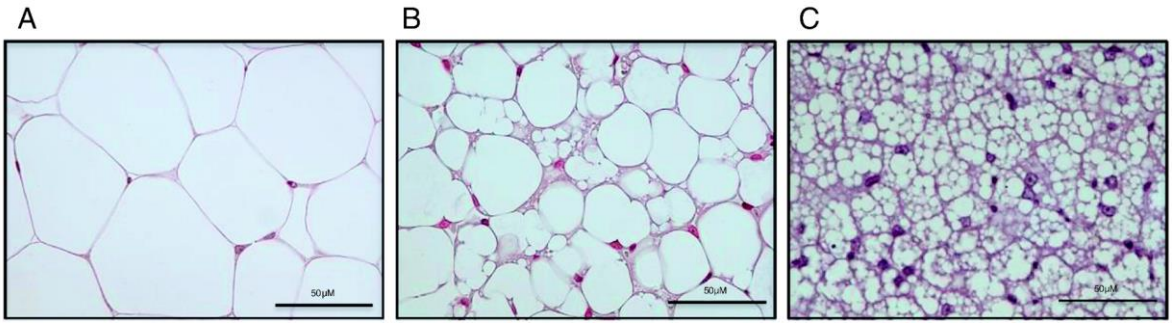

Fig. 5: Morphology of the three different adipocyte types.
Hematoxylin and eosin staining from (A) white adipocytes, (B) beige/brite adipocytes and (C) brown adipocytes. White adipocytes show a unilocular ft droplet whereas brown adipocytes exhibit multiple smaller ones and a high amount of mitochondria. Beige/brite adipocytes present an intermediate phenotype. (Keipert and Jastroch, 2014)

As mentioned above, adipose tissue has been traditionally defined by its ability of energy storage. During times of high food intake and/or decreased energy expenditure, surplus energy is stored in white adipocytes in the form of neutral triglycerides. As soon as the food intake is limited or there is an increased need for energy expenditure, lipid reserves are released for energy generation. In order to achieve this, adipocytes contain lipases enabling cleavage of triglycerides into glycerol and free fatty acids (FFA) which are subsequently released and transported in the blood to the liver or muscle where they are used for fatty acid oxidation (Rosen and Spiegelman, 2006). Therefore, the main function of WAT is not only the energy storage in form of triglycerides but also the energy release in form of fatty acids. When 1994 leptin was discovered to be released by adipose tissue, another dimension was added to our knowledge of adipose tissue function (Zhang et al., 1994). By this, it was demonstrated that adipose tissue is capable of transmitting signals thereby regulating energy balance. Subsequent studies revealed even more cytokine-like factors released by adipocytes, therefore called adipokines, promoting the idea of adipose tissue as an endocrine organ (Trayhurn and Beattie, 2001). Leptin is a hormone that is widely seen as the most important factor secreted by WAT and its functions have been extensively investigated. Leptin seems to interact with a variety of neuroendocrine systems leading to the inhibition of food intake or affecting energy expenditure (Trayhurn and Beattie, 2001). Moreover, leptin is involved in signaling toward the reproductive system, as well as the immune system and in angiogenesis (Friedman and Halaas, 1998). In addition, inhibition of insulin secretion by pancreatic β-cells and the stimulation of sugar transport have been

reported, demonstrating the major impact of leptin in metabolic processes (Trayhurn and Beattie, 2001). Interestingly, leptin exerts most of its effects through hypothalamic pathways, especially in connection with energy intake and expenditure. Therefore, leptin receptors, members of the cytokine class I receptor superfamily, are found in both the central nervous system as well as the periphery (Bjorbæk and Kahn, 2004). Besides leptin, adiponectin is a well known adipokine mediating the effects of WAT. Adiponectin belongs, together with leptin, to the insulin-sensitizing adipokines. Both proteins can induce insulin-stimulated lipogenesis thereby facilitating triglyceride accumulation and adipose expandability (Sethi and Vidal-Puig, 2007). Despite leptin and adiponectin, there are a variety of additional proteins involved in lipid and lipoprotein metabolism in WAT. These include the lipoprotein lipase, apolipoprotein lipase E and perilipin as well as retinol binding protein or fatty acid binding protein 4 (FABP4) (Kershaw and Flier, 2004). On top of the already mentioned adipokines secreted by white adipocytes, there is a plethora of other secreted factors with an amount ranging from 200 to 300 proteins (Ojima et al., 2016). Nonetheless, it needs to be emphasized that fatty acids are the major secretory product of WAT representing their main function as fuel reserve.

In contrast to WAT, brown adipose tissue (BAT) exerts further functions. Brown adipocytes are specialised in thermogenesis; thus, they can produce heat through transferring energy from food by mitochondrial "uncoupling" of oxidative phosphorylation of FFA. Here, the uncoupling protein-1 (UCP-1) plays a major role which is uniquely expressed in brown adipocytes. UCP-1 breaks up the proton gradient which is usually established by the electron transport chain at the inner membrane of mitochondria. Subsequently, heat is generated by energy expense in form of ATP (Cannon and Nedergaard, 2004). In newborns, BAT depots are found in specific body regions such as the neck or the interscapular region ensuring an adequate body temperature. Usually, the amount of BAT decreases with age since there are other mechanisms keeping the body warm (Cousin et al., 1992). The third type of adipose tissue was discovered called beige or brite adipose tissue. Those adipocytes are found in white adipose tissue but show characteristics of brown adipocytes, particularly UCP-1 expression. Speculations about the protective mechanisms of WAT browning against obesity has led to an increased research interest in this area (Lo and Sun, 2013).

In recent years, adipose tissue did not only attracted attention because of its multiple functions in the human body, especially regarding scar regeneration, but also because of the discovery that adipose tissue is a source for mesenchymal stem cells.

1st2nd1st Adipose-derived Stem Cells (ASCs)

The term “stem cell” was first used 1868, but it was more commonly applied with our current understanding of a stem cell at the beginning of the 20th century with the discovery of a putative common progenitor for the hematopoietic system (Ramalho-Santos and Willenbring, 2007). Confirmation of the existence of a hematopoietic stem cell (HSC) was achieved in the 1960s alongside with an extensive characterization of cell surface markers (Becker et al., 1963, Weissman, 2000). Most striking is their capability of self-renewal and multilineage differentiation, two characteristics that are now seen as relevant for a true stem cell (Bianco and Robey, 2001). In addition to HSCs, the existence of non-hematopoietic progenitor cells in bone marrow was verified with those cells showing at least some capacity of self-renewal as well as differentiation potential into mesenchymal cells such as osteocytes, chondrocytes and adipocytes (Friedenstein et al., 1987, Prockop, 1997). Therefore, those progenitor cells were termed as mesenchymal stem cells (MSCs) or bone marrow-derived MSCs (Prockop, 1997). With these observations, growing interest for the field of MSC-based therapies came up: bone marrow-derived MSCs were investigated for their potential in treating diseases such as osteogenesis imperfecta, strokes or myocardial infarctions with some promising therapeutic outcome (Picinich et al., 2007). However, the use of bone marrow-derived MSCs has raised some issues since harvesting of those MSCs is related with pain, side effects and morbidity (Ankrum and Karp, 2010). Therefore, alternative sources for MSCs were being sought with the discovery of certain tissues such as the dental pulp, Wharton jelly, amniotic fluid and indeed adipose tissue (Zuk et al., 2002, da Silva Meirelles et al., 2006).

Especially the discovery of MSCs in adipose tissue, the so-called adipose-derived stem cells (ASCs) led to an explosion in research focusing on ASCs since accessibility and harvesting of those MSCs shows distinct advantages over the original source of bone marrow (Gimble et al., 2007, Zuk et al., 2001). Adipose tissue is easily available in sufficient amounts because of the high abundance of fat in the human body as well as it is often considered as surgical waste in plastic surgery. In addition, adipose tissue obtained by liposuction or excision is associated with little pain and accepted as a safe procedure (Fraser et al., 2006). Moreover, the ASC isolation process can be handled fast and simple with an enormous yield of approximately 2×10^5 cells per gram adipose tissue (Hass et al., 2011). The isolation procedure is based on an enzymatic digestion involving collagenase type I, resulting in the so-called stromal vascular fraction (SVF). The SVF is a highly heterogeneous cell population including ASCs but also endothelial progenitor cells, pericytes or macrophages. ASCs can be selected from the SVF by their ability of plastic adherence (Gimble et al., 2007). One factor being important for the identification and

characterization of ASCs *in vitro* is their cell surface protein profile. Several different marker profiles are being considered as relevant to specifically identify ASCs facing tremendous variations between studies as the surface expression changes as a function of time in passage and plastic adherence (Cawthorn et al., 2012). However, distinct expression patterns were repeatedly shown in various studies, such as $CD34^+$, $CD105^+$ and $CD45^-$ (Dominici et al., 2006). In addition, ASCs are typically verified by their trilineage differentiation potential into osteocytes, chondrocytes and adipocytes (Zuk et al., 2001).

Although the discovery of ASCs in adipose tissue itself is fascinating, the presumption that ASCs could influence fibrotic processes gathered even more attention in the field of regenerative medicine (Schaffler and Buchler, 2007). Indeed, several *in vitro* and *in vivo* studies reported on regenerative effects of ASCs. For instance, injection of ASCs into a rabbit ear model reduced scarring (Zhang et al., 2015). Another study reported on enhanced wound healing in a diabetic nude mice model with ischemic wounds (Kim et al., 2011). Interestingly, an *in vitro* study demonstrated beneficial effects of ASCs on wound healing in fibroblasts via secretory factors (Kim et al., 2007). Although many promising cell-based and animal studies exist that report on positive effects of ASCs, however, well-designed randomized placebo-controlled clinical trials are still missing (van Dongen et al., 2018). This is aggravated by the fact that ASC administration provides many variations, with options that ASCs being cultivated before injection, the usage of the whole SVF or lipografts such as fragmented adipose tissue being transferred. To date, two clinical trials studied for instance the injection of cultured ASCs into patients with non-healing ischemic ulcers (Bura et al., 2014, Lee et al., 2012). After 6 months, 66.7% of patients showed indeed a positive response rate to ulcer healing (Lee et al., 2012). Even if the data obtained so far are promising, however, the mode of action of ASCs in these reports is still unclear and so is the question if ASCs are the only cell type promoting regenerative processes or if other cellular components of the adipose tissue, such as adipocytes, might play a role as well.

1.2.2. Adipogenesis: from ASCs to Adipocytes

The differentiation of ASCs into adipocytes is a complex, multi-step process involving various transcriptional events. Adipogenesis is widely seen as a two-phase procedure with the first phase being described as the determination phase. Here, ASCs are committed to the adipocyte lineage resulting into the conversion of preadipocytes. Preadipocytes are phenotypically not distinguishable from ASCs but lost their potential to differentiate into other cell lineages (Cawthorn et al., 2012). In the second, terminal phase, preadipocytes acquire characteristic adipocyte features presenting a lipid-laden mature adipocyte at the end of this process (Farmer, 2006). Interestingly, the terminal phase of adipogenesis is more extensively characterized than determining factors due to the existence of well-

established cell line models such as the mouse lines 3T3-L1 and C3H10T1/2 or human preadipocytes, which are all already committed to the adipocyte lineage (Rosen et al., 2002).

Overall, adipogenesis is regulated by a comprehensive network of transcriptional activators leading to the expression of hundreds of proteins involved in establishing the mature adipocyte phenotype. At the centre of this network, there are two groups of transcription factors monitoring the differentiation process: peroxisome proliferator-activated receptor gamma (PPARɣ) and CCAAT/enhancer-binding proteins (C/EBPs) (**Fig. 6**). PPARɣ, in particular, is considered as the master regulator of adipogenesis with being both necessary and sufficient for differentiation (Rosen et al., 1999).

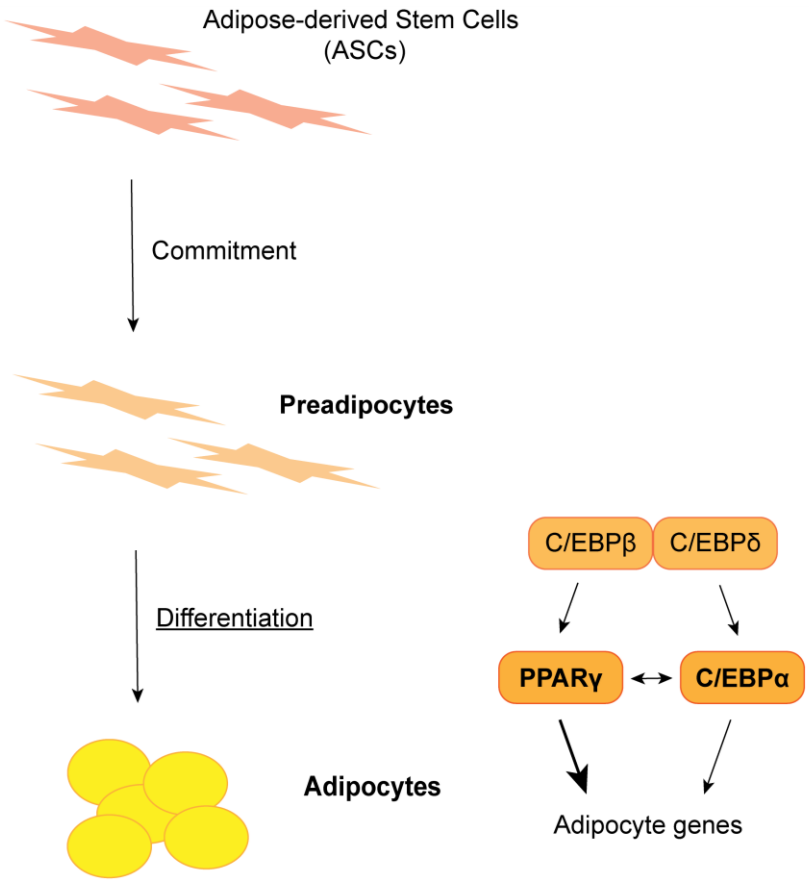

Fig. 6: Schematic overview of adipogenesis with a focus on the differentiation of preadipocytes into adipocytes.
After adipose-derived stem cell (ASC) commitment to preadipocytes, a complex differentiation process into adipocytes is initiated. The two central transcription factors are peroxisome proliferator-activated receptor (PPAR)ɣ and CCAAT/enhancer-binding protein CEBPα which are activated by various factors such as CEBPβ, CEBPδ, Krüppel-like factors (KLFs) and Sterol regulatory element-binding protein-1 (SREBP1)c, subsequently leading to the activation of adipocyte genes.

Indeed, forced PPARɣ expression is sufficient for adipocyte formation and no factor has been discovered so far that promotes adipogenesis in the absence of PPARɣ (Rosen et al., 1999). In concordance with these findings, almost all pro-adipogenic factors seem to function by activating PPARɣ. Furthermore, important signaling pathways in adipogenesis converge on the level of increased PPARɣ expression or activity. PPARɣ belongs to a nuclear receptor superfamily and must therefore heterodimerize with another nuclear hormone receptor (the retinoid X receptor, RXR) in order to bind DNA and induce the transcription of target genes (Tontonoz et al., 1994a). Interestingly, PPARɣ is expressed in two isoforms, due to alternative splicing, with PPARɣ1 being expressed in almost all tissues whereas PPARɣ2 is almost exclusively found in adipose tissue (Rosen et al., 1999). Studies demonstrated that both isoforms can induce adipogenesis but PPARɣ2 plays a major role in insulin sensitivity since PPARɣ2 deficient mice were shown to be insulin resistant (Kubota et al., 1999). PPARɣ has been linked to the induction of FABP4 as well as other adipocyte-specific genes such as adiponectin or perilipin. As for all nuclear receptors, PPARɣ is a ligand-activated transcription factor. A wide variety of natural endogenous ligands and synthetic agonists exists such as thiazolidinediones (TZDs), synthetic agents commonly used in anti-diabetic therapies. Endogenous ligands for PPARɣ include eicosanoids, as for instance the prostanoid 15-deoxy-Δ12,14-prostaglandin-J2 (15dPGJ2) or arachidonic acid derivates such as 15-hydroxy-eicosatetraenoic acid (15-HETE) (Lecka-Czernik et al., 2002). Also, natural fatty acids like linoleic acid, eicosapentaenoic acids, nitrolinoleic acid and LPA belong to known PPARɣ ligands (Tontonoz et al., 1994b).

The other important group of transcription factors, C/EBPs, belong to the basic leucin-zipper class of transcription factors with six different isoforms that have been described, all of which need homo- or heterodimerization with a leucin zipper domain for activation (Darlington et al., 1998). Several factors are known to interplay with C/EBP regulation, for example cyclic adenosine monophosphate (cAMP), a well-known inducer of adipogenesis mediating increased expression of C/EBPα and β. Various gain- and loss-of-function studies revealed the crucial role of this group of transcription factors during adipogenesis (Wu et al., 1999). Especially C/EBPα came into the focus of researchers since ectopic expression of C/EBPα was demonstrated to trigger fat cell formation in fibroblastic cells (Freytag et al., 1994), whereas C/EBPα knockout mice died quickly after birth due to their inability to produce glucose (Wang et al., 1995). Interestingly, C/EBPα can not induce adipogenesis in the absence of PPARɣ while PPARɣ was shown to drive the adipogenic program in C/EBPα-deficient mouse embryonic fibroblasts (Rosen et al., 2002). These observations demonstrate the determinant role of both PPARɣ and C/EBPα, though PPARɣ seems to be the dominant factor. Naturally, the events leading to the expression of both players were

further studied and it is now established that there is a cascade of transcription factors leading to their expression. Here, two other members of the C/EBP family have an impact, C/EBPβ and δ. In more detail, C/EBPβ and δ seem to be expressed earlier in adipogenesis than C/EBPα, as shown by the group of McKnight. They demonstrated C/EBPα induction by ectopic expression of C/EBPβ and δ in 3T3-L1 preadipocytes (Cao et al., 1991, Yeh et al., 1995). Here, however, a link to PPARɣ induction was not investigated but a high number of other studies revealed the involvement of C/EBPs in PPARɣ production (Wu et al., 1995, Wu et al., 1996, Christy et al., 1991, Clarke et al., 1997). These days, it is widely accepted that C/EBPβ and ɣ induce PPARɣ expression which leads to C/EBPα production (Lin and Lane, 1994, Tontonoz et al., 1994b). Nonetheless, adipogenic differentiation does not only depend on C/EBPs and PPARγ but is a complex network of different factors, as depicted in **Fig. 6**. In addition to C/EBPs and PPARγ other factors such as SREBP1c or the Krüppel-like family (KLFs) are vital for adipogenic differentiation (Oishi et al., 2008, Li et al., 2005, Kim and Spiegelman, 1996).

Although the transcriptional control of adipogenesis is extremely well characterized, less is known about ASCs and their preadipocyte commitment. One outstanding factor influencing adipocyte commitment is the zinc-finger protein 423 (Zfp423), as shown by Gupta and coworkers (Gupta et al., 2010). They reported an increased expression of PPARɣ in non-adipogenic NIH-3T3 fibroblasts after ectopic expression of Zfp423. Interestingly, they linked Zfp423-induced PPARɣ expression to the activity of bone morphogenetic proteins (BMPs), members of the TGF-β superfamily. Indeed, BMPs have been considered as pro-adipogenic factors before, especially BMP-2 and -4. BMP-4 treatment, for instance, led to an augmented PPARɣ expression in C3H10T1/2 cells and enhanced their adipogenesis, subsequently (Tang et al., 2004). As shown in **Fig. 7**, BMP-2 and BMP-4, as well as other members of the BMP family, exert their function through binding to hetero-oligomeric receptor complexes consisting of BMP type I (BMPR1) and type II (BMPR2) receptors leading to phosphorylation and thus, activation of Smad1, 5 and 8 (Heldin et al., 1997). For BMP-2, binding of the Smad1/4 complex to the PPARγ2 promotor upon BMP-2 stimulation was shown (Sottile and Seuwen, 2000). How Smads exert these effects remains elusive. Remarkably, Zfp423 contains a Smad binding site and is considered as a Smad coactivator thereby mediating the proadipogenic impact of BMPs (Hata et al., 2000). Notably, another zinc-finger protein, Schnurri-2, also directly binds to Smad1/4 following BMP-2 stimulation, ultimately inducing PPARɣ expression (Jin et al., 2006). Despite BMP-2 and -4, BMP-7 is a known pro-adipogenic factor of the BMP family, although related to brown adipogenesis, since an increased UCP-1 expression was observed in C3H10T1/2 cells following BMP-7 treatment (Tseng et al., 2008).

Even though the interest for a better understanding of adipogenesis is growing, there are even more efforts undertaken in finding anti-adipogenic factors due to increasing health issues originating from obesity. For instance, Wnt (wingless/integrated) signaling is known as a molecular switch, that, when activated, represses adipogenesis (Ross et al., 2000). This was shown especially by the group of MacDonald who performed an overexpression of Wnt1 in 3T3-L1 preadipocytes showing to inhibit adipogenesis (Ross et al., 2000, Bennett et al., 2002). This inhibition was linked to a blocked induction of both PPARγ and C/EBPα.

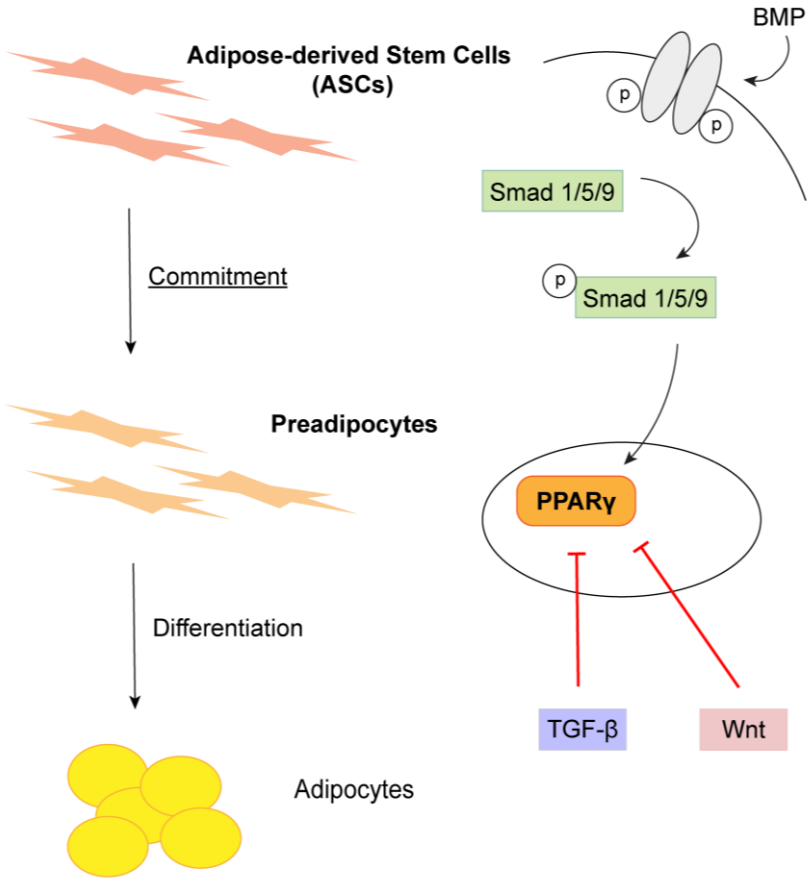

Fig. 7: Commitment to the adipocyte lineage.
The commitment of adipose-derived stem cells (ASCs) to the adipocyte lineage is so far not completely understood. Bone morphogenetic proteins (BMPs) are known pro-adipogenic factors that exert their signals through BMP receptor complexes thereby activating Smad 1/5/9 leading to peroxisome proliferator-activated receptor (PPAR)ɣ induction. In contrast to that, transforming growth factor (TGF)-β as well as Wnt signaling are known pathways inhibiting PPARɣ-mediated adipogenesis.

In the context of anti-adipogenic influences, again, also TGF-β signaling must be mentioned, playing a key part (Choy and Derynck, 2003). Considering the complexity of the adipogenic developmental system, it is somewhat not surprising that TGF-β superfamily members can have mixed effects on adipogenesis. Interestingly, not only BMPs hold a key

part in adipogenesis but also the TGF-β/Activin family. In 3T3-L1 cells for instance, TGF-β treatment inhibited adipogenic conversion (Ignotz and Massague, 1985). After first indications of an interplay between TGF-β and PPARγ, further studies were conducted addressing this relationship. One interesting study dealing with skin biopsies of SSc patients, an autoimmune disease of the connective tissue associated with high levels of TGF-β, demonstrated a reduced PPARγ expression (Wei et al., 2010). Further insights revealed an inverse correlation between pronounced TGF-β activity, for instance by the high mRNA expression of the TGF-β target PAI-1, and impaired PPARγ-regulated gene signature, thereby indicating a reciprocally antagonistic relationship between PPARγ and TGF-β signaling in fibrosis (Wei et al., 2010). Therefore, the counteracting factors of TGF-β signaling as one of the main fibrotic elements and PPARγ, the master regulator of adipogenesis, give first indications for a correlation between fibrotic scar tissue and anti-fibrotic adipose tissue. Interestingly, the application of fat injections into wound areas and fibrotic lesions revealed promising results with regard to tissue regeneration and scar appearance. Further insights into the underlying mechanism of the observed changes following fat grafting could also provide new concepts for the relationship between PPARγ and TGF-β.

1.2.3. Autologous Fat Grafting

Historically, the use of fat transfer can be traced back to the year 1793 with the work of Neubert who first harvested fat from a patient's arm to fill a soft tissue defect in his cheek caused by tuberculosis (Billings and May, 1989). Over the years, more and more reports about autologous fat grafting came up but often included negative observations due to fat reabsorption. It was not until the work of Coleman, whose procedure is still referred to as the gold standard for fat grafting, that results became more reliable (Coleman, 1995). The Coleman technique is based on an initial lipoaspiration step followed by centrifugation of the fatty tissue and its reinjection. Although this technique is still considered as the standard procedure, it has undergone several modifications to improve adipocyte survival. Generally, there are plenty of possible ways for autologous fat grafting because of minor or rather major variations of Coleman's work. Depending on the surgeon's experience and preferences, fat collection can be performed by vacuum aspiration, syringe aspiration or surgical excision (Bellini et al., 2017). Also, fat processing prior to re-injection can comprise some modifications. Fat processing is necessary since the lipoaspirate consists not only of adipocytes but contains collagen fibers, blood and debris which could cause inflammation at the recipient's site. Therefore, the tissue is often sedimented, washed and centrifuged for graft preparation (Cleveland et al., 2015). In addition, there is no consensus on the best technique for fat re-injection, especially when it comes to the choice of cannula diameter

being used for optimal cell viability (Kakagia and Pallua, 2014). Besides all these technical variations, less deliberations are queried for potential applications of fat grafts. One field where autologous fat grafting has been widely used is reconstructive breast surgery. Here, lipofilling can be used for restoring the breast profile after mastectomy, for example. In most cases, lipofilling is combined with the usage of implants or muscle flaps with or without tissue expansion (Simonacci et al., 2017). However, one major difficulty plastic surgeons are still facing is the possibility for graft re-absorption with reports of 50-90% graft loss (Tremolada et al., 2010). Therefore, repeated lipotransfers are preferred for maximum take. In addition to reconstructive surgery, another important field of fat graft application is aesthetical surgery, mainly focussing on facial or hand rejuvenation since adipose tissue holds excellent filling properties (Rohrich and Pessa, 2007, Hoang et al., 2016).

Even more importantly, and as mentioned before, autologous fat grafting can be used for scar treatment, thus representing now one of the most favorable usages of adipose tissue in plastic surgery (Negenborn et al., 2016). In fact, fat transplantation can be used not only to fill atrophic scars but also to reduce scar contractures as a regenerative alternative to other surgical techniques. One of the first reports on the regenerative potential of fat grafting was presented by Rigotti et al., who showed improvements on human skin after treating radiation-induced skin lesions with fat injections (Rigotti et al., 2007) More promising studies emerged on the use of fat for scar treatment. For instance, a case series of three patients demonstrated significant improvement in burn scars following fat transplantation in 2008 (Klinger et al., 2008). Although more studies with intriguing outcomes on scar improvement appeared, most studies were small prospective or retrospective cohort and case studies leaving a demand for randomized, blinded and placebo-controlled studies. A more comprehensive study of Klinger and colleagues indeed demonstrated significant improvements in functionality and appearance of scar tissue (**Fig. 8**).

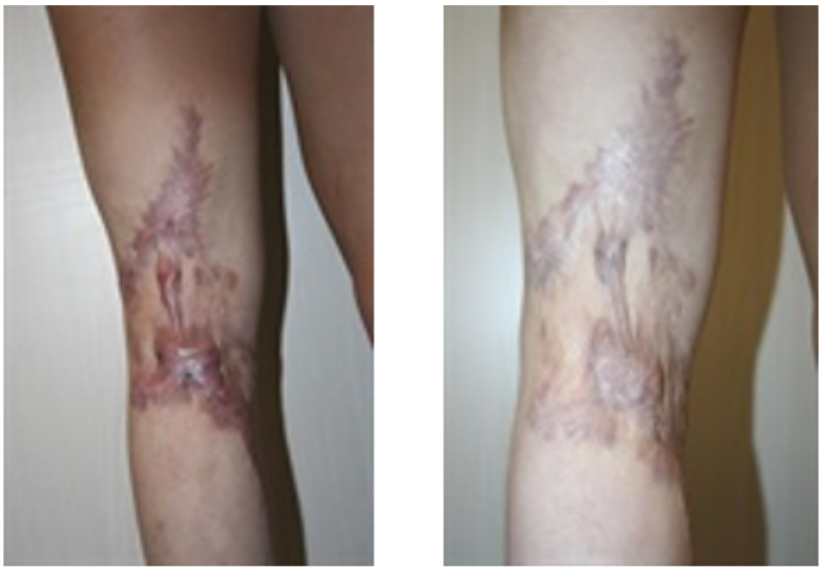

Fig. 8: Beneficial effects of autologous fat grafting.
Left: A hypertrophic scar covers a patient's leg thereby affecting its movement. Right: After autologous fat grafting, the treated tissue appears softer and less coloured. Also a reduction in scar hypertrophy is visible allowing for better leg movement. (Klinger et al., 2013)

In this study, 694 patients with painful and retractile scars were subjected to autologous fat grafting, where fat was injected according to the Coleman technique (Klinger et al., 2013). Notably, included scars derived from burn injuries, road trauma, domestic accidents or various surgery procedures. As a result, pain relief and an increased elasticity of the scarred area was reported in all patients after fat injection. These effects were already observed after 14 days and were constant after 1-year follow-up. Another important observation was a regain of mobility in the treated areas such as joints, eyelids or nasal valve. In addition, histological improvements were observed with new collagen deposition, local hypervascularity and dermal hyperplasia. More generally speaking, treated areas regained characteristics similar to normal skin or in other words, scars became less different from normal skin and less visible.

The exact mechanism by which autologous fat grafting improves scar tissue remains unclear (Fredman et al., 2017), even if there is a wide range of speculations implicating paracrine effects by one or more cellular components of adipose tissue (Kim et al., 2007, Spiekman et al., 2014). For a better understanding of the mode of action of autologous fat grafting, further insights into the interaction between scar tissue and adipose tissue are essential.

1.3. Aim of this thesis

About 100 million patients each year are affected by abnormal scarring after surgery (Sund and Arrow, 2000). Patients dealing with hypertrophic scars or keloids suffer from severe long-term functional and psychological issues. Therefore, there is an unmet clinical need for an effective, targeted therapy and prevention, which would be based on an action or a modulation of a particular factor with clarified mechanism of action that has a beneficial effect on those fibrotic conditions (Hoerst et al., 2019). Notably, the injection of adipose tissue into scarred areas reveals promising results with improved scar characteristics, however, little is known about the underlying mechanisms and cell types involved. Therefore, this thesis aims to unravel the crosstalk between cells of adipose tissue and connective tissue. There are several interesting points this study would like to draw attention to: on the hand, clarification would be necessary in relation to the mode of action of adipose tissue. Here, inter alia, the cellular component being responsible for the observed regenerative effect upon fat grafting needs to be identified. So far, mainly ASCs were studied for their regenerative potential, but adipocytes with their diverse characteristics would present promising candidates as well. Moreover, the actual mediator being released or transmitted from adipose tissue cells needs to be determined. On the other hand, further studies on the observed changes scar tissue undergoes following fat injection are required. What happens to the myofibroblast in this fibrotic tissue? Although it was always believed that myofibroblasts undergo apoptosis after tissue repair, increasing evidence suggests alternative ways for myofibroblasts disappearance, such as re- or trans-differentiation processes. Which intracellular pathways and molecular switches are involved in this regeneration? Those complex and crucial points will be addressed by establishing a co-cultivation between ASCs or adipocytes on the one hand and myofibroblasts or hypertrophic scar fibroblasts on the other hand. Since myofibroblasts' fate following fat grafts is of great interest in this study, myofibroblasts will be analyzed for their characteristic attributes as well as for intracellular changes with the TGF-β network being in the focus.

Answers or even promising indications to the raised questions could help to develop strategies to specifically and ultimately inhibit myofibroblast formation. Altogether, deeper insights about the cellular crosstalk between adipose and connective tissue may contribute to improved treatment options for abnormal scars as well as their prevention. In addition, with a better understanding of skin scarring further insights into the (patho-)physiological process of wound healing and other fibrotic diseases could be gained.

MATERIALS AND METHODS

2.1. Materials

2.1.1. Reagents

β-glycerophosphate	Sigma-Aldrich, Munich, DE
Acrylamide	Sigma-Aldrich, Munich, DE
Alcian Blue	Sigma-Aldrich, Munich, DE
Alizarin Red S	Sigma-Aldrich, Munich, DE
Ammonium persulfate (APS)	Sigma-Aldrich, Munich, DE
Ascorbate-2-phosphate	Sigma-Aldrich, Munich, DE
Bone Morphogenetic Protein (BMP)-4	Miltenyi Biotec, Bergisch-Gladbach, DE
Bovine Serum Albumin (BSA)	Carl Roth, Karlsruhe, DE
Collagenase I	Worthington, Lakewood, NJ, US
DAPI Mounting Medium	Dianova Hamburg, DE
Dexamethasone	Sigma-Aldrich, Munich, DE
Dispase II	Roche Diagnostics, Mannheim, DE
Dithiothreitol (DTT)	Sigma-Aldrich, Munich, DE
DMEM	Sigma-Aldrich, Munich, DE
DMEM/F12	Sigma-Aldrich, Munich, DE
Dimethylsulfoxide (DMSO)	Carl Roth, Karlsruhe, DE
Eosin G	Carl Roth, Karlsruhe, DE
Ethanol absolute	Merck, Darmstadt, DE
Ethanol 96%	Erkel AHK, Berlin, DE
Goat serum	Dianova, Hamburg, DE
GW9662	Sigma-Aldrich, Munich, DE
Hank’s Buffered Salt Solution	Life Technologies, Darmstadt, DE
Hematoxylin	Carl Roth, Karlsruhe, DE
Fetal Bovine Serum	Biochrom, Berlin, DE
IBMX	Life Technologies, Darmstadt, DE
Insulin	Roche, Grenzach-Wühlen, DE
LDN-193189	Sigma-Aldrich, Munich, DE
L-Glutamine	Sigma-Aldrich, Munich, DE
Oil-Red-O	Sigma-Aldrich, Munich, DE
Penicillin/Streptomycin	Sigma-Aldrich, Munich, DE
Phosphate Buffered Saline (PBS)	Sigma-Aldrich, Munich, DE
Protease/Phosphatase Inhibitor Cocktail	Cell Signaling, Massachusetts, US

Roti®-Histofix	Carl Roth, Karlsruhe, DE
Roti®-Histokit	Carl Roth, Karlsruhe, DE
Roti®-Histol	Carl Roth, Karlsruhe, DE
Sodium chloride (NaCl)	Carl Roth, Karlsruhe, DE
Sodium hydroxide (NaOH)	Sigma-Aldrich, Munich, DE
TEMED	Carl Roth, Karlsruhe, DE
Tissue Freezing Medium	Leica Biosystems, Nussloch, DE
Transforming Growth Factor-Beta1 (TGF-β1)	Miltenyi Biotec, Bergisch-Gladbach, DE
Tris	Carl Roth, Karlsruhe, DE
Trypsin/EDTA	Sigma-Aldrich, Munich, DE
Tween-20	Carl Roth, Karlsruhe, DE

2.1.2. Cell Culture Media

Fibroblast Basal Medium (FBM)	DMEM supplemented with: 1 % penicillin/streptomycin 1 % L-glutamine
Fibroblast Growth Medium (FGM)	FBM supplemented with: 7.5 % FBS
ASC Growth Medium	DMEM/F12 supplemented with: 10 % FBS 1 % penicillin/streptomcyin
Adipocyte Differentiation Medium	ASC Growth Medium supplemented with: 1 µM dexamethasone 0.5 mM IBMX 10 µg/mL insulin

2.1.3. Kits

Pierce® BCA Protein Assay Kit	Thermo Fisher Scientific, Schwerte, DE
SignalFire™ ECL reagent	Cell Signaling, Frankfurt/Main, DE
NE-PER Nuclear and Cytoplasmic Extraction	Thermo Fisher Scientific, Schwerte, DE
BMP 2,4,6,7 Elisa Kit	Thermo Fisher Scientific, Schwerte, DE
InnuPREP RNA Mini Kit	Analytik Jena, Jena, DE
iScript cDNA Kit	Bio-Rad, Munich, DE

iTaq™ Universal SYBR® Green Supermix Kit	Bio-Rad, Munich, DE
Cell proliferation Elisa, BrdU Kit	Roche, Basel, Switzerland
Glycerol-3-Phosphate Dehydrogenase (G3PDH) Assay Kit	Abcam, Cambridge, UK

2.1.4. Antibodies

Rabbit anti-β-Tubulin	CST, Massachusetts, US	1:1000 in 5% (w/v) milk
Rabbit anti-α-Smooth Muscle Actin	Novus Biologicals, Minneapolis, US	1:1000 in 5% (w/v) milk
Mouse anti-β-Actin	Abcam, Cambridge, UK	1:10.000 in 5% (w/v) milk
Rabbit anti-Collagen I	Abcam, Cambridge, UK	1:1000 in 5% (w/v) milk
Rabbit anti-Collagen III	Abcam, Cambridge, UK	1:1000 in 5% (w/v) milk
Rabbit anti-PPARɣ	CST, Massachusetts, US	1:1000 in 5% (w/v) milk
Rabbit anti-Histone H3	CST, Massachusetts, US	1:1000 in 5% (w/v) milk
Rabbit anti-GAPDH	CST, Massachusetts, US	1:1000 in 5% (w/v) milk
Rabbit anti-Phospho-p42/44 MAPK (Erk1/2)	CST, Massachusetts, US	1:1000 in 5% (w/v) BSA
Rabbit anti-p44/42 MAPK (Erk1/2)	CST, Massachusetts, US	1:1000 in 5% (w/v) BSA
Rabbit anti-Phospho-SAPK/JNK	CST, Massachusetts, US	1:1000 in 5% (w/v) BSA
Rabbit anti-SAPK/JNK	CST, Massachusetts, US	1:1000 in 5% (w/v) BSA
Rabbit anti-Smad 2/3	CST, Massachusetts, US	1:1000 in 5% (w/v) BSA
Rabbit anti-Phospho-Smad2/Smad3	CST, Massachusetts, US	1:1000 in 5% (w/v) BSA
Rabbit anti-Phospho-Smad1/Smad5/Smad 9	CST, Massachusetts, US	1:1000 in 5% (w/v) BSA
Anti-Rabbit IgG, HRP-linked	CST, Massachusetts, US	1:10.000 in 5% (w/v) milk
Anti-Mouse IgG, HRP-linked	CST, Massachusetts, US	1:10.000 in 5% (w/v) milk
PE anti-human CD34	BioLegend, California, US	5 µl/10^6 cells
FITC anti-human CD105	Miltenyi Biotec, Bergisch-Gladbach, DE	5 µl/10^6 cells
PE anti-human CD45	Miltenyi Biotec, Bergisch-Gladbach, DE	10 µl/10^6 cells
PE IgG1	BioLegend, California, US	5 µl/10^6 cells

IgG Alexa Fluor®488	Abcam, Cambridge, UK	1:400 in PBS
IgG Alexa Fluor®594	Abcam, Cambridge, UK	1:400 in PBS

2.1.5. Primer

Adiponectin	5’ AGGGTGAGAAAGGAGATCC 5’ GGCATGTTGGGGATAGTAA
α-SMA	5’ TGGGCTCTGTAAGGCCGGCT 5’ TCACCCCCTGATGTCTGGGACG
CEBPα	5’ TGGACAAGAACAGCAACGAGT 5’ CAGGCGGTCATTGTCACTGG
Collagen 1 (Col1)	5’ CCTCAAGGGCTCCAACGAG 5’ TCAATCACTGTCTTGCCCCA
Collagen 3 (Col3)	5’ GATCAGGCCAGTGGAAATGT 5’ GTGTGTTTCGTGCAACCATC
Fibronectin	5’ GGTGACACTTATGAGCGTCCTAAA 5’ AACATGTAACCACCAGTCTCATGTG
Id1	5’ CTGCTCTACGACATGAACGGC 5’ TGACGTGCTGGAGAATCTCCA
Leptin	5’ TGCATTCCCAGTGGTCAAAC 5’ TGCATTTGGCTGTTCAGCTG
PPARγ	5’ ATGGAGTTCATGCTTGTGAAGGA 5’ TGCAAGGCATTTCTGAAACCG
ZNF423	5‘ CCAAATCCACGTTGCCAACCA 5‘ TGCTCAATGAGGTGACAGAGGAG
GAPDH	5’ CTCTCTGCTCCTCCTGTTCGAC 5’ TGAGCGATGTGGCTCGGCT

2.1.6. Software

ImageJ, Version 1.46r	National Institute of Health, MD, US
GraphPad Prism	GraphPad Software, La Jolla, CA, US
STRING database, Version 11.0	https://string-db.org/
WinMDI software, Version 2.8	Scripps Institute, La Jolla, CA, US

2.1.7. Consumables

Blotting Pads	VWR, Pennsylvania, US
Cell Culture Inserts Falcon®, 3 µm pore size	Corning, Amsterdam, NL
Cell Culture flasks (75 cm², 150 cm²)	TPP, Melbourn, UK
Cell culture plates (10 cm)	TPP, Melbourn, UK
Cell strainer (70 + 100 µm)	Sigma-Aldrich, Munich, DE
Centrifuge tubes (15, 50 mL)	Sarstedt, Nürnbrecht, DE
Cover slips	Gerhard Menzel, Braunschweig, DE
Embedding molds	Sigma-Aldrich, Munich, DE
Forceps	Carl Roth, Karlsruhe, DE

Hard-Shell 480 PCR Plates	Bio-Rad, Munich, DE
Multiwell cell culture plates (6, 12, 96-well)	VWR, Pennsylvania, US
Nitrocellulose membrane	Bio-Rad, Munich, DE
Nitril gloves	Hansa-Trading HTH, Hamburg, DE
Parafilm	Carl Roth, Karlsruhe, DE
PCR grade tubes	Sarstedt, Nürnbrecht, DE
PCR stripes	Carl Roth, Karlsruhe, DE
Pipette tips (10, 100, 1000 µL)	Sarstedt, Nürnbrecht, DE
Pipette tips with filter (10, 100, 1000 µL)	Sarstedt, Nürnbrecht, DE
Polylysine slides	Gerhard Menzel, Braunschweig, DE
Scalpels	Carl Roth, Karlsruhe, DE
Serological pipettes (5, 10, 25 mL)	Sarstedt, Nürnbrecht, DE
Syringes	Carl Roth, Karlsruhe, DE
Syringe filters (0.45 µm)	Sarstedt, Nürnbrecht, DE

2.1.8. Devices

Autoclave V Series	Systec, Wettenberg, DE
Balance XS205 dualRange	Mettler-Toledo, Giessen, DE
Centrifuge, Eppendorf Centrifuge 5415 C	Eppendorf AG, Hamburg, DE
Centrifuge, Megafuge 1.0 R	Heraeus, Hanau, DE
CO_2 Incubator	Heraeus, Hanau, DE
CO_2-free Incubator	Heraeus, Hanau, DE
Cryotome Leica CM1510 S	Leica Biosystems, Nussloch, DE
Digital camera, EOS 1000D	Canon
FACSCalibur	BD Biosciences, San Jose, CA, US
Fluorescence microscope BZ-8000	Keyence, Neu-Isenburg, DE
FLUOstar Optima	BMG Labtech, Ortenberg, DE
LaminAir HB 2472	Heraeus, Hanau, DE
LightCycler 480	Roche, Mannheim, DE
Microscope, phase contrast Axiovert 135	Carl Zeiss, Jena, DE
Mini-PROTEAN Tetra System	Bio-Rad, Munich, DE
Mr. Frosty	Thermo Fisher Scientific, Waltham, UK
Neubauer cell counting chamber	Carl Zeiss, Jena, DE
PCR thermo cycler, Tgradient	Biometra, Jena, DE
pH meter 766	Knick, Berlin, DE
Pipettes (10, 100, 1000 µl)	Eppendorf, Hamburg, DE
PXi/PXi Touch gel imaging system	Syngene, Cambridge, UK

Trans-Blot Turbo Blotting System	BioRad, Munich, DE

2.2. Methods

2.2.1. Cell Culture

2.2.1.1. Dermal Fibroblast Isolation & Differentiation

Primary human fibroblasts were isolated from juvenile foreskin following circumcision (approved by the ethics committee of the Charité–Universitätsmedizin Berlin, Germany, EA1/081/13). Therefore, juvenile foreskins were washed in PBS, minced into 3 cm thick pieces and placed in a dispase solution (1,2 U/ml dispase in PBS) overnight at 4 °C. The next day, the epidermis was separated from the dermis by using forceps. Subsequently, the dermis pieces were placed in a 6-well cell culture plate and cultivated in Dulbecco's modified Eagle's medium (DMEM, Sigma-Aldrich, Munich, Germany) supplemented with 7.5% FBS, 2 mM L-glutamine, 100 units/ml penicillin and 100 µg/mL streptomycin. Cultures were maintained at 37 °C in a humidified atmosphere containing 5% CO2. After one week in culture, the dermis pieces were removed and the outgrown fibroblasts sub-cultivated when confluent. Fibroblasts in passage 1 were trypsinized, resuspended in DMEM supplemented with 10% dimethyl sulfoxide (DMSO) and frozen until needed for further experiments. For every experiment, cells (passage 2-3) from three different donors were pooled. To generate myofibroblasts, fibroblasts were serum-starved for 72h followed by 96h of stimulation with 10 ng/ml TGF-β1.

2.2.1.2. 3D Cultivation of Myofibroblasts

Primary human fibroblasts were trypsinized and adjusted to a concentration of $2*10^6$ cells/ml in FBS. Collagen type I was mixed with Hank's Buffered Saline Solution (HBSS) followed by pH neutralization with 1 M NaOH. Subsequently, the cell suspension was combined with the collagen solution in a 1:1 ratio and poured into a cell culture insert (3 µm pore size) for 6-well plates with a growth area of $4.2cm^2$. Upon gel solidification, fibroblast growth medium was added, the system transferred to an incubator with 5% CO_2 and 95% humidity and the medium changed every second day. After a cultivation period of 7 days, medium was supplemented with 10 ng/ml TGF-β for 72h. Subsequently, models were serum starved for 24h or incubated with conditioned medium (CM) from adipocytes.

2.2.1.3. Hypertrophic Scar & Keloid Fibroblast Isolation

Isolation of fibroblasts from hypertrophic scars and keloids as well as their cultivation was conducted in the lab of Prof. Dr. Susan Gibbs at the Department of Molecular Cell Biology and Immunology at Vrije Universiteit Medical Center (VUmc), Amsterdam, Netherlands. Hypertrophic scars and keloid fibroblasts were isolated from skin samples of patients undergoing scar removal via excision. The discarded scar tissue was used in anonymous fashion in compliance with the VU University Medical Center's ethical guidelines and the "Code for Proper Use of Human Tissues" in accordance with the Dutch Federation of

Medical Scientific Organizations (see www.fmwv.nl). Scarred tissue was washed in PBS, minced into pieces of 0.5 cm² and placed on gauze soaked with dispase II solution (1U/ml in PBS). Following overnight incubation at 4 °C, the dermis was separated from the epidermis by using forceps. Subsequently, dermis pieces were incubated in a dispase II/collagenase II solution (10 mg/ml, 2.5 h, 37 °C) with manually shaking every 15 minutes. After a first filtration using a drip chamber (Beldico, Marche-en-Famenne, Belgium), cell solutions were filtered again by using cell strainers (100 µm and 70 µm). After centrifugation (5 min, 4 °C, 300 *g*), cells were counted and cultures were maintained in DMEM, containing 7.5% FBS, 100 units/ml penicillin and 100 µg/mL streptomycin (37 °C, 5% CO_2) and used for experiments in passages 2-3.

2.2.1.4.ASC Isolation

Adipose-derived stem cells (ASCs) were isolated from adipose tissue obtained from breast reconstruction and abdominal plastic surgeries (approved by the ethics committee of the Charité–Universitätsmedizin Berlin, Germany, EA2/121/15, with patient's consent). Adipose tissue was washed in PBS, minced and incubated with a collagenase mix composed of 1 mg/ml collagenase type I, 4% BSA and 1% penicillin/streptomycin for 50 min at 37 °C under agitation. Every 10 min tubes were shaken manually. The cell suspension was then passed through 100-µm and 70-µm strainers, centrifuged (300 g, 5 min) and seeded in DMEM/F12 supplemented with 10% FBS, 100 units/ml penicillin and 100 µg/mL streptomycin. A medium change was performed the following day to remove debris. For induction of adipogenesis, ASCs inpassage 2-3 were further cultivated in DMEM/F12 supplemented with 10% FBS, 10 µg/mL insulin, 1 µM dexamethasone, 0.5 mM IBMX, and 1% penicillin/streptomycin for 14 days.

2.2.1.5. Conditioned Medium Preparation

For CM preparation, ASC and induced adipocytes were used in passage 2-3 and grown until confluence. To obtain conditioned medium (CM) from ASCs and adipocytes, cells were cultivated and differentiated as described previously. After washing in PBS, ASC and adipocyte culture media were replaced with serum-free media for 24h to avoid FBS contamination. Subsequently, CM was collected, centrifuged and stored at -80 °C until further use.

2.2.1.6. Incubation with Conditioned Medium

Confluent cell layers of myofibroblasts or fibroblasts isolated from hypertrophic scars were washed twice with PBS and then incubated with CM from either ASCs or adipocytes. Following 24h, cells for harvested and used for subsequent analysis. Myofibroblasts cultured in standard serum-free medium served as the control.

2.2.1.7. Transwell and Direct Co-Culture Cultivation

ASCs were seeded on a cell culture insert (3 µm pore size, PET membrane, Corning, Amsterdam, Netherlands) with a growth area of 4.2 cm^2 in a 6-well cell culture plate and cultivated either in adipogenic differentiation medium or ASC growth medium for 14 days. In parallel, fibroblasts were differentiated into myofibroblasts (see 0) in a 6-well plate. Upon completed differentiation, the cell culture insert seeded with ASCs or adipocytes was transferred onto the 6-well plate pre-seeded with myofibroblasts. After 24h, myofibroblasts were harvested for further analysis.

The direct co-culture was achieved by differentiating ASCs into adipocytes in a 6-well cell culture plate. After 14 days of cultivation, equal amount of myofibroblasts were added for 24h. Myofibroblasts as well as adipocytes alone served as a control.

2.2.1.8. Inhibition Studies

Inhibition studies using two different antagonists were performed with the PPARγ inhibitor GW9662 (1 µM) or the BMP receptor type I antagonist LDN-193189 (200 nM). GW9662 is an irreversible antagonist that binds to the ligand binding site of PPARɣ thereby inhibiting its activity. The dorsomorphin derivate LDN-193189 on the other hand is a highly selective to the BMP receptor type I thereby inhibiting signaling through this pathway. Monolayers of myofibroblasts and hypertrophic scar fibroblasts were pretreated either with 1 µM GW9662 or 200 nM LDN-193189 for 30 min followed by 24 h incubation with CM from adipocytes. Cells cultured in serum-free medium served as the control.

2.2.2. Trilineage Differentiation of ASCs

2.2.2.1. Adipogenic Differentiation

ASCs were subjected to the adipogenic differentiation (see details above) cocktail for 14 days. In particular, dexamethasone is a glucocorticoid that functions as an inducer of C/EBPα. IBMX increases the intracellular cAMP concentration and insulin is known to mimic the insulin-like growth factor thereby activating PPARɣ. To verify the presence of *in vitro* differentiated adipocytes, lipid droplets were visualized by the lipophilic dye Oil Red O. The cells were washed with PBS followed by fixation in 4% PFA for 10 min. After an additional washing step, cells were incubated in 0.5% Oil Red O staining solution for 30 min. Adipocytes were then washed in water until staining solution was removed and imaged with a phase contrast microscope (Axiovert 135, Carl Zeiss, Jena, DE).

2.2.2.2. Osteogenic Differentiation

Osteogenesis was encouraged by cultivating ASCs for 14 days in differentiation medium containing 10% FBS, 0.1 µM dexamethasone, 50 µM ascorbate-2-phosphate and 10 mM β-glycerophosphate. Successful differentiation was verified by calcium depositions

visualized by Alizarin Red staining. Cells were washed, fixed and incubated with 40 mM Alizarin Red staining solution for 20 min. Following washing, cells were imaged with a phase contrast microscope (Axiovert 135, Carl Zeiss, Jena, DE).

2.2.2.3. Chondrogenic Differentiation

For chondrogenic induction, ASCs were cultivated using the micromass technique. Since chondrocytes rapidly lose their phenotype in culture, specific conditions need to be created to form chondrocytes from precursor cells. Therefore, a high-density cultivation is necessary resulting in cell condensation and subsequently, ECM deposition (Archer et al., 1985). Micromasses were achieved by pipetting 10 µl of cell suspension containing 100,000 ASCs into wells of a 6-well cell culture plate. After 2 h, ASC growth medium was added. 24h later, the culture medium was switched to chondrogenic differentiation medium containing 1% FBS, 6.25 µg/mL insulin, 10 ng/mL TGF-β1 and 50 nM ascorbate-2-phosphate. After 14 days, chondrogenic differentiation was verified by Alcian Blue staining. Alcian Blue stains acidic polysaccharides such as glycosaminoglycans in cartilages.

2.2.3. Western Blot

For the investigation of various target protein concentrations in myofibroblasts, treated cells were washed in ice-cold PBS. Subsequently, myofibroblasts were lysed in radioimmunoprecipitation assay (RIPA) buffer for 30 min on ice, harvested and centrifuged (13,000 g, 30 min, 4 °C). Protein concentration was calculated using the Pierce® BCA Protein Assay Kit. Subsequently, 20 µg of protein lysate was prepared for sodium dodecyl sulfate polyacrylamide gel electrophoresis (SDS-PAGE). SDS-PAGE separates proteins according to their molecular mass based on their different migration rate through a gel under the influence of an electrical field. Since proteins with the same molecular weight would migrate differently depending on their charge and 3D structure, SDS is used. SDS is a detergent that, together with heat, disrupts the tertiary structure of proteins and coats the proteins with a negative charge. Therefore, samples were diluted in standard SDS-PAGE sample buffer supplemented with 100 mM dithiothreitol (DTT) and boiled at 95 °C. DTT is a reducing agent that breaks down protein-protein disulfide bonds. In parallel, gels were prepared for SDS-PAGE (see Table 1).

Table 1: Running and Stacking gel composition for SDS-PAGE.

	dH_2O	**Acrylamid**	**Gel buffer**	**SDS (10%)**
Running Gel	4.1 ml	3.3 ml	2.5 ml 2 M Tris (pH 8.8)	0.1 ml
Stacking Gel	6.1 ml	1.3 ml	2.5 ml 0.5 M Tris (pH 6.8)	0.1 ml

After mixing components, 50 µl ammonium persulfate (APS) and 10 µl TEMED were added to the running gel for polymerization and quickly poured into gel cassettes. Following running gel solidification, the stacking gel was added, and an appropriated comb was inserted. Protein samples were now subjected to SDS-PAGE (150 mV, 60-90 min). After separation, proteins were transferred onto nitrocellulose membranes (0.45 µm pore size) using a semi-dry transfer system (Bio-Rad, Munich, DE). Therefore, gel and membrane together with blotting pads were layered in a transfer cassette. By applying electrical load (200 mA, 30 min), the negatively charged proteins transfer onto the membrane. Subsequently, the membrane was blocked in Tris-buffered saline containing 0.1% Tween-20 (TBST) supplemented with 5% skimmed milk powder or 5% BSA for 1h at room temperature to reduce the amount of unspecific binding of proteins. The membrane was further incubated with primary antibodies, targeting the protein of interest, diluted in 1:1000 in TBST with 5% skimmed milk at 4 °C overnight (see 2.1.4.). Following washing in TBST, anti-rabbit or anti-mouse horseradish peroxidase (HRP)-conjugated secondary antibodies were applied for 1h at room temperature. The blots were washed again, developed using SignalFire™ (Enhanced ChemiLuminescent) ECL reagent and visualized with a PXi/PXi Touch gel imaging system. Due to the interaction of the ECL substrate with the HRP-conjugate a signal is generated reflecting the amount of target protein in the sample. Immunoblotting quantification was performed using ImageJ software. ImageJ was applied to analyze protein expression via densitometry. Target protein intensity was compared to that of the loading control (β-Actin or β-Tubulin).

2.2.4. Cellular Subfractionation

To separate the nuclear and cytoplasmic fractions of myofibroblasts, an NE-PER Nuclear and Cytoplasmic Extraction Reagents Kit was used. Prior to cellular subfractionation, myofibroblasts were stimulated with adipocyte-CM for 24h or maintained in serum-free medium (control). Subsequently, the cells were trypsinized and centrifuged (500 g, 3 min), and the cell pellets were further processed according to the manufacturer’s instructions.

2.2.5. Enzyme-linked Immunosorbent Assay (ELISA)

In order to analyze a potential BMP secretion of ASCs and adipocytes into CM, various sandwich ELISAs were performed. Therefore, collected CM from ASCs and adipocytes were analyzed by using human BMP 2, 4, 6 and 7 ELISA Kits according to the manufacturer's instructions. Here, 96-well plates have been pre-coated with a target-specific antibody. Subsequently, samples or standards are applied and bind to the immobilized antibody. An additional, secondary antibody is used to generate a measurable signal. This HRP-linked antibody binds to the target-sample complex and thus, the intensity

of the signal, measured at a wavelength of 562nm, directly reflects the amount of target protein.

2.2.6. Histology

For histological analysis, myofibroblast 3D models were embedded in tissue freezing medium, shock-frozen with liquid nitrogen and subsequently cut into vertical sections (7 µm) using a cryotome (Leica Microsystems, Wetzlar, DE). Sections were then stained with hematoxylin and eosin (HE) in order to study their cellular structure. Hematoxylin stains nuclei blue whereas eosin colors eosinophilic structures such as the cytoplasm. First, sections were fixed in 4% formaldehyde. Subsequently, sections were processed as shown in Table 2.

Table 2: Technical procedure of HE staining.

Solution	Application period [min]
double-distilled H_2O	0.5
Mayer's hemalum solution	5
tap water	5
Eosin G solution	0.5
Ethanol 96% I	2
Ethanol 96% II	2
Ethanol 100% I	2
Ethanol 100% II	2
Roti®-Histol I	2
Roti®-Histol II	2

2.2.7. Immunofluorescence

In order to detect and localize α-SMA in myofibroblasts incorporated in the collagen matrix, cryosections were processed for immunofluorescence staining. Here, sections were fixed with 4% formaldehyde, blocked with normal goat serum (1:20 in PBS) and incubated overnight at 4 °C with primary antibodies (in PBS, 0.0025% BSA, 0.025% Tween 20, see 0). Subsequently, slides were incubated for an additional hour at room temperature with secondary antibodies (1:400 in PBS, 0.0025% BSA, 0.025% Tween 20). Afterwards, the sections were embedded in DAPI mounting medium and analysed by fluorescence microscopy (BioZero, Keyence, Neu Isenburg, DE).

2.2.8. Flow Cytometry

For verification of the ASC phenotype, the presence of the ASC-specific surface markers CD34 and CD105 and the hematopoietic stem cell marker CD45 was assessed via flow cytometry. Therefore, 100.000 ASCs in P0, P3 or P7 were trypsinized, washed and centrifuged (300 g, 5 min). After resuspension in binding buffer (PBS + 2mM EDTA + 0.5% BSA) and centrifugation, cells were incubated with FITC-linked antibodies (CD45 and CD105) or PE-linked (CD34) in binding buffer for 10 min on ice, respectively, as well as with an IgG1 isotype control (HRP-linked). Cell were assessed via flow cytometry with FACSCalibur (BD, New Jersey, US). Cell debris was excluded by forward and side scatter gating. Data were analyzed using WinMDI software (Version 2.8).

2.2.9. Annexin V/Propodium Iodide (PI) Staining

To exclude any potential apoptotic effects of adipocyte-CM on myofibroblasts, an Annexin V/PI staining was performed. Annexin V binds to phosphatidylserine residues that appear on the cell surface as an early event in apoptosis. PI, in contrast, is dye that is normally impermeable for the cell membrane of viable cells but intercalates with the DNA of damaged cells. Myofibroblast were either incubated with CM from adipocytes or serum-free medium. As a positive control, cells were treated with 10% DMSO. After 24h, myofibroblasts were detached and centrifuged (300 g, 5 min). Subsequently, myofibroblasts were resuspended in binding buffer (PBS + 2mM EDTA + 0.5% BSA). After an additional centrifugation, 5 µl Annexin V-FITC in 195 µl binding buffer were added and cells incubated for 10 min at 4 °C. Myofibroblast were washed, centrifuged and again resuspended in binding buffer. Prior to analysis, 10 µl PI were added. Cells were assessed via flow cytometry with FACSCalibur (BD, New Jersey, US). After excluding debris by scatter gating, cells were gated for the two fluorophores Annexin V-FITC (FL1) and PI (FL2). Data were analyzed using WinMDI software (Version 2.8).

2.2.10. Glycerol-3-Phosphate Dehydrogenase (GPDH) Assay

As an additional evaluation of adipocyte characteristics, a GPDH assay was performed (by Patrick Graff, supervised diploma student). Following 14 days of adipogenic differentiation, GPDH activity of the cells was measured using the Glycerol-3-phosphate dehydrogenase (G3PDH) assay kit according to the manufacturer’s instructions. GPDH is an enzyme that catalyzes the conversion between dihydroxyacetone phosphate and glycerol-3-phosphate in lipid biosynthesis. The colorimetric assay measures the oxidation of NADH to NAD during this reaction.

2.2.11. Real-time Quantitative Polymerase Chain Reaction (qPCR)

For gene expression analysis, initially, RNA needed to be extracted from cells. Therefore, confluent cell layers were washed in PBS prior to 5 min incubation in RNA lysis buffer (from the InnuPREP RNA Mini Kit, Analytik Jena, Jena, Germany). After transfer of the lysed cell suspension to RNAse-free tubes, the RNA was isolated according to the manufacturer's instructions. Prior to qPCR analysis, RNA samples needed to be converted into complementary DNA (cDNA) by using the retroviral enzyme reverse transcriptase. For cDNA synthesis, the iScript cDNA Kit (BioRad, Munich, DE) was used. Subsequently, qPCR samples were prepared using an iTaqTM Universal SYBR® Green Supermix Kit. The qPCR was performed using the LightCycler 480 (Roche, Mannheim, DE). The qPCR approach and the running protocol are listed in **Table 3**. For analysis of gene expression data, the relative quantification approach was used. Here, the obtained Cp-values are normalized to the housekeeping gene as a reference (glyceraldehyde-3-phosphate dehydrogenase, GAPDH).

Table 3: Components and cycling conditions for qPCR

qPCR reaction volume containing:		**Cycling conditions**		
		Temperature [°C]	Duration [sec]	Cycle number
PCR water	2 µl	95	300	1 ×
Forward primer (10 µM)	0.5 µl	95	10	45 ×
Reverse primer (10 µM)	0.5 µl	60	10	
SYBR green master mix	5 µl	72	10	
Sample volume	2 µl	95	10	1 ×
		65	60	
		40	10	
		4	indefinite	

2.2.12. Bromodeoxyuridine (BrdU) Assay

To assess potential effects of CM-incubation on the myofibroblast's proliferation, the proliferation of *in vitro* differentiated myofibroblasts was measured. Following 24h incubation with adipocyte-CM, proliferation was analyzed by using the cell proliferation

Elisa, BrdU Kit according to the manufacturer's instructions. This assay is based on the measurement of bromodeoxyuridine incorporation during DNA synthesis of cycling cells.

2.2.13. Scratch Assay

The scratch assay is a very basic wound healing assay where a “wound” is created in a cell monolayer by scratching. After the scratch, cell migration and growth towards the gap is monitored. First, myofibroblast were grown in 6-well cell culture plates and after reaching confluency, the monolayer was scratched across the center of the well by using a 200 µL pipet tip. Following scratching, cells were washed, and serum free or conditioned medium from adipocytes was applied. Images were taken at 0h and 24h by using a phase contrast microscope (Axiovert 135, Carl Zeiss, Jena, DE).

2.2.14. Contractility Assay

In order to measure their contractility, myofibroblasts were embedded in a collagen gel. Therefore, *in vitro* differentiated myofibroblasts were generated, trypsinized and mixed with a collagen type I solution to a final concentration of 1 mg/mL. Subsequently, the gel solution was poured into a 6-well cell culture plate and left for solidification for 20 min at room temperature. Carefully, gels were dissociated from the well by gently running the tip of a 200 µl tip. 600 µl serum free or conditioned medium were added for 24h. Diameter change of gels was recorded using a digital camera (Fujifilm X 20, Fujifilm, Tokyo, JP)) from a fixed distance above the gel. Contraction was quantified by calculating the gel surface area using ImageJ.

2.2.15. DigiWest®

For an in-depth analysis of myofibroblast protein expression, the high-throughput DigiWest® analysis was performed. Therefore, myofibroblasts were stimulated with adipocyte-CM or serum-free medium for 24h. Subsequently, cells were washed twice in ice-cold PBS, detached and then centrifuged at 4 °C (2 min, 13,000 g). This description of the DigiWest® protein profiling procedure as well as its realization was conducted by NMI TT Pharmaservices as described previously (Treindl et al., 2016, Hoerst et al., 2019). Briefly, SDS-PAGE and Western blotting onto PVDF membranes was performed using the NuPAGE system (Life Technologies, Darmstadt, Germany). Blots were washed in PBS containing 0.1% Tween-20 (PBST). The proteins were biotinylated on the membrane using NHS-PEG12-Biotin in PBST and then washed in PBST and dried. Each sample lane was sliced into 96 fractions of 0.5 mm each, and the proteins were eluted in 96-well plates using elution buffer (8 M urea, 1% Triton-X100 in 100 mM Tris-HCl, pH 9.5). The eluted proteins from each molecular weight fraction were loaded onto one distinct color of neutravidin-coated MagPlex beads (Luminex Corporation, Texas, USA) and pooled afterwards. A total of 10 µg of protein per cell sample was used for 96 different antibody incubations. Aliquots

of the DigiWest® bead mixes were added to 96-well plates containing assay buffer (Blocking Reagent for ELISA (Roche, Penzberg, Germany)) supplemented with 0.2% milk powder, 0.05% Tween-20 and 0.02% sodium azide. After the assay buffer was discarded, diluted primary antibodies were added (see Appendix, **Table 6**). Following overnight incubation, bead mixes were washed twice with PBST, and phycoerythrin-labeled diluted secondary antibodies were added. Beads were washed twice, and assay results were measured on a Luminex FlexMAP 3D system. Antibody-specific signals were quantified using the DigiWest® data analysis tool to identify the peaks of correct molecular weight and to calculate peak areas. For comparative analyses between the samples, protein expression values were normalized to the total protein amount.

2.2.16. Mass Spectrometry

Liquid chromatography/electron spray ionization mass spectrometry (LC/ESI–MS) was performed by Dr. Oliver Klein (Charité-Universitätsmedizin Berlin) as described previously (Becker et al., 2018, Hoerst et al., 2019). Also, the description of this method section was provided by Dr. Oliver Klein. Briefly, 1 ml of CM from three independent donors (A, B, C) was rebuffered in Amicon® Ultra centrifugal filters with 0.11 mM CHAPS (0.05 M Tris –HCL (pH 7.5) / 0.05 M KCL, 20% glycerin), 8 M urea/0.1 M/Tris-HCL (pH 8.5) and 50 mM ammonium bicarbonate (ABC, Sigma-Aldrich, Munich, Germany) to a finale volume of 40 µl. Subsequently, 5 0 µl of 0.2 µg/µL trypsin (Promega, Mannheim, Germany) in 50 mM ABC was added and incubated with the sample overnight at 37 °C. Peptides were extracted with 60 µl of 0.1% TFA and directly analyzed by LC/ESI–MS. Peptide separation was performed (2-60% acetonitrile/ in 0.1% formic acid, flow rate 400 nl/min) using an analytical UHPLC system (Dionex Ultimate 3000 RSLC, Thermo-Fisher, Waltham, MA, USA) and analyzed with an ESI-QTOF mass spectrometer (Impact II, Bruker Daltonics, Billerica, MA, USA). Mass spectra were evaluated using MASCOT software (version number 2.2, Matrix Science, Boston, MA, USA) by automatically searching the SwissProt 51.9 database (553474 sequences; 198069095 residues, Cambridgeshire, UK). The MS/MS ion search was performed with the following set of parameters: (i) taxonomy, Homo sapiens (human) (20172 sequences); (ii) proteolytic enzyme, trypsin; (iii) maximum of accepted missed cleavages, 2; (iv) mass value, monoisotopic; (v) peptide mass tolerance, 10 ppm; (vi) fragment mass tolerance, 0.05 Da; and (vii) variable modifications, oxidation of methionine. Only proteins with scores corresponding to $p<0.05$ and with at least two independent peptides were considered. Visualization of protein interaction networks was performed with the String database using a high confidence interaction score (0.7) and experiments, databases, gene fusion and neighborhood as active interaction sources. GO enrichment

analysis was performed using the open access platform Term Finder with cellular component as the ontology aspect.

2.2.17. Statistical Analysis

Statistical tests were conducted by using the GraphPad Prism software (GraphPad Software, La Jolla, CA). The data from at least three independent experiments are presented as the means ± standard error of the mean (SEM). Significance was determined with a one-sample t-test followed by Bonferroni correction for multiple testing; *$p \leq 0.05$, and **$p \leq 0.01$. Each sample (CM ASC or CM adipocytes) was tested against the control but not against each other.

RESULTS

3.1. Generation & Characterization of ASCs and Adipocytes

First, the cultivation conditions for ASCs and *in vitro* differentiated adipocytes needed to be established. The adipose tissue from plastic surgery was either obtained as a lipoexcision or liposuction. Subsequently, cell isolation was performed by enzymatic digestion via collagenase type I followed by centrifugation resulting in the SVF. No difference was seen with regard to the cell yield when comparing liposuction and lipoexcision giving approximately 200,000 cells per gram tissue (**Fig. 9**).

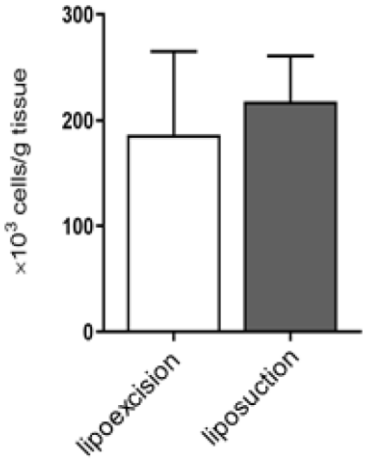

Fig. 9: Analysis of stromal vascular fraction yields from lipoexision or liposuction.
Adipose tissue was obtained from lipoexcision or liposuction and subsequently minced, subjected to collagenase digestion followed by centrifugation and counted. Data are represented as mean ± SEM, n = 4-6. Assay performed by P. Graff (supervised as a diploma student).

ASCs were then selected from the SVF by their plastic adherence and their identity was confirmed by verifying the high expression of the mesenchymal surface markers CD34 and 105 and low expression of the hematopoietic marker CD45 (**Fig. 10a**). Furthermore, their potential of trilineage differentiation into adipocytes, osteoblasts and chondrocytes (**Fig. 10b-d**) was successfully examined. Here, adipogenic differentiation of ASCs was verified by Oil Red O staining, osteogenic differentiation by Alizarin red staining and chondrocytes were stained with Alcian Blue. Effective differentiation after 14 days of cultivation in adipogenic differentiation medium was on the one hand verified by the presence of lipid droplets (**Fig. 11b**). On the other hand, *in vitro* differentiated adipocytes were analyzed for specific target gene expression as well as for their glycerol-3-phosphate dehydrogenase (GPDH) activity (**Fig. 11**).

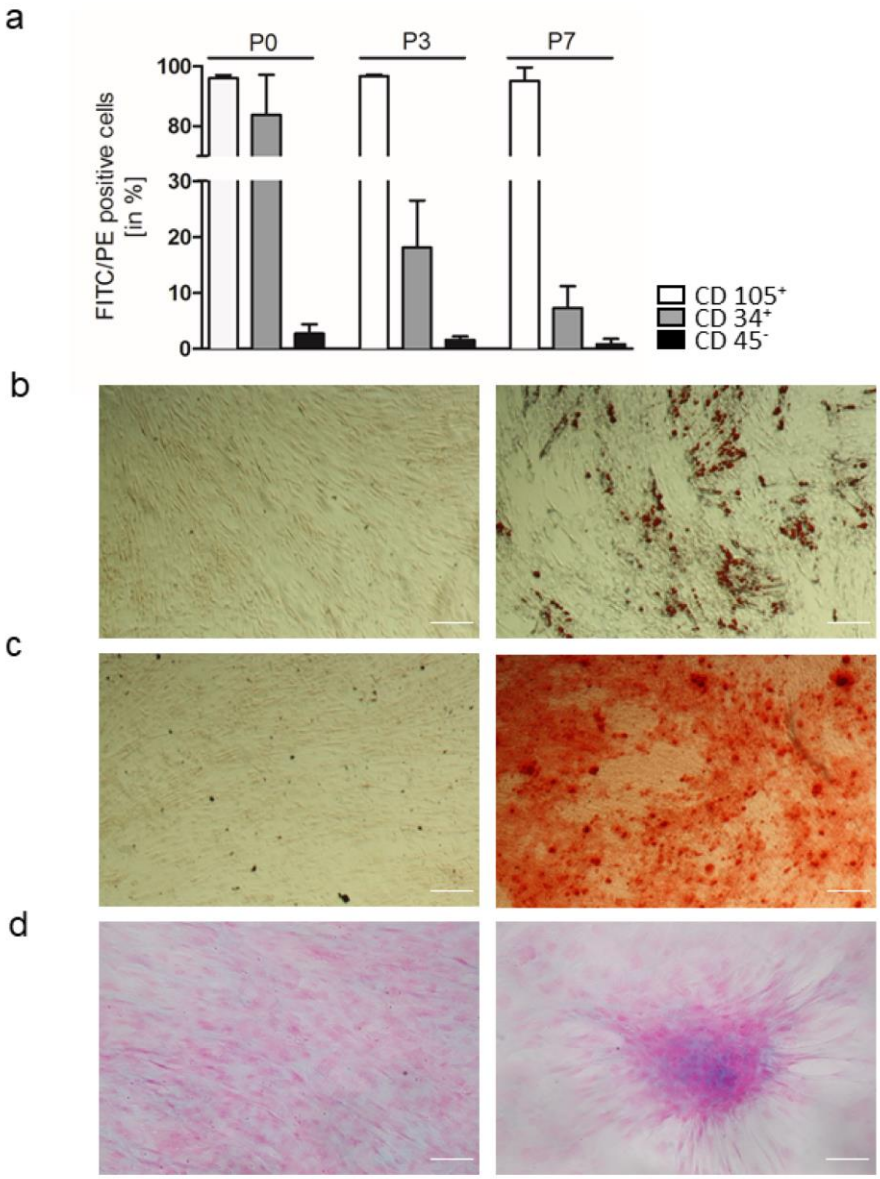

Fig. 10: Verification of adipose-derived stem cell (ASC) characteristics.
a) ASCs in passages 0, 3 and 7 were analysed by flow cytometry for the expression of characteristic surface markers (▭ CD 34, ▭ CD 105) and low expression of CD45 (■). Data are represented as mean ± SEM, n = 3-4. (b) Adipogenic differentiation of ASCs was verified by Oil Red O staining, (c) osteogenic differentiation by Alizarin Red staining and (d) chondrogenic differentiation by Alcian Blue staining. Control = DMEM/F12 + 10% FBS (left panel), differentiation (right panel). Scale bar = 100 µm. (Hoerst et al., 2019)

Notably, adipocytes revealed an increased gene expression for the transcription factors PPARγ and CEB/Pα and the adipogenic factors adiponectin and leptin compared to their precursors. Moreover, a significant increase in the GPDH activity was detected, an enzyme involved in lipid metabolism.

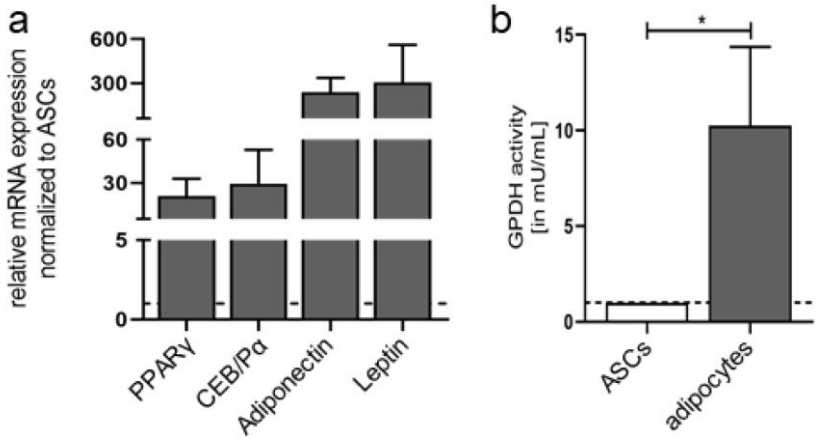

Fig. 11: Characterization of *in vitro* differentiated adipocytes.
Following 14 days of adipogenic differentiation relative mRNA levels for PPARγ, CEB/Pα, adiponectin and leptin were assessed (a) as well as the GPDH activity compared to ASCs (b). PPARγ = peroxisome proliferator-activated receptor gamma, CEB/Pα = CAAT enhancer binding protein alpha, ASCs = adipose-derived stem cells, GPDH = glycerol-3-phosphate dehydrogenase. Data are represented as SEM, n= 3. GPDH assay was performed by P. Graff (supervised as an diploma student).

3.2. Myofibroblast Generation & Characterization

For investigating potential effects of ASCs or *in vitro* differentiated adipocytes on scarring, an appropiate cellular system had to be found. Since the *in vitro* differentiation of fibroblasts into myofibroblasts by the addition of TGF-β1 is a common experimental design, this approach was chosen (**Fig. 12**).

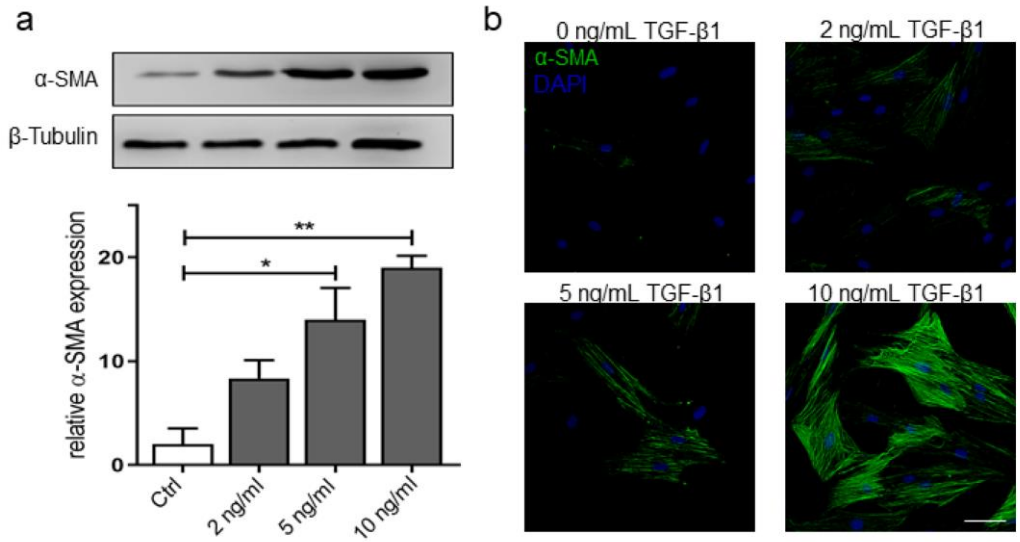

Fig. 12: Myofibroblast generation by TGF-β1 stimulation.
Human juvenile dermal fibroblasts were treated for 72h with TGF-β1 (2, 5, 10 ng/mL) and analyzed for *de novo* expression of α-SMA expression by Western Blot and immunofluorescence. (a) Representative Western Blot and semi-quantification by densitometry showing the α-SMA expression compared to β-Tubulin. (b) Representative immunofluorescence pictures after TGF-β treatment with α-SMA (green) and DAPI (blue). Scale bar = 50 µm. Ctrl = Control, α-SMA = alpha-smooth muscle actin, TGF-β1 = transforming growth factor beta 1. Data are presented as SEM, n=3.

First, the optimal cultivation conditions for the generation of myofibroblasts needed to be studied. By the addition of increasing concentrations of human recombinant TGF-β1 to juvenile dermal fibroblasts, an enhanced α-SMA expression was observed accordingly *(***Fig. 12***)*. More precisely, α-SMA protein expression was studied by Western Blot analysis and immunofluorescence. Interestingly, fibroblasts treated with 10 ng/ml TGF-β for 72h revealed an α-SMA positive phenotype with α-SMA being incorporated into stress fibers reflecting the myofibroblasts as a contractile smooth muscle-like cell type (**Fig. 12b**). Therefore, the condition with 10 ng/ml TGF-β1 for 72h was chosen as an optimal requirement for myofibroblast generation.

3.3. Co-cultivation of Adipocytes and Myofibroblasts

Following the establishment of optimal culturing conditions of ASCs and adipocytes as well as myofibroblasts, a suitable model for studying their crosstalk was required. Analyses of intercellular communications allow for the application of several co-culture techniques summarized in **Fig. 13**. The main difference between these conditions lies in the direct or in-direct contact of the cells. Within a direct co-culture, the cell membranes of two cell types are in direct contact thereby allowing the exchange of cellular components via distinct junctions in the cell membrane. In contrast to that, the use of conditioned medium or a transwell system enables the interaction via soluble factors thereby representing paracrine effects of the cells.

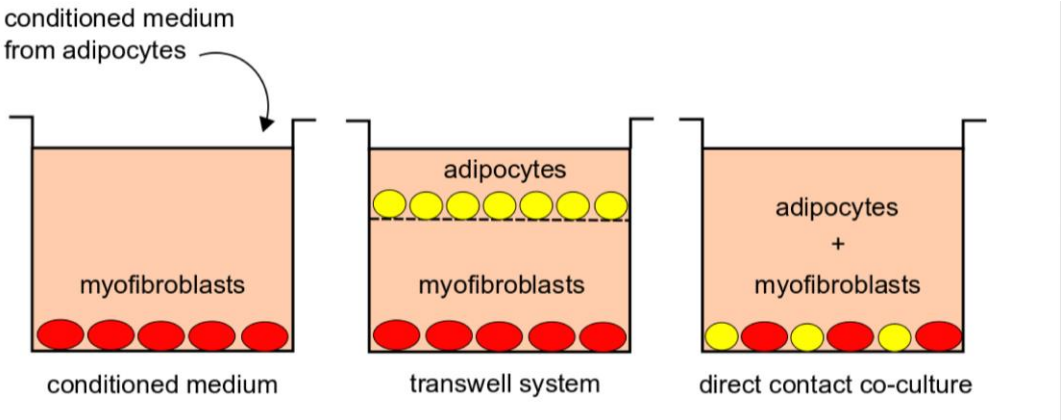

Fig. 13: Schematic overview of different co-culture approaches.
Myofibroblasts were grown as monolayers and stimulated by adipocytes via conditioned medium or in a transwell system. In addition, myofibroblasts were co-cultivated with adipocytes in a direct contact-coculture.

In this study, all three concepts were tested with myofibroblasts being exposed to co-cultures with either adipocytes or ASCs. (**Fig. 14**). As being the main target, myofibroblasts gene expression was examined after 24h exposure to CM from adipocytes, shared medium with adipocytes in a transwell system or after direct contact to adipocytes (**Fig. 14 a, b**).

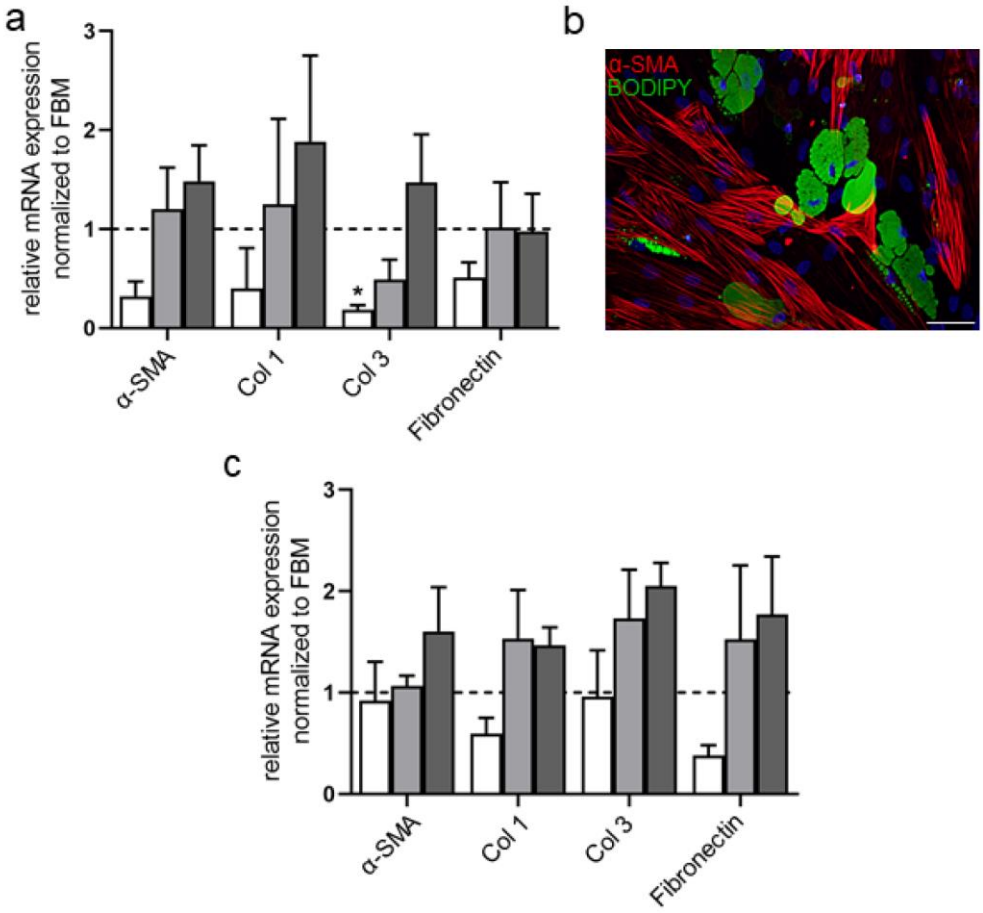

Fig. 14: Co-cultivation approaches of myofibroblasts with adipoytes or ASCs.
(a) Myofibroblasts were treated for 24h with adipocyte-CM ▭, cultivated in a transwell with adipocytes ▭ or exposed to adipocytes in a direct co-culture ▬ for 24h, and subsequently analyzed for their gene expression of α-SMA (alpha-smooth muscle actin), Col 1 (collagen 1), Col 3 (collagen 3) and fibronectin compared to GAPDH. Data were normalized to FBM (fibroblast basal medium, dotted line). (b) Immunofluorescence image of the direct co-culture with α-SMA (red), BODIPY (green), DAPI (blue). Scale bar = 50 µm. (c) Myofibroblasts were co-cultivated with adipose-derived stem cells (ASCs) with the same approaches as described in (a). Data are presented as SEM, n = 3.

Gene expressions for the ECM components collagen 1, collagen 3 and fibronectin were analyzed as well as the myofibroblast marker α-SMA. Interestingly, all genes showed a major decrease in their expression when CM was added but not in the presence of adipocytes in a transwell or in direct contact. When myofibroblasts were co-cultivated with ASCs, interestingly, the CM treatment induced a reduction in characteristic myofibroblasts gene expression as well but less distinct (**Fig. 14c**). After this initial screen, the CM approach was pursued for further testing.

3.4. Phenotypic Changes in Myofibroblasts following CM Exposure

For investigating CM-induced changes in myofibroblasts, myofibroblasts protein expression was studied for characteristic attributes including α-SMA and the ECM proteins collagen 1 and 3. Interestingly, incubation of myofibroblasts with adipocyte-CM for 24h resulted in significantly reduced expression of α-SMA (-29.5% ± 4.9%; **Fig. 15a**). Further, a clear trend towards reduced deposition of collagen 1 (-66.4% ± 16.4%; **Fig. 15c**, $p = 0.056$) and collagen 3 (-41.3% ± 17.1%; **Fig. 15e**, $p = 0.073$) was observed (Hoerst et al., 2019). Myofibroblast treatment with CM from ASCs also yielded in a decreased expression of those three proteins, however, not comparable to adipocyte-CM. Since myofibroblasts were generated *in vitro*, another cell source was included in the CM-studies which was directly obtained from scar tissue. Hence, fibroblasts from hypertrophic scars were isolated (at VUmc in Amsterdam, Netherlands, in cooperation with Prof. Dr. Susan Gibbs) and incubated with CM equally. In this case, the effect of adipocyte-CM was even more pronounced with a significantly downregulated expression for -SMA and collagen 3, and a clear tendency for reduced collagen 1 (**Fig. 15b** with - 80.5% ± 9,6%; **d** with - 61,7%; **f** with - 51.1% ± 9.6%). Notably, incubation with ASC-CM resulted again in less distinct effects (Hoerst et al., 2019).

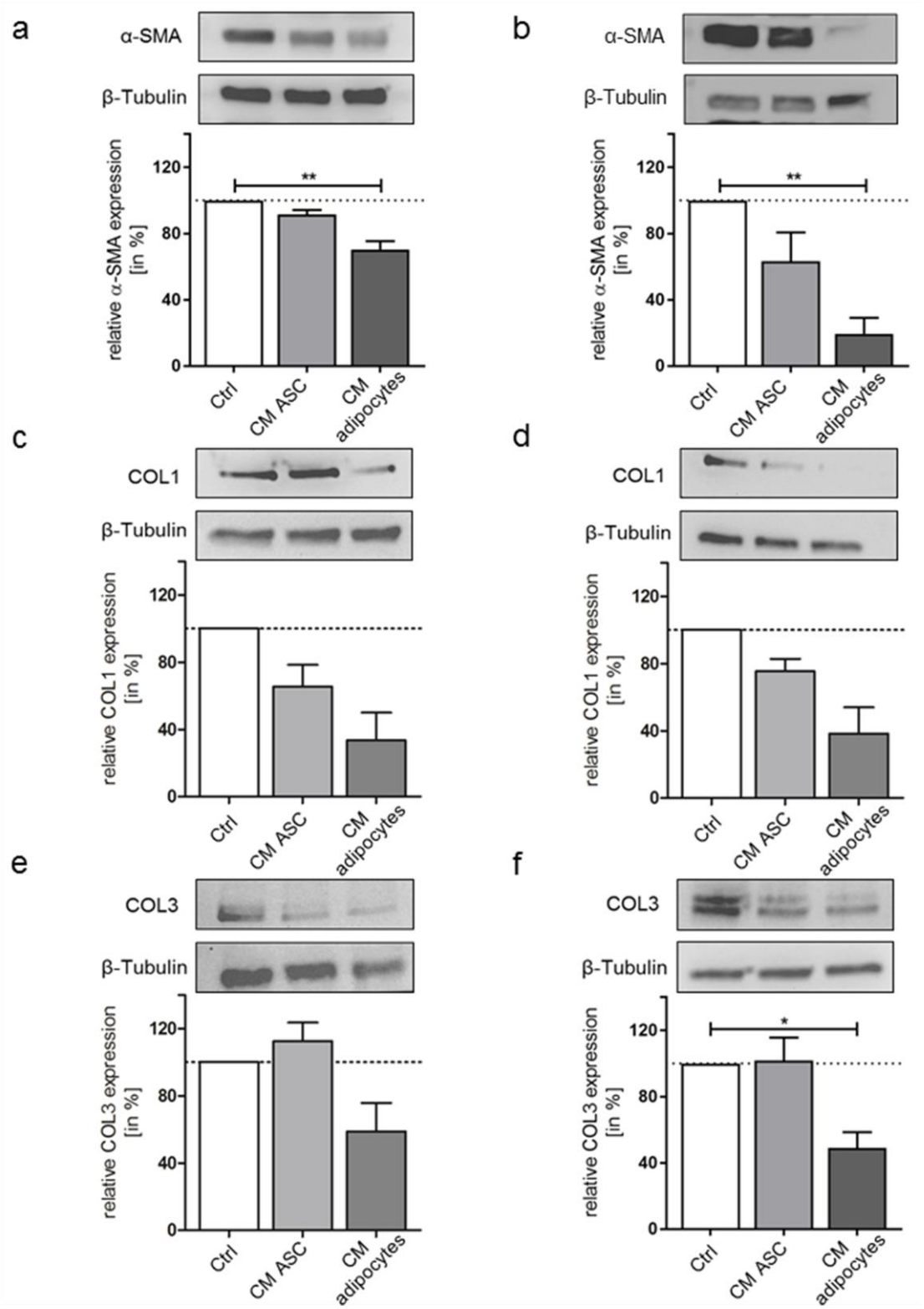

Fig. 15: **α-SMA expression is significantly downregulated in myofibroblasts and hypertrophic scar fibroblasts following incubation with adipocyte-CM.**
Representative Western blots and associated semi-quantification by densitometry showing the relative protein expression of α-smooth muscle actin (α-SMA), collagen 1 (COL1) and collagen 3 (COL3) in TGF-β-induced myofibroblasts (a, c, e) and hypertrophic scar fibroblasts (b, d, f) after exposure to conditioned medium (CM) from adipocytes and adipose-derived stem cells (ASCs). Ctrl = control, serum-free medium treatment. The data are presented as the mean ± SEM; n = 3-5 (*$p \leq 0.05$, and **$p \leq 0.01$). (Hoerst et al., 2019)

Since CM incubation resulted in a tremendous reduction of myofibroblast attributes, more features of those cells were investigated. Considering the contractile activity of myofibroblasts during wound healing, implementation of this parameter into the CM studies was inevitable. Therefore, myofibroblasts were seeded in a collagen matrix and stimulated with adipocyte-CM. Interestingly, myofibroblast contraction was reduced in the presence of adipocyte-CM (-37.8% ± 1.6%) indicating a reversal of this myofibroblast characteristic as well (**Fig. 16a, b**). However, myofibroblast proliferation and migration remained unaffected (**Fig. 16c, d**) (Hoerst et al., 2019).

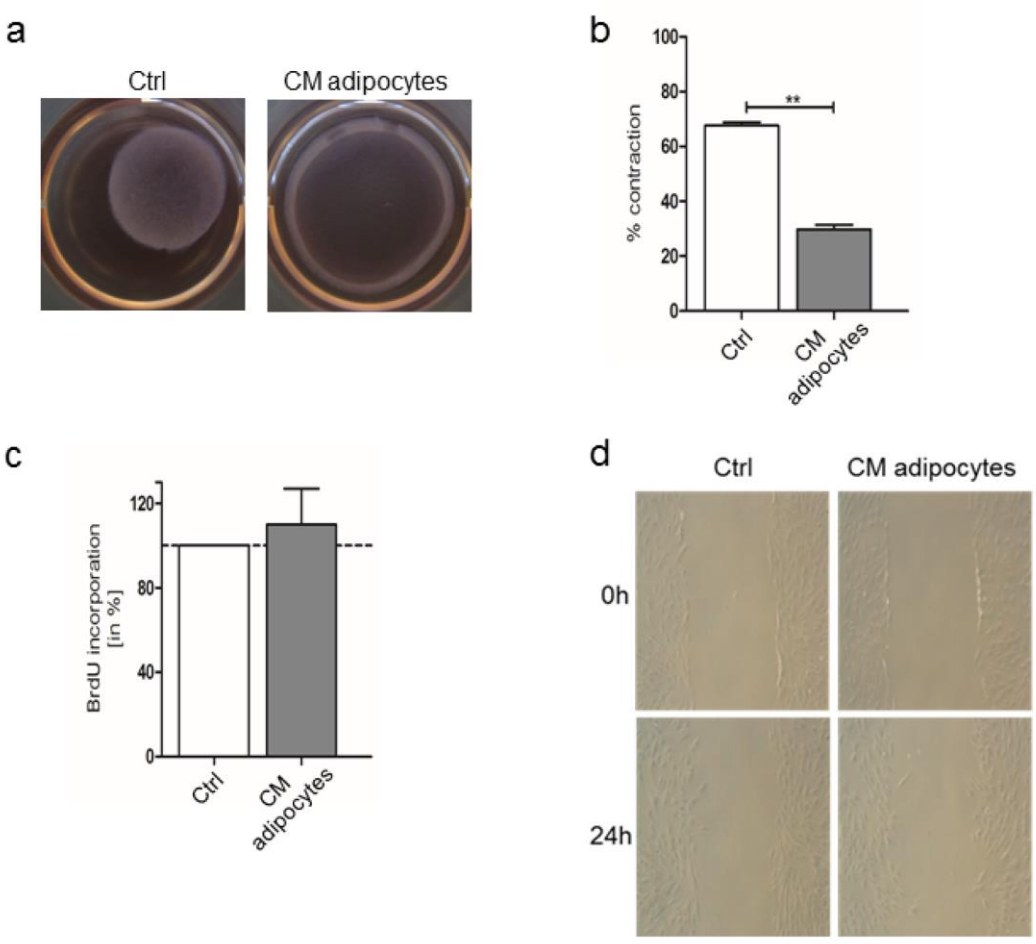

Fig. 16: Conditioned medium (CM) reduced myofibroblast contractility but did not affect myofibroblast proliferation or migration

(a) Representative images of in vitro differentiated myofbroblasts, 24 h after seeding in collagen gels on Ctrl (= control, serum-free) medium or adipocyte-conditioned medium (CM). (b) Contraction of gels represented as percentage of contraction compared to original volume. (c) Myofibroblast proliferation, assayed by BrdU incorporation, after 24 h incubation with control or conditioned medium from adipocytes. (d) Representaive images of myofibroblast migration following scratching and CM-treatment for 24h. The data are presented as the mean ± SEM, n = 3-4 (**p ≤ 0.01). (Hoerst et al., 2019)

Additional to characteristic myofibroblast features, potential side effects of adipocyte-CM on cell viability were considered. Therefore, an Annexin V staining for the detection of apoptotic cells and a propidium iodide (PI) staining for potential necrosis was performed (**Fig. 17**). Myofibroblasts cultured on basal medium (95.79%) or with adipocytes-CM (95.87%) were both still viable and, hence, an induction of cell death triggered by adipoyte-CM could be excluded.

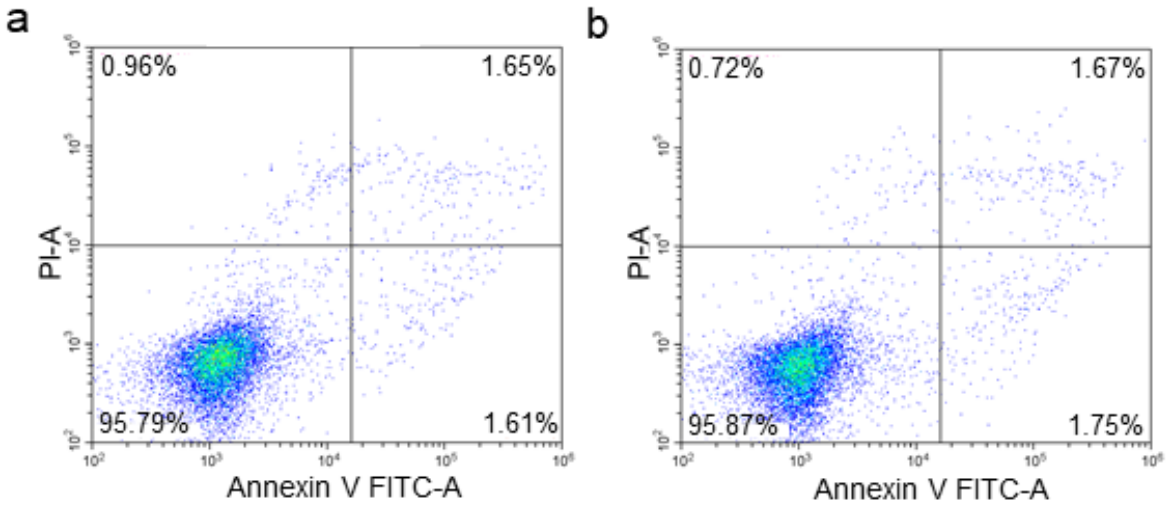

Fig. 17: Myofibroblasts treated with adipocyte-CM were negative for Annexin V/PI staining. *In vitro* generated myofibroblasts were left untreated (a) or subjected to conditioned medium (CM) from adipocytes (b) followed by Annexin V/PI staining and flow cytometry analysis. Annexin V FITC-A vs Propidium Iodide-A (PI-A) plots from show the populations corresponding to viable and non-apoptotic (Annexin $V^{-}PI^{-}$, left lower), early (Annexin $V^{+}PI^{-}$, right lower), and late (Annexin $V^{+}PI^{+}$, right upper) apoptotic cells. DMSO-treated myofibroblasts served as a positive control (see Appendix **Fig. 30**).

3.5. TGF-β Signaling in Myofibroblasts

Due to the remarkable results of CM, particularly from adipocytes, on myofibroblasts and hypertrophic scar fibroblasts characteristics, further insights into intracellular changes of both cell types were desirable. Since TGF-β signaling plays a pivotal role in myofibroblast generation and perpetuation, canonical and non-canonical TGF-β signaling elements were addressed in subsequent studies. Here, again, myofibroblasts and hypertrophic scar fibroblasts were incubated with CM from ASCs and adipocytes and analyzed for regulations in their protein expression. Notably, no significant alterations in phosphorylated Smad 2/3 were observed (**Fig. 18a**) indicating that the canonical TGF-β pathway is not affected by CM.

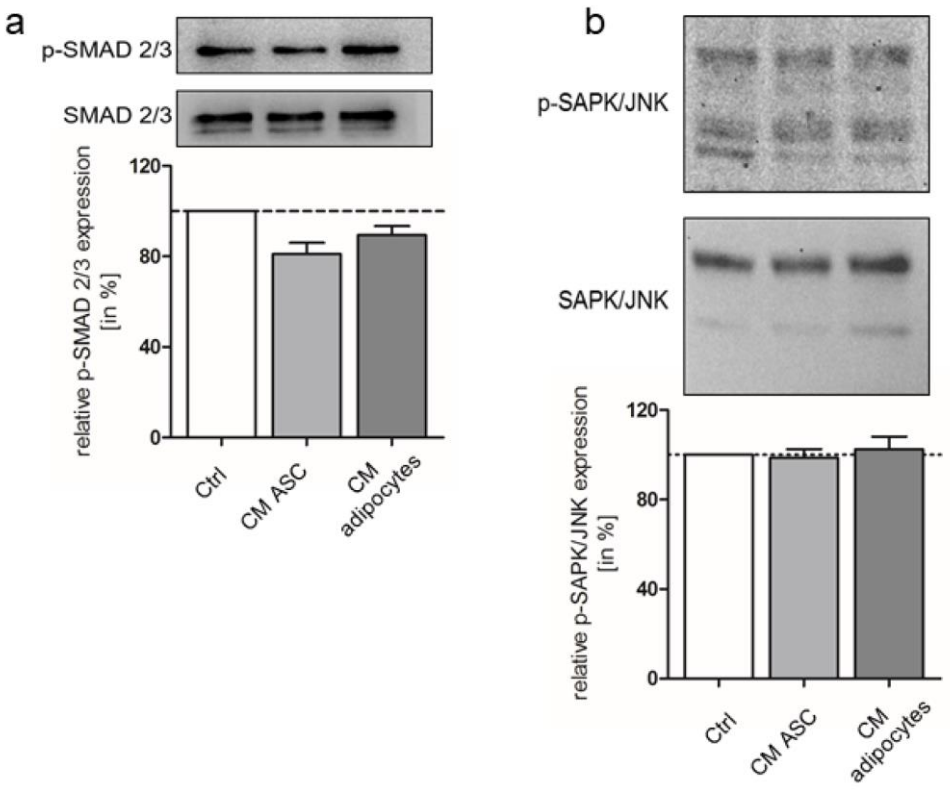

Fig. 18: Protein expression of SMAD 2/3 and stress-activated protein kinase/Jun-amino-terminal kinase SAPK/JNK in myofibroblasts and hypertrophic scar fibroblasts.
Representative Western blots and relative protein expression semi-quantified by densitometry of myofibroblasts (A) and hypertrophic scar fibroblasts (B) following incubation with conditioned medium (CM) from adipose-derived stem cells (ASCs) and adipocytes. Protein expression analyses of phosphorylated proteins compared to SMAD 2/3 and SAPK/JNK are shown (Ctrl = control, serum-free medium treated). Data are presented as mean ± SEM, n = 3. (Hoerst et al., 2019)

However, since TGF-β also signals through Smad-independent pathways, such as via MAPKs, three target proteins were investigated. Like Smad 2/3, phosphorylated SAPK/JNK showed no regulated expression pattern as well upon CM stimulation (**Fig. 18b**). By contrast, a significant decrease in phosphorylated ERK 1/2 was found in myofibroblasts and hypertrophic scar fibroblasts following CM-incubation (**Fig. 19a, b**). Similarly, a significant reduction in phosphorylated p38 levels (**Fig. 19c, d**) was observed. Again, adipocyte-CM induced a stronger downregulation compared to ASC-CM (Hoerst et al., 2019).

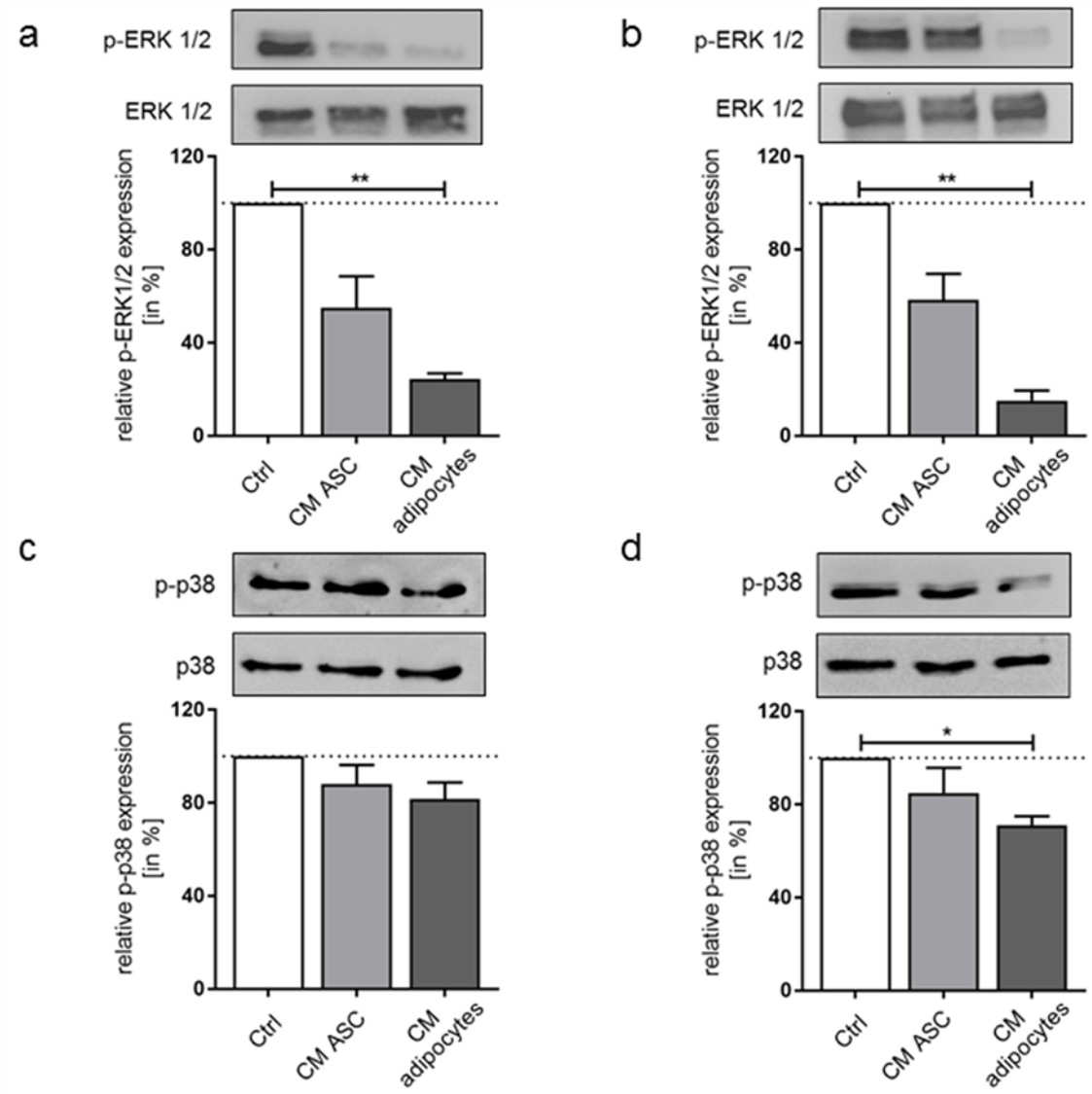

Fig. 19: Non-canonical TGF-β signaling elements are reduced in myofibroblasts following CM incubation.

Representative Western blots and relative protein expression (semi-quantified by densitometry) of phosphorylated ERK 1/2 (p-ERK 1/2) and phosphorylated p38 (p-p-38) in TGF-β-induced myofibroblasts (a, c) and hypertrophic scar fibroblasts (b, d) following incubation with CM from adipose-derived stem cells (ASCs) and adipocytes. Ctrl = control, serum-free medium treatment. The data are presented as the mean ± SEM; n = 3-5 (*p ≤ 0.05, and **p ≤ 0.01), (Hoerst et al., 2019).

3.6. PPARγ Expression in Myofibroblasts

Since a reciprocal, antagonistic relationship has been described for TGF-β and the nuclear receptor PPARγ, a potential contribution of PPARγ to the observed alterations in myofibroblasts induced by adipocyte-CM was considered (**Fig. 20**).

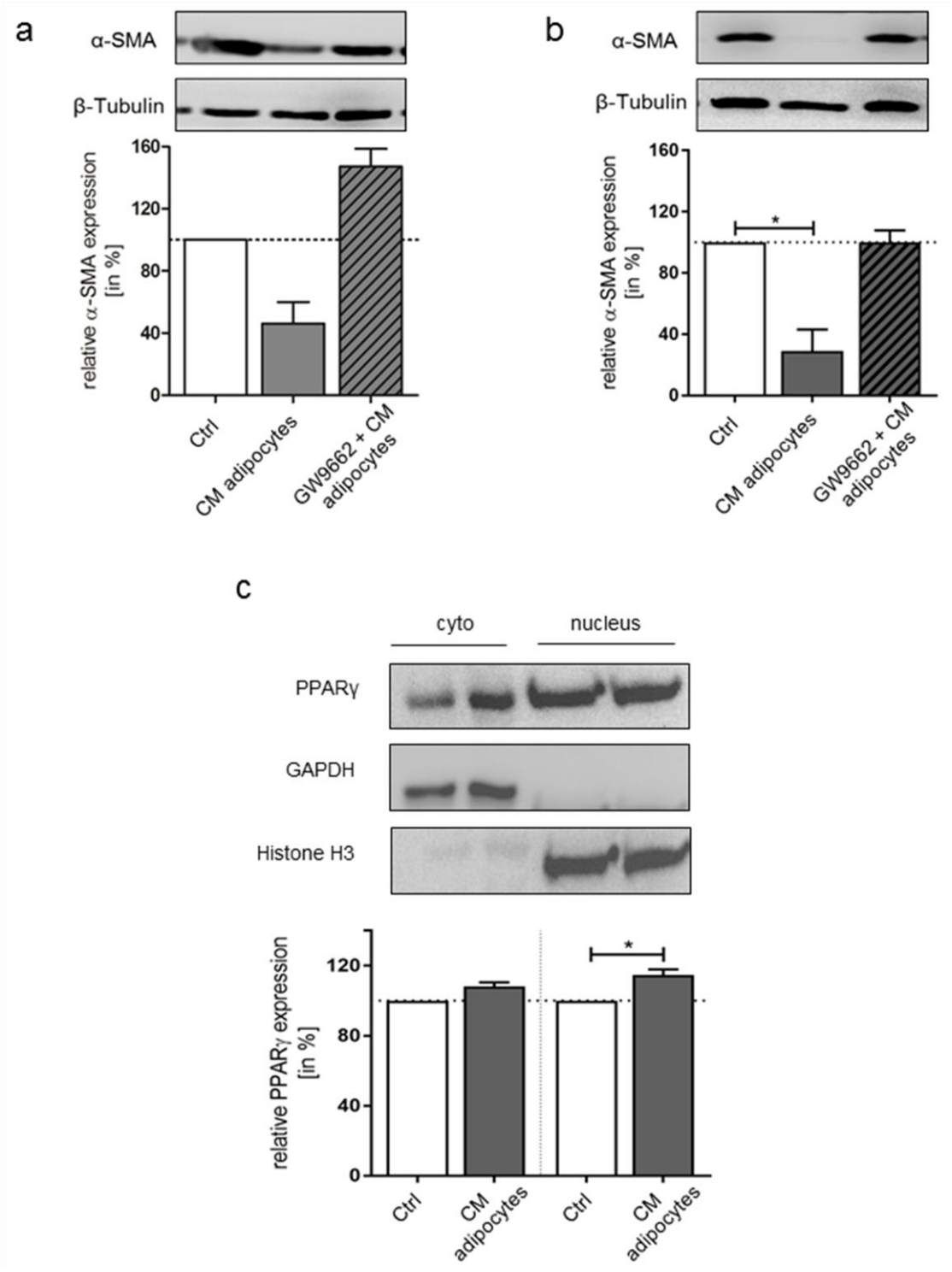

Fig. 20: Antagonizing PPARγ abolishes the α-SMA reduction observed after exposure to adipocyte-CM.

Representative Western blots and relative protein expression (semi-quantified via densitometry) of α-SMA in TGF-β-induced myofibroblasts (a) and hypertrophic scar fibroblasts (b) after preincubation with GW9962 followed by CM-treatment. β-Tubulin served as the loading control. (c) Representative Western blots and relative protein expression (semi-quantified by densitometry) of peroxisomal proliferator-activated receptor γ (PPARγ) after subfractionation of TGF-β-induced myofibroblasts. GAPDH served as the loading control for cytoplasmic fractions; Histone H3 for nuclear fractions. Ctrl = control, serum-free medium treatment. The data are presented as the mean ± SEM; n = 3 (*p ≤ 0.05), (Hoerst et al., 2019).

Therefore, myofibroblasts and fibroblasts from hypertrophic scars were preincubated with the PPARγ antagonist GW9662 prior to exposure to CM. Interestingly, this preincubation with GW9662 completely abolished the α-SMA downregulation (**Fig. 20a, b**) indicating a possible role of PPAR for mediating the effects of CM from adipocytes (Hoerst et al., 2019).

Furthermore, the influence of CM from adipocytes on the PPARγ expression in myofibroblasts was studied. More precisely, PPARγ expression before and after TGF-β-induced myofibroblast exposure to adipocyte-CM was assessed by subfractionating allowing for an expression analysis in cytoplasmic and nuclear compartments separately. Indeed, an increased trend in PPARγ expression by 8% ± 2.4% in cytoplasmic extracts was observed and significantly increased PPARγ expression in nuclear fractions (14.6% ± 3.3%) (**Fig. 20c**) (Hoerst et al., 2019).

3.7. CM Analysis of ASCs and *in vitro* differentiated Adipocytes

Since the studies with CM, especially with CM generated from adipocytes, revealed promising effects on myofibroblasts and hypertrophic scar fibroblasts, further clarification of the CM content was necessary. Therefore, a Liquid Chromatography based mass spectrometry shotgun proteomics approach was conducted for both CM-ASCs and CM-adipocytes (in cooperation with Dr. Oliver Klein from Charité-Universitätsmedizin Berlin). This approach demonstrated the secretion of 160 proteins from ASCs and 288 from *in vitro* differentiated adipocytes. A subsequent literature comparison revealed that 90 out of those 288 proteins are commonly identified in adipocyte-CM (**Fig. 21**, (Hoerst et al., 2019, Ojima et al., 2016, Zvonic et al., 2007, Alvarez-Llamas et al., 2007, Zhong et al., 2010)). Interestingly, using a search tool for the retrieval of interacting genes and proteins, wound healing processes (GO: 0042060) were significant ($p \leq 0.01$) enriched and included 23 proteins. In addition, 5 of these proteins could be assigned to the GO term regeneration (GO: 0031099; **Fig. 21**, (Hoerst et al., 2019)).

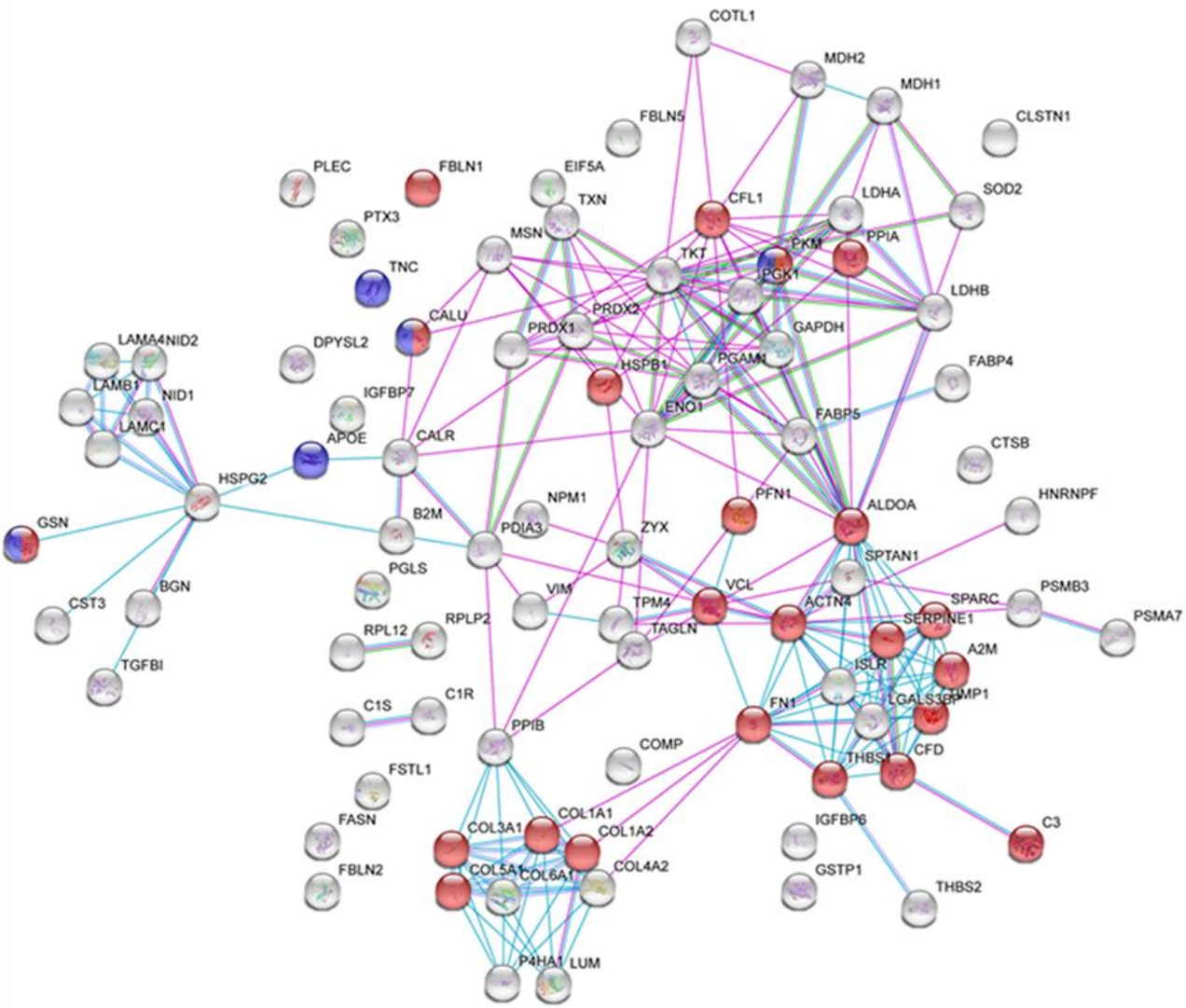

Fig. 21: Secretome analysis of *in vitro* differentiated adipocytes shows secretion of 288 mediators.

STRING analysis of the 90 out of 288 proteins that have been previously identified in the adipocyte secretome. Among these, 23 are associated with wound healing (red spheres) and 5 with regeneration (blue spheres) according to GO terms. The lines indicate known protein interactions based on curated databases (turquoise), experiments (pink), predicted interactions for neighborhood (green) or gene fusion (red). (Hoerst et al., 2019)

In addition to the adipocyte secretome, the 160 identified proteins in ASC-CM were also compared to relevant literature (Rosenow et al., 2010, Zhong et al., 2010, Kim et al., 2015, Kim et al., 2010). Here, 41 proteins from our analysis were commonly found, but when subjected to STRING analysis and examined for the same GO terms, only 9 proteins were found to be associated to wound healing and none to regeneration (**Fig. 22**). Interestingly, 7 proteins were associated with angiogenesis (GO:0001525). Even though a wide range of interesting and potential regenerative factors were identified in adipocyte CM, no conclusion regarding the effective mediator in CM could be drawn from this analysis.

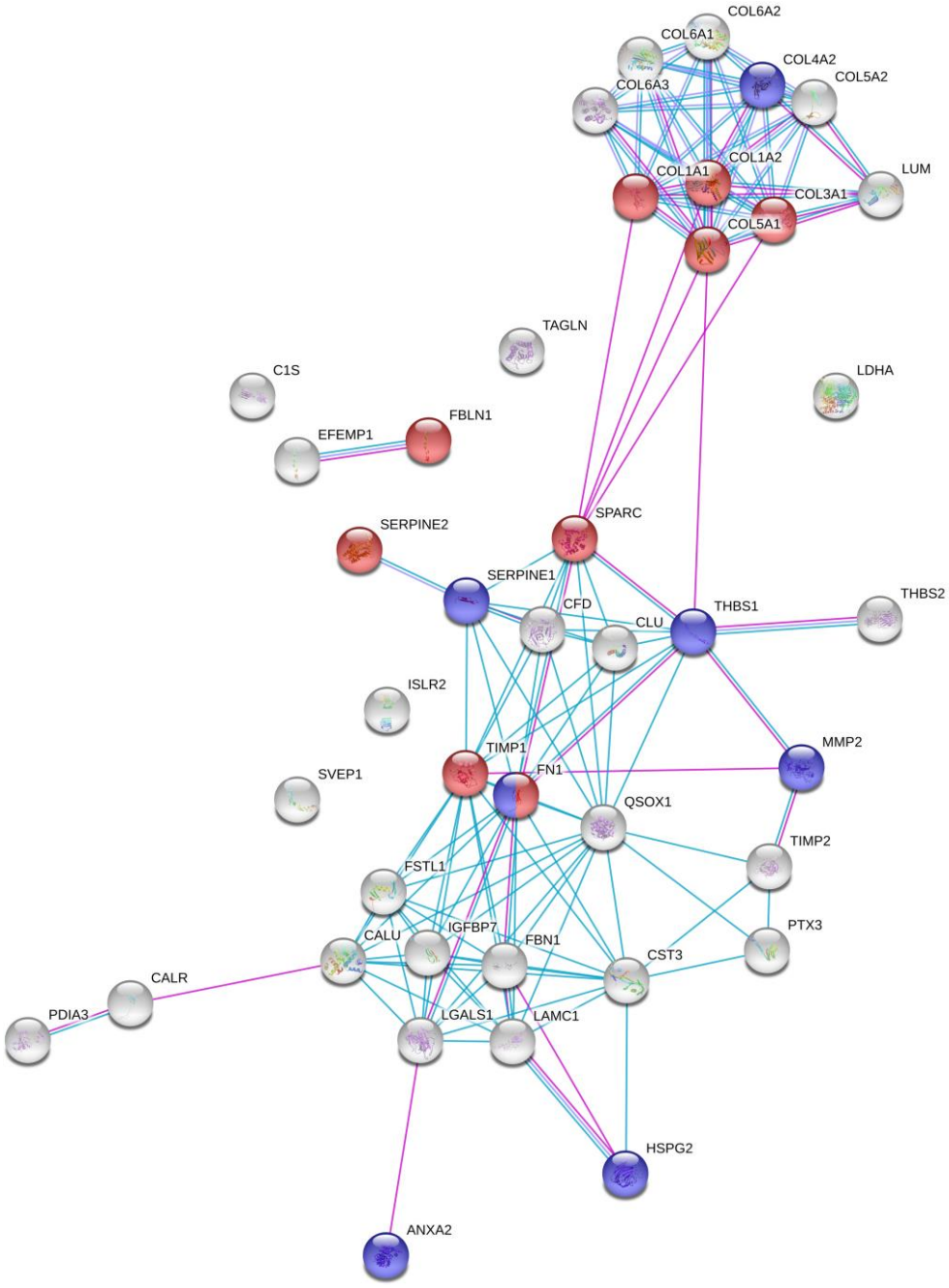

Fig. 22: Secretome analysis of ASCs reveals less secreted proteins compared to adipocytes. STRING analysis of 41 out of 160 proteins found in previous literature. Here, only 9 proteins are associated with wound healing (red spheres) and angiogenesis (blue spheres) according to GO terms and none were found for regeneration. The lines indicate known protein interactions based on curated databases (turquoise), experiments (pink), predicted interactions for neighborhood (green) or gene fusion (red).

3.8. BMP Signaling in Myofibroblasts

Since the involvement of bone morphogenetic proteins (BMP)-2 and -4 in myofibroblast reprogramming has been recently shown (Plikus et al., 2017), BMP secretion by ASCs and adipocytes was analyzed via ELISA, and the results showed distinct levels of BMP-4 (**Fig. 23a**), whereas BMP-2, -6 and -7 were not detected. To further analyze the role of BMP-4,

TGF-β-induced myofibroblasts were preincubated with the BMP receptor type I inhibitor LDN-193189, which abolished the effects of adipocyte-CM, resulting in unchanged α-SMA levels (**Fig. 23b**) (Hoerst et al., 2019).

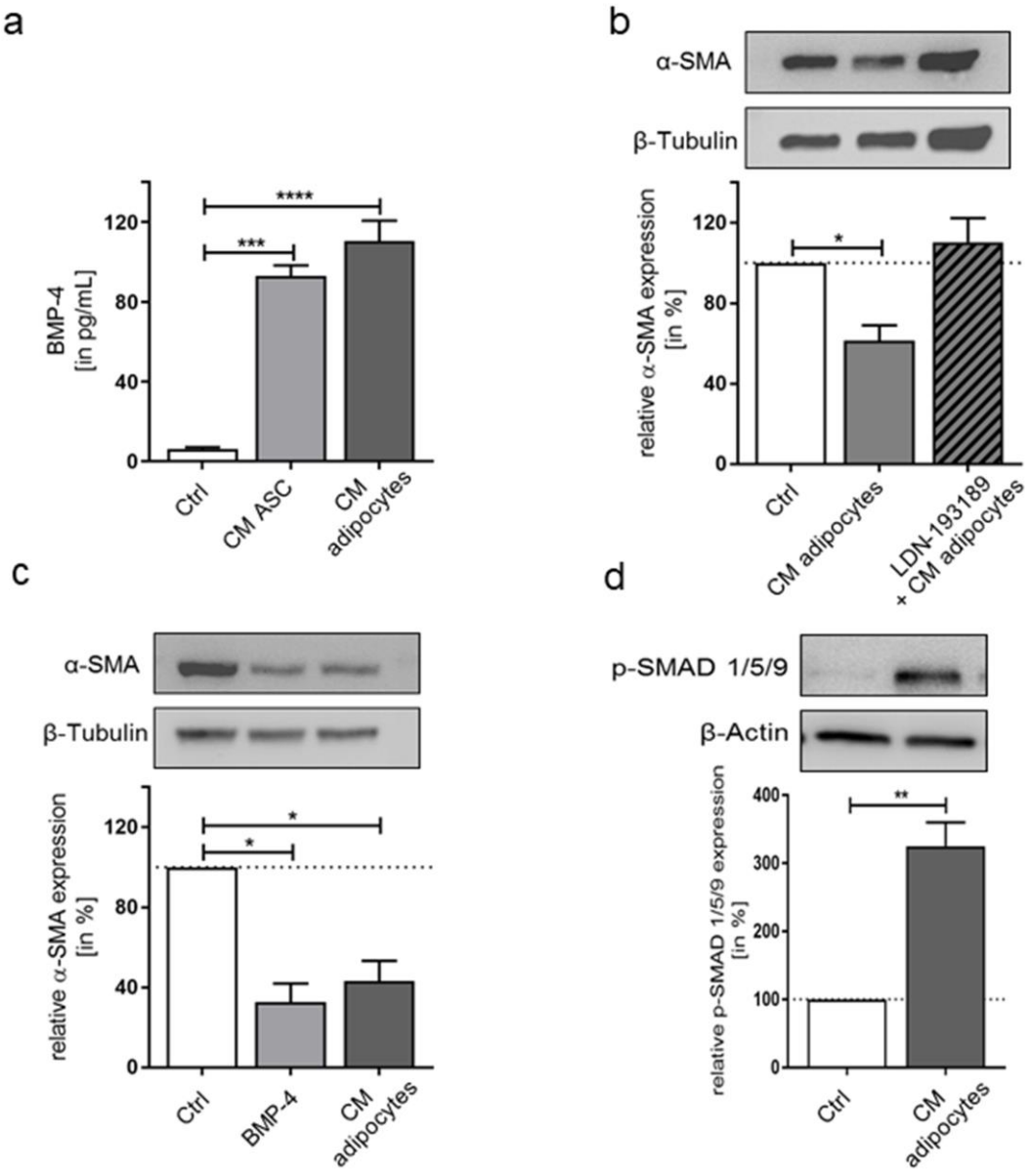

Fig. 23: BMP-4 is involved in myofibroblast reprogramming.
(a) Bone morphogenetic protein (BMP)-4 secretion from adipocytes and adipose-derived stem cells (ASCs) measured by ELISA (Ctrl = control, serum-free DMEM/F12). (b) Representative Western blots of α-SMA expression following TGF-β-induced myofibroblast preincubation with the BMP receptor inhibitor LDN-193189 prior to incubation with adipocyte-CM. (c) α-SMA protein expression in TGF-β-induced myofibroblasts after stimulation with 20 ng/mL recombinant BMP-4 or adipocyte-CM. (d) Representative Western blots of p-SMAD 1/5/9 expression in TGF-β-induced myofibroblasts following adipocyte-CM incubation. The relative protein expression of target proteins was semi-quantified by densitometry and compared with β-actin or β-tubulin expression. The data are presented as the mean ± SEM; n = 3-5 (*p ≤ 0.05, **p ≤ 0.01, ***p ≤ 0.001, ****p ≤ 0.0001) (Hoerst et al., 2019)

To verify the involvement of BMP-4, 20 ng/mL recombinant human BMP-4 was added to TGF-β-induced myofibroblasts and led to distinct α-SMA downregulation comparable to that induced by incubation with adipocyte-CM (**Fig. 23c**). In addition, activation of BMP signaling, and hence the phosphorylation pattern of the SMAD 1/5/9 complex, was analyzed (**Fig. 23d**). Indeed, the expression of phosphorylated SMAD 1/5/9 increased significantly in TGF-β-induced myofibroblasts following incubation with adipocyte-CM (Hoerst et al., 2019).

3.9. Potential Myofibroblast Trans-differentiation into Adipocytes

A recent study has indicated the potential of BMP-4 to induce adipogenic transformation of scar fibroblasts *in vitro* and *in vivo* (Plikus et al., 2017). In their *in vitro* experiments, the authors treated hypertrophic scar as well as keloid fibroblasts with BMP-4 to induce adipogenic commitment followed by a hormone cocktail mediating adipogenic differentiation. To test whether adipocyte-CM could induce a similar trans-differentiation, a similar study to Plikus report was performed. Following the protocol by Plikus et al., myofibroblasts as well as fibroblasts from hypertrophic scars and keloids (both scar cell types isolated and cultivated at Prof. Dr. Gibbs' lab at the VUmc in Amsterdam, Netherlands) were stimulated with 20 ng/mL BMP-4 or adipocyte-CM for 48h, followed by further cultivation in adipogenesis medium for another 10 days. However, no lipid droplet formation or significant increases in characteristic adipogenic genes or proteins were observed (**Fig. 24**).

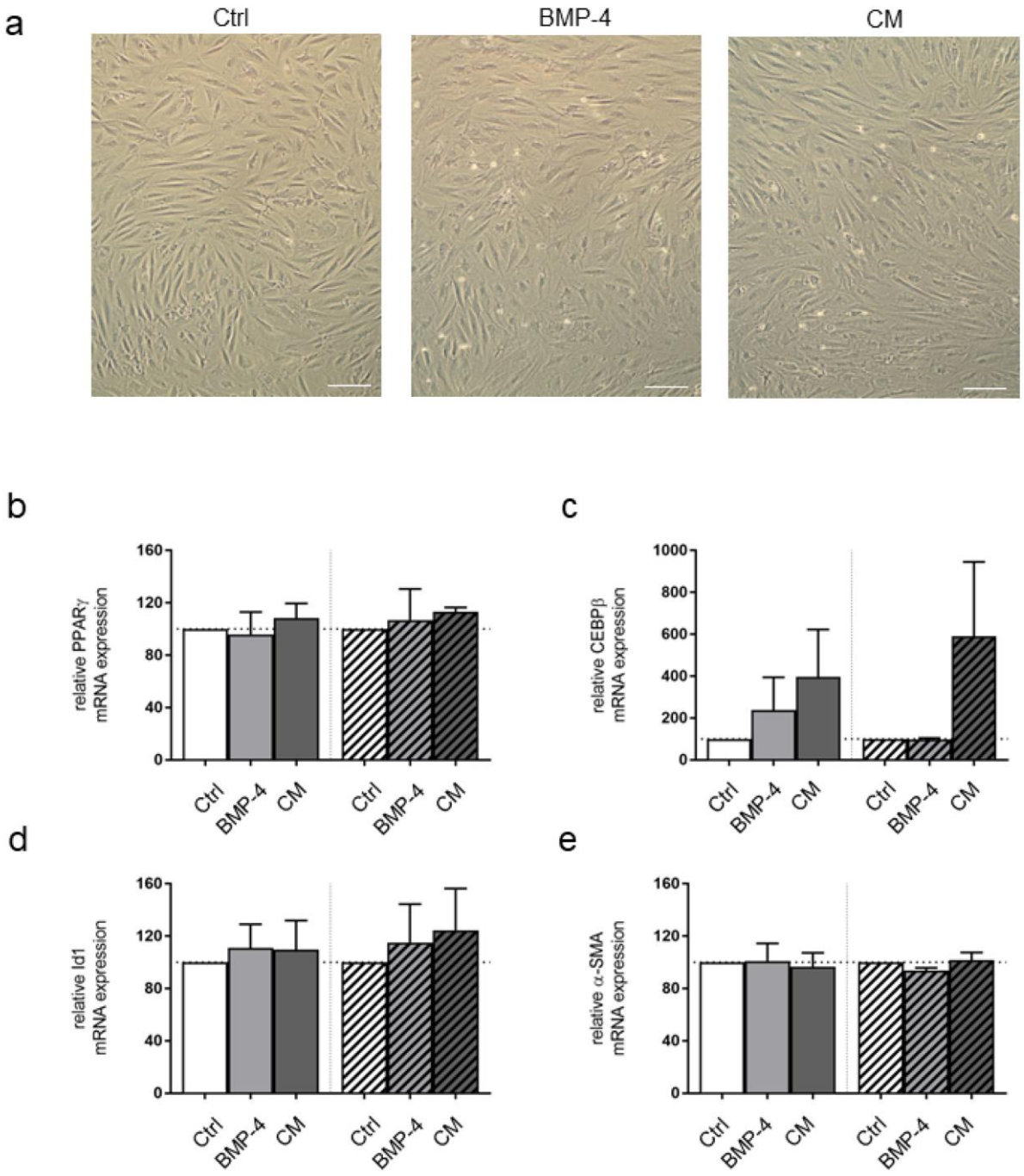

Fig. 24: Incubation with BMP-4 and conditioned medium (CM) did not induce myofibroblast trans-differentiation into adipocytes.

(a) Representative images of hypertrophic scar fibroblasts following incubation with BMP-4 or adipocyte-CM and adipogenesis medium. Control (=Ctrl) cells were incubated in adipogenesis medium only. Scale bar = 100 µm. Relative mRNA levels for (b) peroxisome proliferator-activated receptor γ (PPARγ), (c) CCAAT-enhancer-binding protein β (CEBPβ), (d) Inhibitor of DNA binding 1 (Id1) and (E) α-smooth muscle actin (α-SMA) in hypertrophic scar (□) and keloid (▨) fibroblasts. Data are presented as mean ± SEM. n = 3 (Hoerst et al., 2019).

Following these observations, another approach was tested. Since gene expression data are very time-dependent, a time course experiment for the first 24h of CM-treatment was conducted (**Fig. 25**).

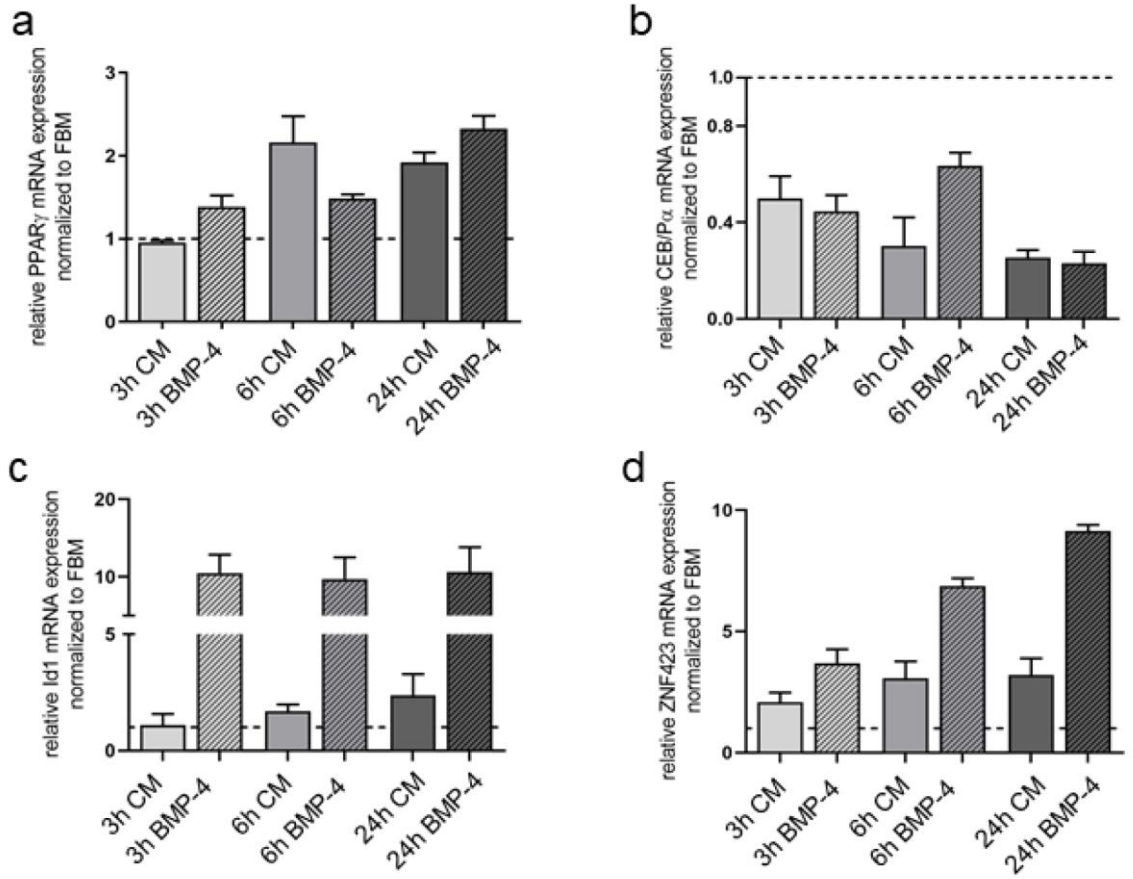

Fig. 25: Time-course of myofibroblasts gene expression after adipocyte-CM or BMP-4 stimulation.

Relative mRNA expression for PPARγ (a), CEB/Pα (b), Id1 (c) and ZNF423 (d) compared to GAPDH and normalized to FBM (fibroblast basal medium, dotted line) in myofibroblasts follwoing 24h exposure to adipocyte-CM or 20ng/ml BMP-4. PPARγ = peroxisome proliferator-activated receptor gamma, CEBPα = CAAT enhancer binding protein alpha, BMP-4 = bone morphogenetic protein-4. ZNF423 = zinc finger protein 423. Data are presented as SEM, n=3.

Here, myofibroblasts were stimulated for 3, 6 and 24h with adipocyte-CM and analyzed for target gene expression. For comparison of the adipocyte-CM impact, effects of 20 ng/ml BMP-4 for the three time points were analyzed in parallel. Notably, nuclear receptor PPARγ showed a time-dependent increase in mRNA levels triggered by adipocyte-CM as well as BMP-4. In contrast to that, reduced CEBPα mRNA expression was found at any point and for both conditions. However, both BMP-4 downstream targets Id1 and ZNF423 showed an augmented gene expression after adipocyte-CM and BMP-4 stimulation. It is hardly surprising that BMP-4 induced a stronger increase in mRNA levels due to its high concentration compared to what was found in adipocyte-CM (110,5 ± 10.1 pg/ml, **Fig. 23**).

3.10. High-throughput Analysis of Myofibroblast Protein Expression

For a more comprehensive analysis of the effects of adipocyte-CM on TGF-β-induced myofibroblasts, a bead-based DigiWest® analysis, a high-throughput Western blot

approach, was performed by Dr. Gerrit Erdmann and Anja Briese from NMI TT Pharmaservices (**Fig. 26**).

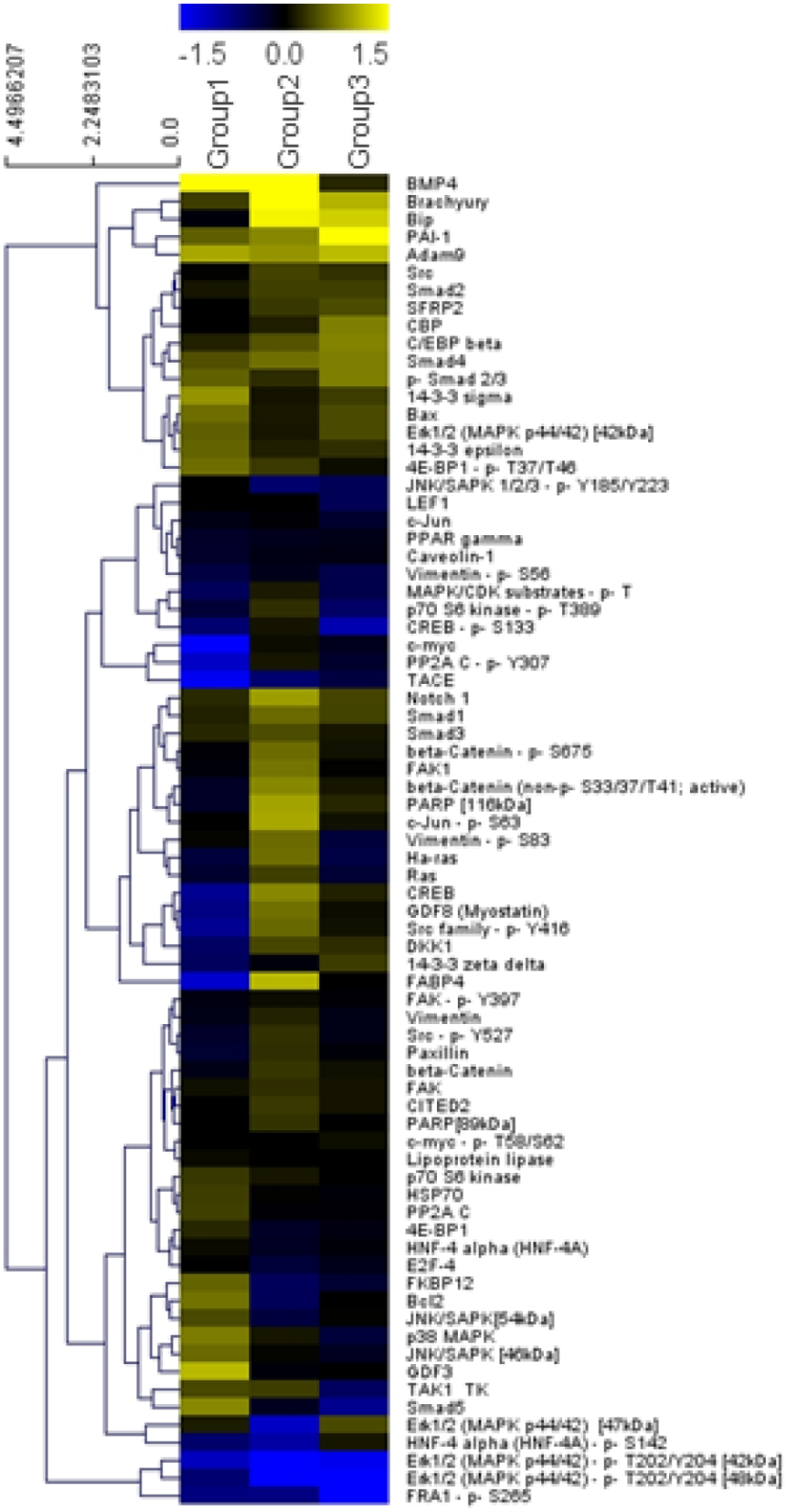

Fig. 26: High-throughput analysis of myofibroblast protein expression indicates distinct alteration of BMP and PPARγ signaling following incubation with adipocyte-CM.
TGF-β-induced myofibroblast protein expression following adipocyte-CM stimulation was analyzed by the DigiWest® bead-based multiplex Western blot analysis. For clustering, ratios were calculated between CM-treated and untreated samples from each group followed by log2 transformation. Hierarchical clustering (HCL) was performed on the log2 transformed ratios using MeV 4.9.0 Software. Each group represents a of pool cells from three independent donors (Hoerst et al., 2019).

Hierarchical clustering (HCL) analysis revealed up- (yellow) or downregulation (blue) of 77 proteins (**Fig. 26**). However, it must be noted that donor variability needs to be considered. Two out of three pooled myofibroblast samples showed significantly increased BMP-4 protein expression after incubation with adipocyte-CM. Interestingly, the expression levels of the transcription factor CCAAT/enhancer-binding protein β (CEBPβ) and transcriptional coactivator Cbp/P300- interacting transactivator with Glu/Asp rich carboxy-terminal domain 2 (CITED2), both of which are associated with PPARγ activation, were enhanced (**Fig. 27a**). The expression of phosphorylated ERK 1/2 was consistently reduced in all samples (**Fig. 27b**), which confirms previous findings (**Fig. 19a, b**) (Hoerst et al., 2019).

HCL analysis further indicated alterations in Wnt signaling elements, although currently no clear conclusion can be drawn because both inducers and inhibitors of Wnt pathways seemed to be modulated after myofibroblast incubation with adipocyte-CM. Notably, increased expression of plasminogen activator inhibitor (PAI)-1 and Notch-1 (**Fig. 27c**) were observed, both of which are associated with myofibroblast differentiation (Hoerst et al., 2019).

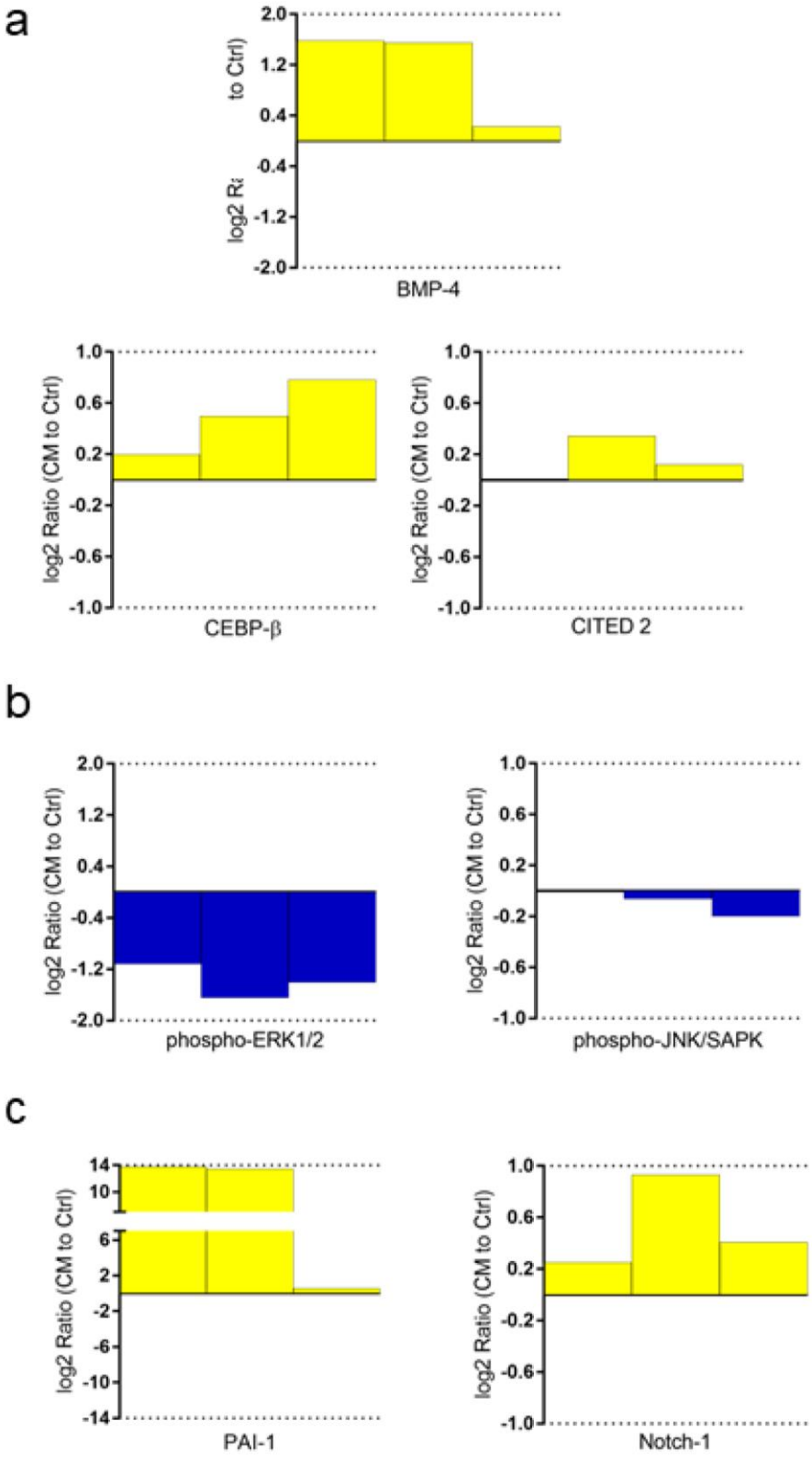

Fig. 27: Detailed expression levels of selected proteins from Fig. 26.
Protein expression levels of (a) CITED2, BMP-4 and CEBPβ; (b) p-ERK 1/2 and p-JNK/SAPK; (c) PAI-1 and Notch1 in the three analyzed groups. (Hoerst et al., 2019)

3.11. Establishment of a 3D Myofibroblast Model

After obtaining those promising results from a two-dimensional (2D) co-cultivation approach, an attempt for establishing a three-dimensional (3D) model was conducted. Since 2D cell culture experiments lack the complexity of the physiological human situation, a 3D model could represent a more reliable tool for investigating the given intricate structures of scarring. Therefore, a first approach consisting of myofibroblasts embedded in a 3D matrix was addressed. More precisely, dermal fibroblasts were incorporated into a collagen gel and placed onto a cell culture insert. Following 7 days of culture, fibroblasts were stimulated with TGF-β to obtain myofibroblasts. Subsequent incubation with adipocyte-CM resulted in a decreased α-SMA expression verified by Western Blot and immunofluorescence (**Fig. 28**). In view of those first results, this approach of a 3D myofibroblasts model holds the potential for further studies of myofibroblasts in a more complex environment.

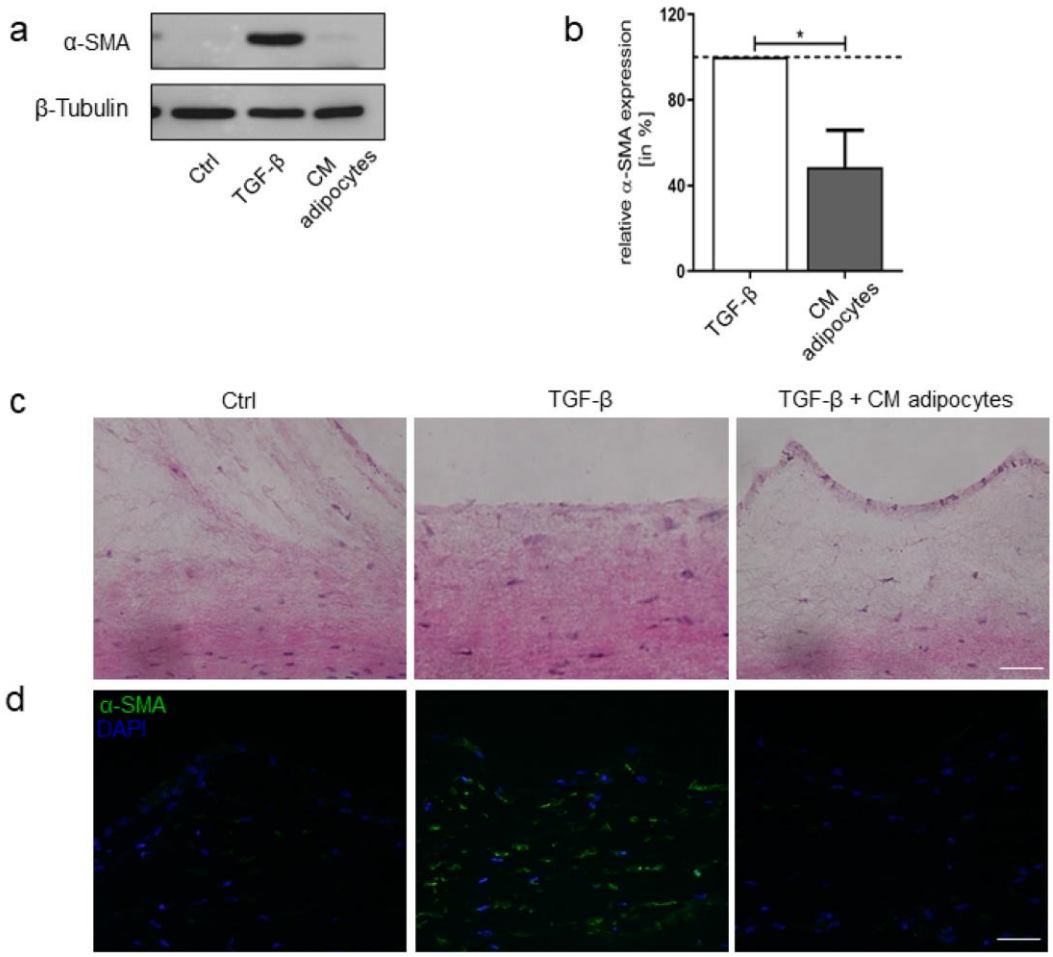

Fig. 28: Establishment of a 3D myofibroblast model.
Dermal fibroblasts were seeded into a collagen gel and differentiated into myofibroblasts after 7 days cultivation. Following 24h exposure to adipocyte-CM, the myofibroblast model was subjected to further analysis. (a) Representative Western Blot of alpha smooth muscle actin (α-SMA) and β-Tubulin with (b) semi-quantification by densitometry. (c) Histological and (d) immunofluorescence images with α-SMA (green) and DAPI (blue), scale bar = 50 µm. Data are represented as SEM, n = 4.

DISCUSSION

4.1. Suitable *In Vitro* Models for Studying Scar Regeneration

So far, a large spectrum of experimental models ranging from simple monolayer cell culture experiments to 3D tissue-engineered models and animal models are available for investigating cellular communication. It seems to be a matter of course that a suitable model always depends on the fundamental question and that is, indeed, challenging for studying human scar regeneration. Scar models are essential for approaching questions such as the pathogenesis of scarring, identifying new drug targets or testing potential therapeutics. Naturally, human studies represent the ultimate approach and are required for the validation of potential novel therapeutics identified in animal or *in vitro* scar models. However, due to ethical issues and probably also due to interindividual differences with regard to the extent and duration of scar appearance, patients are rarely used for investigating the pathogenesis of abnormal scars (van den Broek et al., 2014). In an attempt to overcome the problems faced in patient studies, researchers have been trying to extrapolate results from animal studies. Even though a large number of models exist to study scarring, dealing with mice, rabbits, pigs and other animals, the basic skin physiology and immunology and hence, wound healing processes vary widely from the human situation (Hillmer and MacLeod, 2002, Ramos et al., 2008, Seo et al., 2013, Seok et al., 2013). Therefore, those animals do not develop abnormal scars such as hypertrophic scars and keloids as observed in humans. The animal that shares most similarities with human skin physiology is the pig. Interestingly, porcine skin has a similar dermal-epidermal thickness ratio and epidermal lipid composition (Summerfield et al., 2015). Besides parameters, such as general structure, thickness and hair follicle content, pigs, especially the red Duroc pig, have been shown to develop hypertrophic scars similar to humans (Simon and Maibach, 2000). Zhu and colleagues presented scars in red Duroc pigs following deep dermal wounds with disorganized collagen bundles and characteristic nodule formation like in human hypertrophic scars (Zhu et al., 2003). However, pigs are large animals, difficult to handle and expensive, probably just some of the reasons why the red Duroc pig has not become a gold standard of scar models (Ramos et al., 2008). To tackle the discrepancies between humans and animals, humanized animal models have been developed. Here, healthy human split-thickness skin grafts have been transplanted onto the back of nude mice to establish a hypertrophic scar mouse model (Momtazi et al., 2013, Yang et al., 2007a). Similarly, keloid skin has been transplanted onto nude mice (Estrem et al., 1987, Kischer et al., 1989, Shetlar et al., 1985). Since these mice are immune-deficient the chance of graft rejection is reduced. However, this immunodeficiency also means that the immune component of wound healing and scarring is only poorly represented (Seok et al., 2013). Along with ethical issues, the ideal solution for studying scar regeneration would be a suitable *in vitro* model. The simplest approach of

in vitro studies is to use the conventional cell monolayer. This was, indeed, also applied in this thesis. First, the cultivation and differentiation of all cell types used in this study needed to be established. With regard to adipose tissue those were ASCs and adipocytes. While the ASC characterization by specific surface markers and their trilineage differentiation was implemented successfully (**Fig. 10**), the cultivation of adipocytes was challenging. Owing to their high lipid content, mature adipocytes in culture clump, float on top of the medium and therefore, do not get equal and sufficient access to the medium. As a result, most adipocytes undergo cell lysis within 72h after cell isolation (Zhang et al., 2000). One possible way to overcome these problems would be the ceiling culture, where adipocytes adhere to the top inner surface of a cell culture flask which is completely filled with medium. Although this method allows for the cultivation of adipocytes, however, treatments or co-cultivation approaches with other cell types remain challenging (Dong et al., 2015). Therefore, in the present study, adipocytes were *in vitro* differentiated from ASCs. By the verification of lipid droplets, adipocyte specific gene expression and an increased GPDH activity, successful adipocyte differentiation was confirmed (**Fig. 11**). However, it needs to be considered that *in vitro* differentiated adipocytes still vary from mature adipocytes, for instance by the fact that they contain multiple small lipid droplets instead of one large fat vacuole. Nonetheless, *in vitro* differentiated adipocytes present a valuable cellular model facilitating the study of differences between adipocytes and their precursors (Armani et al., 2010).

In addition to ASCs and adipocytes, another cell type needed to be introduced which was the myofibroblast phenotype. Notably, *in vitro* myofibroblast generation based on TGF-β treatment has been shown before (Rønnov-Jessen and Petersen, 1993, Vaughan et al., 2000). The successful *in vitro* differentiation was verified by *de novo* expression of the myofibroblast marker α-SMA (**Fig. 12**) as well as other specific features such as contractility (**Fig. 16**). Moreover, another primary source for scar fibroblasts was acquired by establishing a cooperation with the group of Prof. Dr. Susan Gibbs in Amsterdam, Netherlands, where hypertrophic scar and keloid fibroblasts were isolated and cultivated. To bring those different cell types together and study a potential intercellular crosstalk between adipose tissue and connective tissue cells, different co-culture approaches were investigated (**Fig. 13**). Here, only the CM approach revealed promising results by reducing myofibroblast characteristics. This is in line with previous studies that investigated the regenerative potential of ASCs and postulated paracrine effects of those cells (Kim et al., 2007, Verhoekx et al., 2013, Spiekman et al., 2014). Interestingly, even more studies exist that addressed the characterization of cells isolated from scar tissue, especially hypertrophic scar and keloid-derived fibroblasts and keratinocytes (Funayama et al., 2003, Khoo et al., 2006, Lim et al., 2009, Phan et al., 2003). Even though all studies, including the

present one, showed promising results and produced valuable insights into scar characteristics, the lack of physiological relevance of those very basic monolayer studies is obvious. Therefore, models with a three-dimensional (3D) structure would be ideal. With having the aim of this study in mind, there are two essential items that need to be considered about a suitable 3D model: on the hand, a complex model mimicking the fibrotic tissue structure of a native scar would be needed. On the other hand, a component that represents the injected adipose tissue needs to be integrated to study scar regeneration upon fat grafting. For both mentioned tissues, promising models already exist. For instance, fibroblasts have been seeded on a collagen lattice with biaxial load being applied subsequently to mimic mechanical tension in scar tissue (Derderian et al., 2005). With the discovery of an important crosstalk between keratinocytes and fibroblasts regarding ECM production (Ghaffari et al., 2009), organotypic skin equivalents have moved to the fore of studying scar pathogenesis. Skin equivalents where dermal fibroblasts were replaced by hypertrophic scar or keloid fibroblasts have been developed as well as models with an epidermis populated with keratinocytes derived from keloids (Chiu et al., 2005, Butler et al., 2008, Bellemare et al., 2005). However, the use of those models for testing therapeutics is limited due to the lack of valid biomarkers (van den Broek et al., 2014). Interestingly, much progress on 3D models of adipose tissue has been made. Adipose tissue engineering has made great advantages with various synthetic and non-synthetic biomaterials being used. Synthetic polymers such as polylactic acid (Shanti et al., 2008), polyglycolic acid (Lin et al., 2008), and the copolymer polylactic-co-glycolic acid (Kang et al., 2008) have been used with promising results supporting adipogenesis *in vitro*. Indeed, natural products are preferred with respect to biocompatibility as well as their mechanical and biological properties. Here, the use of materials found in the native ECM or generated by biological systems is favored, such as collagen and silk fibroin (Mauney et al., 2007). Although there are promising approaches and models for both players in this scar regeneration process, so far, no 3D model exists which combines both components, scar tissue and adipose tissue. To address this issue, first attempts have been made in this thesis to establish a 3D scar regeneration model. Due to the fact that scar-derived fibroblasts were only available in cooperation with the Gibbs lab in Amsterdam, the idea of a 3D myofibroblast model based on dermal normal fibroblasts grew. Since the Hedtrich lab is experienced in the development of skin equivalents, this established model was used as a template (Eckl et al., 2011, Küchler et al., 2011). Therefore, dermal juvenile fibroblasts were incorporated in a collagen gel and subsequently treated with TGF-β in order to generate myofibroblasts. Following successful generation verified by α-SMA expression, 3D myofibroblasts were treated with adipocyte-CM and a similar α-SMA downregulation was observed as in myofibroblast monolayers (**Fig. 28**). Needless to say, this model is still very simple and

artificial. Other cellular components of fibrotic tissue such as endothelial cells or keratinocytes are missing as well as an immune component. Moreover, other ECM components and cytokines are not considered. The adipose tissue is also represented by CM only. Here, an additional 3D layer of adipocytes or ASCs in collagen, for instance, could be beneficial to mimic a complex 3D environment. In addition to the cellular simplicity of the model, the genetic predisposition factor that plays at least in keloids an important role, is not considered here. Also, existing scar models have a lifetime of only a few weeks while abnormal scars grow for months or even years. To conclude, for establishing a suitable *in vitro* scar regeneration model for studying the processes of cellular and matrix remodeling upon autologous fat grafting in human patients with pathological scars, there is still a long way to go. One solution for those limitations could be the new technology of organ-on-a-chip that has been introduced in the last years (Baker, 2011, Giese et al., 2010, Huh et al., 2010). Interestingly, the organ-on-a-chip system is based on engineered tissues that consist of multiple cell types interacting with each other. Even more importantly, those tissues are grown in a microfluidic chip which allows for an ideal and controlled supply of the organ. Recently, a WAT-on-a-chip has already been introduced (Loskill et al., 2017, Liu et al., 2019). In addition, several skin-on-a-chip models have been reported (Ataç et al., 2013, van den Broek et al., 2017, Lee et al., 2017). Once a scar-on-a-chip model has been developed, an in-depth analysis of the ongoing process during scar remodeling could be followed thoroughly.

Until then, and even though cell monolayer studies have their limitations, they provide a useful platform for studying intracellular signaling mechanisms. Here, their simplicity is an advantage since external influences such as the treatment with CM are directly reflected in the cell monolayer. In the present study, several intracellular changes have been observed in the myofibroblast following adipocyte-CM as well as ASC-CM incubation. Whether adipocytes or ASCs may have a greater influence on scar regeneration will be discussed in the next chapter.

4.2. Adipose Tissue and its Cellular Components as a Regenerative Tool

Over the past years, new insights into the functionality and composition of adipose tissue have stimulated speculation about its regenerative potential (Hoerst et al., 2019). Transfer of adipose tissue, also known as fat grafting, lipografting or lipofilling, is widely recognized as a novel and promising technique for volume corrections, dermal rejuvenation and scar treatment (Klinger et al., 2013, Coleman and Saboeiro, 2007). As described in 1.2.3, clinical reports and trials on the beneficial effects of adipose tissue on fibrotic conditions emerge, however, less is known about the cellular component responsible for those fascinating observations. With the discovery of adipose tissue as a source for adipose-derived stem cells (ASCs), many of the advantageous effects observed after fat grafting were attributed to ASCs. Until now, the use of ASCs as a cell therapy for fibrosis has not been thoroughly investigated in clinical trials yet (McVicker and Bennett, 2017). In one study, ASCs were used to treat chronic ulcers in 10 patients with promising results showing improved healing (Akita et al., 2012). When ASCs were injected in soft tissue defects of 29 patients, reduced fibrosis and dermal scarring was observed (Tiryaki et al., 2011). More studies exist where ASCs have been used to enrich the lipograft, which is called cell-assisted lipografting (CAL). By the addition of ASCs, the graft survival shall be improved which was proven by various studies (Kølle et al., 2013, Tanikawa et al., 2013, Peltoniemi et al., 2013). Regarding the use of ASCs that have been cultivated *in vitro* before injection, only two clinical trials exist until now (Bura et al., 2014, Lee et al., 2012). Here, their use for critical limb ischemia has been explored, especially with the focus of revascularization. In both studies, ASCs were injected intramuscularly in patients who suffered from non-healing ischemic ulcers. The study of Bura and co-workers included 12 patients from whom 66.7% reported on ulcer healing after six months. In addition, reduced pain and increased mobility was observed. In the other study, four out of seven patients needed amputation after ASC injection. The three non-amputated patients described pain relief after six months. However, despite the amputations, no other side effects were reported in both studies. Interestingly, the improved ulcers in both studies were attributed to augmented angiogenesis by the administrated ASCs (van Dongen et al., 2018). Even though the ASC injection into ischemic ulcers showed benefits in both studies, large proportions of patients remained unaffected. The therapeutic effect of ASCs might be connected to a loss of ASCs via the circulatory or lymph system (Parvizi and Harmsen, 2015). Other factors that contribute to the therapeutic outcome are donor characteristics such as age and co-morbidity (Fossett et al., 2012). Also, the enzymatic isolation and cultivation of ASCs before injection could induce ASCs senescence (Gruber et al., 2012). Indeed, randomized, controlled large trials are necessary to revise these results.

In animal models of wound healing, ASCs were tested for their regenerative potential as well. Interestingly, ASCs increased the healing rate of wounded areas and, after wound closure, less scarring was observed (Lam et al., 2012, Uysal et al., 2014). Lam and colleagues introduced ASCs to excisional wounds created in mice by using an ECM patch and observed improved wound healing rates. Moreover, ASCs improved healing of diabetic ischemic limbs in a diabetic nude mice model after injection (Kim et al., 2011). These *in vivo* data indicate that ASCs can prevent scar formation by accelerating wound healing. A comparison to the available clinical studies is difficult since wounds can be induced in animal models but the commonly used model organisms such as rats or mice do not develop pathological scars as observed in humans (see 4.2.).

Having a look at *in vitro* studies, ASCs also show beneficial effects. An interesting study from Spiekman et al. revealed an inhibition of TGF-β mediated myofibroblast formation in the presence of CM from ASCs (Spiekman et al., 2014). Interestingly, another group working with myofibroblasts from Dupuytren's disease obtained similar data indicating paracrine effects of ASCs (Verhoekx et al., 2013). All these different models and experimental settings provide valuable aspects on the regenerative potential of ASCs, however, concepts about the mode of action are still speculative.

In contrast, thus far, the regenerative potential of other cellular components of adipose tissue such as adipocytes has rarely been studied. In fact, only a few studies have reported on the effects of adipocytes on wound healing (Hoerst et al., 2019). Among them, Schmidt and Horsley demonstrated that enhanced proliferation of adipocyte precursor cells and adipocyte repopulation in skin wounds after inflammation is crucial for adequate wound healing (Schmidt and Horsley, 2013). They used A-ZIP mice lacking all white adipose tissue, and thereby presented the importance of adipocytes for fibroblast recruitment and dermal reconstruction. Further studies focused on the primary adipokines adiponectin and leptin which seem to facilitate re-epithelialization (Salathia et al., 2013, Frank et al., 2000). For instance, in adiponectin-deficient mice wound re-epithelialization is severely delayed. By the addition of adiponectin to cultured keratinocytes, interestingly, cell proliferation and migration was enhanced and administration of adiponectin to mice skin wounds led to a faster wound healing rate (Jin et al., 2015, Shibata et al., 2012). Notably, similar effects were observed for leptin. Full-thickness skin wounds showed an accelerated re-epithelialization and contraction when leptin was applied systemically or locally in leptin-deficient mice (Frank et al., 2000, Ring et al., 2000). Even though there are several studies pointing towards a regenerative potential of adipocytes, more evidence and clarification is needed. Together with ASCs, two promising candidates for the observed scar regeneration exist, but knowledge about the determining factors and underlying mechanism is lacking.

Hence, to study the regenerative potential of both ASCs and adipocytes, the effects of ASCs and *in vitro* differentiated adipocytes on myofibroblasts and on fibroblasts from hypertrophic scars were investigated in this thesis. Therefore, one first approach was to study the secretome of ASCs and adipocytes determined using mass spectrometry shot gut proteomics approach. Notably, data derived from a secretome analysis require careful interpretation because the results strongly depend on the experimental setup (Chevallet et al., 2007, Hoerst et al., 2019). Indeed, the analysis of secreted proteins represents a major challenge for current proteomic techniques. Low protein concentrations and contaminations from intracellular proteins released into the medium upon cell lysis are only two issues, to name a few. The main problem so far is, indeed, that various techniques for investigating the cell's secretome exist, all with variable outcome (Chevallet et al., 2007). Therefore, a comparison of literature was conducted after the here performed analysis. Due to the complex functions of adipocytes, it was not surprising that we found more proteins secreted from adipocytes (288 proteins) than their precursors (160 proteins), which is also in line with comparative literature (Zhong et al., 2010, Ojima et al., 2016). Interestingly, 90 out of the 288 identified proteins in adipocyte-CM have been previously found in the adipocyte secretome. In-depth analysis related to GO terms revealed that 23 of the proteins were associated with wound healing and 5 were associated with regeneration (**Fig. 21**), including collagen types 1, 3, and 5 and TIMP1, fibulin 1 and fibronectin 1 (Hoerst et al., 2019). A similar analysis was performed with the CM from ASCs, with the result that only 9 proteins can be assigned to wound healing and none to regeneration (**Fig. 22**). With only these two parameters in mind, protein amount and the GO terms wound healing and regeneration, this would indicate a higher regenerative potential from adipocytes than ASCs.

In line with that, investigations of paracrine effects of adipocytes or ASCs on myofibroblasts resulted in similar speculations. Interestingly, incubation of myofibroblasts with adipocyte-CM showed a significant reduction in the myofibroblast marker α-SMA as well as reduced expression of the ECM components collagen 1 and 3 (**Fig. 15**), indicating myofibroblast reprogramming or dedifferentiation. This effect was most pronounced in fibroblasts isolated from hypertrophic scars and superior to the effect of ASC-CM (Hoerst et al., 2019). For the latter, the regulatory effects on α-SMA expression have been previously demonstrated (Spiekman et al., 2014, Verhoekx et al., 2013, Li et al., 2016). Interestingly, the results of this thesis indicate stronger effects mediated by adipocytes compared to ASCs potentially due to the highly complex secretome of adipocytes. However, it has to be noted that this study has been working with *in vitro* differentiated adipocytes and the effect of mature adipocytes should be addressed in the future (Hoerst et al., 2019). Compared to mature adipocytes, *in vitro* differentiated adipocytes are smaller in size and never obtain the typically unilocular appearance adipocytes *in vivo* possess. In addition, *in vitro* adipogenesis

is a complex progress which requires the supplementation of an unphysiological hormonal cocktail (Siersbæk et al., 2012). Therefore, the secretome of *in vitro* differentiated adipocytes may vary from mature adipocytes. However, since the isolation and cultivation of mature adipocytes from adipose tissue is a difficult to handle process and limited in the amount of resulting viable adipocytes (Zhang et al., 2000), mature adipocytes were not isolated but *in vitro* differentiated from ASCs. Elaborating the question whether adipocytes or ASCs have a stronger impact on scar regeneration, more aspects of the *in vivo* situation need to be considered. A number of recent studies has focused on the fate of cells composing the fat graft after injection (Eto et al., 2012, Pu, 2016, Hong et al., 2018). Naturally, fat grafts require nutritional infusion until vascularization from the recipients site occurs. In the past, failed grafts showed loss of adipocytes and graft conversion into fibrotic tissue as well as oil cysts (Niechajev and Sevćuk, 1994). Due to shear stress and mechanical tension during the grafting procedure the large, fragile lipid-laden adipocytes are prone to cell death. Currently, two theories about the fate of the different cells in the fat graft exist: the “graft survival theory”, first described by Pu et al. considers graft survival trough imbibition until neovascularization in the recipient takes place (Pu, 2016). In contrast to this, the “graft replacement theory” describes another progress after graft application. Eto and co-workers presented the three-zone survival theory based on *in vivo* mouse studies (Eto et al., 2012). Here, inguinal fat pads were transplanted into scalped areas which were stained up to 14 days following procedure. They observed a surviving area where adipocytes were still viable, a regenerating area where adipocytes died but ASCs survived and replaced dead adipocytes by forming new ones, and the third, necrotic area where both adipocytes and ASCs died. From these observations they concluded that only a few adipocytes can survive the procedure, but the dead adipocytes are soon replaced by differentiating ASCs which were co-transplanted. Indeed, ASCs or preadipocytes are 20 times smaller than adipocytes and thus, show a higher tolerance to ischemia (von Heimburg et al., 2005).This theory was supported by another study that also reported on adipogenesis and even angiogenesis by stromal cells (Fu et al., 2013). With regard to angiogenesis, Hong and colleagues demonstrated that injected ASCs can transform into endothelial cells (Hong et al., 2018). They also observed new fat formation by donor ASCs as well as recipient ASCs which would combine the “graft survival” and “graft replacement” theory. Also, the CM analysis in the present study supports the idea of ASC-mediated angiogenesis since ASC secrete proteins associated to angiogenesis (**Fig. 22**). The adipocyte secretome, in contrast, does not permit these considerations. Taking all these considerations into account, the obtained data from adipocytes and ASCs cannot be examined independently from each other. Even though adipocytes constantly induced stronger effects in myofibroblasts and hypertrophic scar fibroblasts in this *in vitro* study, this cannot be directly transferred to the

in vivo situation. Here, ASCs would be necessary to form new adipocytes. Therefore, the interplay between the highly active, secretory adipocytes and resilient ASCs inducing adipogenesis and angiogenesis might be responsible for implementing the regenerative potential of adipose tissue. In addition, it should be mentioned that other cell types residing in the SVF, such as pericytes, macrophages and endothelial cells, may also contribute to tissue regeneration which have not been considered in the present study.

Despite all the advantageous and impressive reports and studies regarding autologous fat grafting, there are also concerns about the use of this technique. Since fat transfer methods as well as isolation procedures and cultivation conditions *in vitro* are still highly variable, uniform procedures are required. Until now, fat grafting may lead to unpredictable clinical outcomes in terms of graft take and viability confirming the need for well-designed placebo-controlled clinical trials (Longaker et al., 2014). While the positive results of fat grafting on wound healing and fibrotic conditions have been investigated in small-scaled studies and reports only, the therapeutic effect needs to be corroborated in controlled trials (van Dongen et al., 2018). Especially specific applications for fat grafting such as breast reconstruction after breast cancer must be evaluated carefully. Here, particularly ASCs are discussed controversially since those cells may increase the risk for cancer recurrence (Bielli et al., 2014, Massa et al., 2015, Ito et al., 2017).

As became evident in this chapter, adipose tissue and its cellular components revealed improvements in various wound healing models and showed positive findings on scarring. Unfortunately, the underlying mechanism is often not addressed or leaves room for speculations. Therefore, the present situation in combination with findings of this thesis will be pointed out in the next chapter.

4.3. Insights into the Mechanisms of Scar Regeneration

Since myofibroblasts represent one of the key cell types during wound healing and their persistent activity is associated with the occurrence of fibrosis, the fate of myofibroblasts in fibrotic tissue following fat injections is of great interest.

At the beginning of this study, when adipocyte-CM was applied onto myofibroblast, a significant reduction in myofibroblast characteristics was observed (**Fig. 15**). These characteristics comprised the myofibroblast marker α-SMA and the ECM production of collagen 1 and 3 due to the lack of other valuable marker for this cell type (1.1.3). CM incubation on hypertrophic scar fibroblasts, that were used as an additionally primary source from scar tissue, resulted in an even stronger downregulation of those characteristic proteins. In addition, the contractility of the myofibroblast phenotype was tested in a collagen lattice, with the similar result that myofibroblast contraction was diminished in the presence of adipocyte-CM (**Fig. 16**). Following those first promising results, further insights into intracellular signaling cascades in the myofibroblast were gained. Due to its pivotal role in myofibroblast formation and persistence, canonical and non-canonical TGF-β signaling pathways were investigated upon CM-incubation. These data indicate the occurrence of Smad-independent changes in TGF-β signaling because the MAPKs ERK and p38 exhibited reduced phosphorylated expression in adipocyte-CM-treated myofibroblasts and hypertrophic scar fibroblasts (**Fig. 19**). This is in line with previous literature. Although the Smad3 pathway is considered as one of the major fibrotic inducers, other studied revealed essential roles of ERK and p38 in models of fibrosis (Pannu et al., 2007, Stambe et al., 2004).

The α-SMA reduction seems to be at least partially mediated by PPARγ receptor activation because no α-SMA downregulation was observed when PPARγ was blocked (**Fig. 20**). Interestingly, previous studies have reported anti-fibrotic effects of PPARγ induced by attenuation or even inhibition of TGF-β signaling (Ghosh et al., 2004, Burgess et al., 2005, Aoki et al., 2009). More precisely, PPARɣ activation by naturally occurring or synthetic agonists suppressed profibrotic responses induced by TGF-β. For instance, the PPARɣ ligand 15d-PGJ2 dose-dependently attenuated TGF-β-mediated production of connective tissue growth factor or ECM products such as fibronectin in hypertrophic scar fibroblasts (Zhang et al., 2009). Moreover, the PPARɣ agonist rosiglitazone prevented the development of skin fibrosis in a model of bleomycin-induced scleroderma (Wu et al., 2009). So far, the underlying mechanisms of the TGF-β-antagonizing effect of PPARγ are not completely defined. An upregulation of the tumor suppressor phosphatase and tensin homolog (PTEN) was considered as an anti-fibrotic mediator since PTEN has been shown to inhibit α-SMA and other TGF-β target genes in mouse fibroblasts (White et al., 2006, Lee

et al., 2006). Apart from that, the inverse relationship to TGF-β involving a suppression of PPARɣ by enhanced TGF-β activity provides more clues. Notably, reduced PPARγ expression and enhanced TGF-β signaling is associated with progressive fibrogenesis (Wei et al., 2010, Hoerst et al., 2019). Interestingly, one study revealed a TGF-β activated Smad repressor complex that induces PPARɣ downregulation at the transcriptional level. The authors showed histone deacetylation in the PPARɣ promotor after binding of the repressor complex to specific regulatory elements (Lakshmi et al., 2017). In the present study, subfractionation of CM-treated myofibroblasts increased the PPARγ expression in cytoplasmic and nuclear fractions (**Fig. 20**). Interestingly, high-throughput protein analysis showed an upregulation of CITED2 in myofibroblasts after incubation with adipocyte-CM (**Fig. 26**). CITED2 is a transcriptional activator for both TGF-β and PPARγ (Chou et al., 2006, Tien et al., 2004), and it may be speculated that both TGF-β-dependent Smads and PPARγ compete for the same pool of CITED2 molecules for efficient target gene activation (Hoerst et al., 2019). In addition, the high-throughput analysis also compromised proteins involved in Wnt signaling. Notably, Wnt signaling is a third component that has been shown to interact both with TGF-β and PPARɣ (Vallée et al., 2017). The inhibitory effects of the Wnt family on PPARɣ were already recognized in 2000 (Ross et al., 2000). In a study of Macdougald and colleagues the anti-adipogenic effect of Wnts by PPARɣ suppression was shown. Thereby, Wnt family members can shift an adipogenic program towards the osteoblastic lineage in bone marrow-derived stem cells (Takada et al., 2007). In the present study, regulated Wnt signaling through CM stimulation would present a reasonable explanation of the observed impact of PPARɣ and was, therefore, investigated in myofibroblasts but showed no clear results (**Fig. 26**). Even though the Dickkopf-related protein 1 (DKK-1), which is known to be involved in the inhibition of the Wnt pathway, was increased, however, other proteins such as c-myc were upregulated, thus indicating Wnt activation. Therefore, these opposing results give no clear indication about Wnt activity. Altogether, these results indicate that direct as well as indirect activation of PPARɣ signaling shifts the balance toward anti-fibrotic effects (**Fig. 29**) (Hoerst et al., 2019). However, thus far, the component of adipocyte-CM that directly activates the PPARγ receptor is unknown and so is the specific mechanism between PPARɣ and TGF-β activities.

Although the decreased expression levels of α-SMA and collagen 1 and 3 indicate a dedifferentiation of myofibroblasts, their specific fate remains to be elucidated, which is challenging because specific markers to characterize and distinguish myofibroblasts and fibroblasts have not yet been identified (Hoerst et al., 2019). A recent study from Plikus et al. reported myofibroblast reprogramming into the adipogenic lineage induced by BMP-2 and BMP-4 secreted from hair follicles during wound healing in mice (Plikus et al., 2017). Concordant results were obtained from *in vitro* assays with BMP-4 stimulated keloid

fibroblasts (Hoerst et al., 2019). Interestingly, the authors observed a fibroblast-to-adipocyte *in vitro* differentiation in keloid fibroblasts but could not induce a similar conversion of hypertrophic scar fibroblasts. Inspired by the Plikus study, the influence of BMPs in this project was investigated. Notably, BMP-4 was secreted by adipocytes, and inhibition of BMP receptor type I abolished the reduction in α-SMA expression in myofibroblasts, indicating an involvement of BMP-4 in myofibroblast reprogramming (**Fig. 23**) (Hoerst et al., 2019)

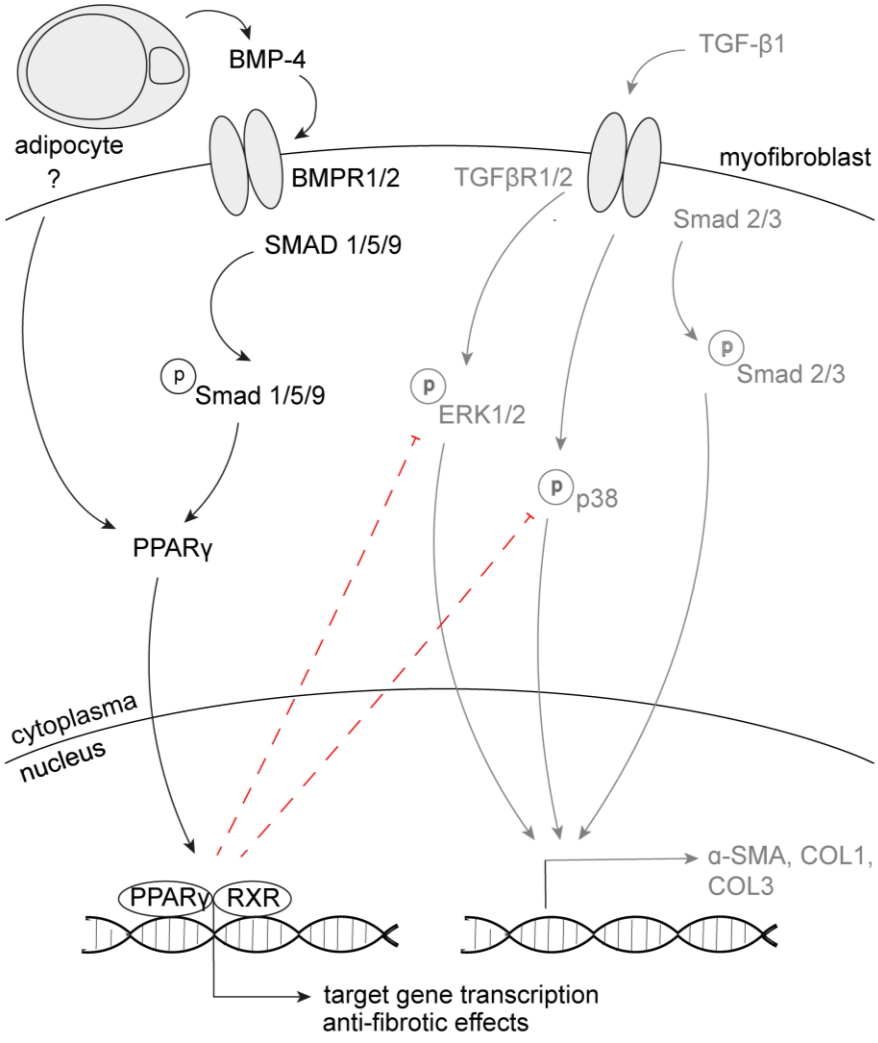

Fig. 29: Paracrine effectors secreted by adipocytes trigger myofibroblast reprogramming via BMP-4 secretion and PPARγ activation.
Schematic depiction of the cellular crosstalk between adipocytes and myofibroblasts. Usually myofibroblasts are triggered by transforming growth factor (TGF)-β1 during wound healing mediating target gene expression such as α-smooth muscle actin (α-SMA) via canonical (SMAD 2/3) and non-canonical (ERK, p38) signaling pathways (highlighted in grey). Upon fat grafting, adipocytes secreting bone morphogenetic protein (BMP-4) induce peroxisomal proliferator-activated receptor (PPAR)γ activation in myofibroblasts leading to target gene expression and anti-fibrotic effects. TGFR = TGF-receptor; BMPR = BMP receptor; RXR = retinoid X receptor. (Hoerst et al., 2019)

Moreover, DigiWest® analysis showed enhanced BMP-4 protein expression in myofibroblasts following stimulation with adipocyte-CM (**Fig. 27**), which is in line with recent findings in human esophageal myofibroblasts (Zhang et al., 2018). Members of the BMP family, especially BMP-2, 4, and 7, are known for their anti-fibrotic potential by opposing the actions of TGF-β signaling (McVicker and Bennett, 2017, Shlyonsky et al., 2011, Pegorier et al., 2010). However, in contrast with Plikus et al., an adipogenic differentiation of myofibroblasts or hypertrophic scar fibroblasts (**Fig. 24**) could not be induced (Hoerst et al., 2019). Since Plikus and colleagues were also not successful in trans-differentiating hypertrophic scar fibroblasts, keloid fibroblasts were included in this study. However, also here no adipocytes were formed. Although the experimental setting (48h BMP-4 stimulation for adipogenic commitment, followed by 10 days of adipogenic differentiation medium) was copied from Plikus et al., some parameters varied such as the adipogenesis medium composition which was kept as used in this study before. In addition, minor other factors may have differed which were not provided in their publication. Apparently, diverse factors such as experimental duration, medium supplements and serum content all contribute to a cell's behaviour *in vitro* and therefore, primary cell culture experiments are difficult to reproduce and prone for variations. Nevertheless, even though no phenotypical change with the formation of lipid droplets was observed, some data may indicate the onset of adipogenic differentiation because increased CEBPβ expression and activation of BMP-4/SMAD 1/5/9-signaling, both of which are key activators of adipogenesis, were found in myofibroblasts after incubation with adipocyte-CM (**Fig. 27**) (Hoerst et al., 2019). In addition, a time-course gene expression analysis revealed an upregulation of PPARɣ as well as the BMP targets Id1 and Zfp423 following BMP-4 stimulation (**Fig. 25**). Interestingly, adipocyte-CM induced similar results although to a less extent. These results are in line with recent data demonstrating enhanced expression of PPARγ in 3T3-L1 adipocytes (Schreiber et al., 2017) and differentiation of precursor cells into the adipocyte lineage (Huang et al., 2009, Hammarstedt et al., 2013) after incubation with BMPs. However, further studies are necessary to draw final conclusions. Here, the experimental setting needs to be considered and perhaps modified. The CM studies were conducted for 24h only, which appeared to be sufficient for a reduction of characteristic protein expression (**Fig. 15**). However, the transformation of one cell type into another lineage, which was shown by Plikus et al., potentially needs more time. Their *in vitro* study was conducted for a total of 12 days which was enough at least for a conversion of keloid fibroblasts. Notably, the high-throughput protein analysis performed in the present study provided evidence that myofibroblast characteristics are still present, as indicated by the high expression levels of PAI-1 or Notch-1 (**Fig. 27**), which are both strongly associated with fibrosis (Ghosh and Vaughan, 2012).

Therefore, more insights into the protein expression level of CM-treated myofibroblasts are required and might benefit from further knowledge about their transcriptional control.

Since an adipogenic conversion of myofibroblast could not be proven, another assumption for the myofibroblast fate after fat injection is a redifferentiation back to fibroblasts. Since the annexin V/PI staining was negative (**Fig. 17**), apoptosis and thus, disappearance of myofibroblasts in the fibrotic tissue, can be excluded. Interestingly, several studies reported that myofibroblasts can disappear by a reversal of the differentiation (Hecker et al., 2011, Wettlaufer et al., 2016, Horowitz and Thannickal, 2018). One study proposed the role of the transcription factor MyoD in the dedifferentiation of TGF-β induced lung fibroblasts. Here, MyoD downregulation mediated by ERK signaling was demonstrated in myofibroblast deactivation (Hecker et al., 2011). Another group showed that the lipid mediator prostaglandin E_2 was able to induce dedifferentiation in a lung fibroblast cell line treated with TGF-β (Wettlaufer et al., 2016). These data support the concept that myofibroblast are not terminally differentiated cells, however, the reversibility of this phenotype is so far not completely understood.

Overall, the data of the present study addressing mechanisms of scar regeneration indicate that adipocytes can induce myofibroblast reprogramming. These paracrine effects are mediated by direct and indirect activation of PPARɣ signaling as well as by the release of BMP-4 and subsequent stimulation of BMP signal transduction; both of these signaling pathways are known for their TGF-β-antagonizing and hence anti-fibrotic effects (**Fig. 29**) (Hoerst et al., 2019).

Although the important and unique role of myofibroblasts in wound healing and scar processes is indisputable, it might be speculated whether the complex progress of scar remodeling can be attributed to a myofibroblast conversion only. As described before, angiogenesis could play a key role as well. Since ASCs are often mentioned in this context (**Fig. 22**, (Dong et al., 2015, Li et al., 2003)), this presumption is not far-fetched. One aspect why angiogenesis seems to be critical in scar regeneration is the need for new blood vessel formation to guarantee fat graft survival. Since this can be provided not only by the recipient site but also by ASCs (Kachgal and Putnam, 2011), endothelial cells (Koh et al., 2011) and potentially also adipocytes (Park et al., 2001) originating from the injected adipose tissue, the graft might exert further pro-angiogenic functions on promoting scar improvement (Javazon et al., 2007). However, whether enhanced angiogenesis is beneficial for a reduction of scar appearance remains questionable. Several studies suggest contradictory effects since pronounced angiogenesis was associated with scar formation (Diao et al., 2010, Gira et al., 2004, Wilgus et al., 2008). Interestingly, systemic administration of the

anti-angiogenic endostatin reduced hypertrophic scarring in a rabbit ear model (Ren et al., 2013). Overall, more evidence for pro- and anti-angiogenic effects on pathological scars is needed and must be assessed carefully.

In addition to angiogenesis, other aspects such as ECM remodeling in scar reduction need to be evaluated more extensively. With considering all the different factors potentially involved in tissue regeneration, again suitable models need to be addressed as being crucial. Due to the lack of relevant models, mechanistic studies on the regenerative potential of adipose tissue on native scar remodeling specifically are underrepresented. Existing studies have mainly focussed on wound healing acceleration or inhibition of scar formation by fat graft components. Insights into those processes are of great importance but effects and mechanisms in pre-existing scars and their transformation may vary widely.

4.4. Conclusion

With this study, more insights into the complex intercellular crosstalk of adipose tissue and scar tissue were gained. These data demonstrate the regenerative potential of adipocytes and provide new insights into the regenerative processes triggered by autologous fat grafting. Here, the importance and contribution of adipocytes to scar regeneration was highlighted. The effect of adipocytes over ASCs was superior, however, the transferability of these results to the *in vivo* situation remains questionable since adipocytes and ASCs behaviour in their natural habitation might result in a different clinical outcome. Raising the point of an applicable and adequate model for studying intracellular signaling pathways, the chosen approach of the *in vitro* co-cultivation of myofibroblasts and hypertrophic scar fibroblasts with conditioned medium of adipocytes indeed presented a suitable model for studying intracellular signaling pathways. By addressing TGF-β signaling, an interesting, reciprocal relationship with the nuclear receptor PPARɣ became clear. Even though the mechanism of PPARɣ activation by secreted factors of adipocytes requires further investigation, a pivotal role of BMP-4 in this regard was considered in this study. A trans-differentiation of myofibroblasts would provide a reasonable explanation for the observations made on scar regeneration *in vitro* and *in vivo* but, however, this could not be confirmed in this study. Even though the specific fate of myofibroblasts remains to be elucidated, an initiated myofibroblast reprogramming was clearly shown. A more detailed understanding of these mechanisms may pave the way toward novel strategies for scar prevention or treatment.

4.5. Prospects

The complex contributing factors underlying scar remodelling remain challenging for clinicians, dermatologists and researchers. While both processes before and after treatment, the development and progression of pathological scars as well as their positive transformation upon fat injection, are only understood to some degree, ideal treatment and prevention options for abnormal scars are far from optimal. Since human studies on the one hand have their ethical restrictions and are difficult to achieve, animal studies on the other hand provide only little potential to extrapolate findings to the human situation (see 0), the focus should be on *in vitro* studies. The presented two-dimensional approach in this study provides a valuable tool for studying intracellular changes in the myofibroblast and hypertrophic scar fibroblasts. So far, only ASCs and adipocytes have been tested for their regenerative potential in this setting. Therefore, it remains open to what extent other cell types of the stromal vascular fraction (SVF) such as pericytes, endothelial cells, macrophages etc. residing in the autologous fat grafts may also contribute to myofibroblast dedifferentiation. This requires specific attention since BMP-4 production, for example, has been recently shown in endothelial cells (Wertheimer et al., 2018). However, these aspects were beyond the focus of the current work but clearly require further attention in future investigations (Hoerst et al., 2019). In addition, further attention should be drawn on the actual mediator of PPARɣ activation. Notably, one recent discovery in the field of cell-cell communications are exosomes. Exosomes are extracellular vesicles secreted by cells and may contain proteins, lipids, mRNAs or microRNAs (miR). This content can be transferred to an acceptor cell and may have functional effects in those recipient cells. With regard to adipose tissue, a fascinating study recently provided more insights. Ying and colleagues studied the exosome profile of adipose tissue macrophages in obese mice and found exosomes containing miR-155 (Ying et al., 2017). Interestingly, miR-155 has been shown to be a target of PPARɣ (Chen et al., 2013, Han et al., 2018). Moreover, Ying et al. demonstrated that miR-155 knockout mice are insulin sensitive and glucose tolerant. Although the survey of adipose tissue-derived miRs has already started (Thomou et al., 2017), more extensive studies on the adipose tissue secretome profile, especially with regard to its effects on PPARɣ activation and expression in myofibroblasts, are inevitable. Returning to the question of suitable *in vitro* models, more advances in establishing a scar regeneration model are necessary. The presented 3D model in this study is, indeed, quite simple but showed first favorable results. By integrating a layer of adipocytes, the most promising cell type concluded from the here obtained results, the model would already benefit with regard to complexity. Indeed, other cell types such as keratinocytes or endothelial cells would be necessary, too. As mentioned before (0), the organ-on-a-chip

technology would provide a promising tool integrating all these different cell types. In addition to 3D models, human skin biopsies might contribute to gain more insights about scar remodeling as well. If it were possible to obtain scar biopsies before and after fat injection, cellular and histological changes in the excised tissue could be observed right away. Getting access to such biopsies, indeed, would be challenging but the expected data would be more than promising. An aspect that has not been mentioned before, is the type of adipose tissue being used for studying scar regeneration. Naturally, the adipose tissue that is harvested and injected in plastic surgery is subcutaneous white adipose tissue. The fact that the human body also comprises brown and brite adipose tissue should be included in future considerations dealing with scar remodeling. Since brown and beige adipose tissue holds promising potential their effect on scar regeneration could provide valuable knowledge on regenerative possibilities. Interestingly, brown adipose tissue was discovered as an endocrine organ as well (Villarroya et al., 2017). Therefore, a comparison of secretory factors released by brown and white adipocytes with regard to tissue remodeling could provide new, promising insights.

Overall, the investigation of adipose tissue mediated-scar regeneration needs further standardized methods with regard to secretome analysis and *in vitro* model generation. Once the complete secretome of adipocytes is accessible and suitable complex cell-based models are available, lacking evidence might be provided for the remaining open questions of this complex scar remodeling.

REFERENCES

Abe, R., Donnelly, S. C., Peng, T., Bucala, R. & Metz, C. N. 2001. Peripheral blood fibrocytes: differentiation pathway and migration to wound sites. *The Journal of Immunology,* 166**,** 7556-7562.

Akita, S., Yoshimoto, H., Akino, K., Ohtsuru, A., Hayashida, K., Hirano, A., Suzuki, K. & Yamashita, S. 2012. Early experiences with stem cells in treating chronic wounds. *Clinics in Plastic Surgery,* 39**,** 281-292.

Alvarez-Llamas, G., Szalowska, E., De Vries, M. P., Weening, D., Landman, K., Hoek, A., Wolffenbuttel, B. H. R., Roelofsen, H. & Vonk, R. J. 2007. Characterization of the Human Visceral Adipose Tissue Secretome. *Molecular & Cellular Proteomics,* 6**,** 589-600.

Ankrum, J. & Karp, J. M. 2010. Mesenchymal stem cell therapy: Two steps forward, one step back. *Trends in Molecular Medicine,* 16**,** 203-209.

Annes, J. P., Munger, J. S. & Rifkin, D. B. 2003. Making sense of latent TGFβ activation. *Journal of Cell Science,* 116**,** 217-224.

Aoki, Y., Maeno, T., Aoyagi, K., Ueno, M., Aoki, F., Aoki, N., Nakagawa, J., Sando, Y., Shimizu, Y., Suga, T., et al. 2009. Pioglitazone, a peroxisome proliferator-activated receptor gamma ligand, suppresses bleomycin-induced acute lung injury and fibrosis. *Respiration,* 77**,** 311-9.

Archer, C. W., Rooney, P. & Cottrill, C. P. 1985. Cartilage morphogenesis in vitro. *Development,* 90**,** 33-48.

Armani, A., Mammi, C., Marzolla, V., Calanchini, M., Antelmi, A., Rosano, G. M., Fabbri, A. & Caprio, M. 2010. Cellular models for understanding adipogenesis, adipose dysfunction, and obesity. *Journal of Cellular Biochemistry,* 110**,** 564-572.

Ataç, B., Wagner, I., Horland, R., Lauster, R., Marx, U., Tonevitsky, A. G., Azar, R. P. & Lindner, G. 2013. Skin and hair on-a-chip: in vitro skin models versus ex vivo tissue maintenance with dynamic perfusion. *Lab on a Chip,* 13**,** 3555-3561.

Bainbridge, P. 2013. Wound healing and the role of fibroblasts. *Journal of Wound Care,* 22.

Baker, M. 2011. Tissue models: a living system on a chip. *Nature,* 471**,** 661.

Baum, C. L. & Arpey, C. J. 2005. Normal cutaneous wound healing: clinical correlation with cellular and molecular events. *Dermatologic Surgery,* 31**,** 674-686.

Bayat, A., Mcgrouther, D. & Ferguson, M. 2003. Skin scarring. *Bmj,* 326**,** 88-92.

Becker, A. J., Mcculloch, E. A. & Till, J. E. 1963. Cytological demonstration of the clonal nature of spleen colonies derived from transplanted mouse marrow cells. *Nature,* 197, 452–454

Becker, M., Maring, J., Schneider, M., Herrera Martin, A., Seifert, M., Klein, O., Braun, T., Falk, V. & Stamm, C. 2018. Towards a novel patch material for cardiac applications: tissue-specific extracellular matrix introduces essential key features to decellularized amniotic membrane. *International Journal of Molecular Sciences,* 19**,** 1032.

Bellemare, J., Roberge, C. J., Bergeron, D., Lopez-Vallé, C. A., Roy, M. & Moulin, V. J. 2005. Epidermis promotes dermal fibrosis: role in the pathogenesis of hypertrophic scars. *The Journal of Pathology: A Journal of the Pathological Society of Great Britain and Ireland,* 206**,** 1-8.

Bellini, E., Grieco, M. P. & Raposio, E. 2017. The science behind autologous fat grafting. *Annals of Medicine and Surgery,* 24**,** 65-73.

Bennett, C. N., Ross, S. E., Longo, K. A., Bajnok, L., Hemati, N., Johnson, K. W., Harrison, S. D. & Macdougald, O. A. 2002. Regulation of Wnt signaling during adipogenesis. *Journal of Biological Chemistry,* 277**,** 30998-31004.

Bianco, P. & Robey, P. G. 2001. Stem cells in tissue engineering. *Nature,* 414**,** 118.

Bielli, A., Scioli, M. G., Gentile, P., Agostinelli, S., Tarquini, C., Cervelli, V. & Orlandi, A. 2014. Adult adipose-derived stem cells and breast cancer: a controversial relationship. *Springerplus,* 3**,** 345.

Biernacka, A., Dobaczewski, M. & Frangogiannis, N. G. 2011. TGF-β signaling in fibrosis. *Growth Factors,* 29**,** 196-202.

Billings, J. E. & May, J. J. 1989. Historical review and present status of free fat graft autotransplantation in plastic and reconstructive surgery. *Plastic and Reconstructive Surgery*,83, 368-381

Bjorbæk, C. & Kahn, B. B. 2004. Leptin signaling in the central nervous system and the periphery. *Recent Progress in Hormone Research,* 59**,** 305-332.

Bombaro, K. M., Engrav, L. H., Carrougher, G. J., Wiechman, S. A., Faucher, L., Costa, B. A., Heimbach, D. M., Rivara, F. P. & Honari, S. 2003. What is the prevalence of hypertrophic scarring following burns? *Burns,* 29**,** 299-302.

Brockes, J. P. & Kumar, A. 2002. Plasticity and reprogramming of differentiated cells in amphibian regeneration. *Nature Reviews Molecular Cell Biology,* 3**,** 566.

Bujak, M., Ren, G., Kweon, H. J., Dobaczewski, M., Reddy, A., Taffet, G., Wang, X.-F. & Frangogiannis, N. G. 2007. Essential role of Smad3 in infarct healing and in the pathogenesis of cardiac remodeling. *Circulation,* 116**,** 2127-2138.

Bura, A., Planat-Benard, V., Bourin, P., Silvestre, J.-S., Gross, F., Grolleau, J.-L., Saint-Lebese, B., Peyrafitte, J.-A., Fleury, S. & Gadelorge, M. 2014. Phase I trial: the use of autologous cultured adipose-derived stroma/stem cells to treat patients with non-revascularizable critical limb ischemia. *Cytotherapy,* 16**,** 245-257.

Burgess, H. A., Daugherty, L. E., Thatcher, T. H., Lakatos, H. F., Ray, D. M., Redonnet, M., Phipps, R. P. & Sime, P. J. 2005. PPARgamma agonists inhibit TGF-beta induced pulmonary myofibroblast differentiation and collagen production: implications for therapy of lung fibrosis. *American Journal of Physiology-Lung Cellular and Molecular Physiology,* 288**,** L1146-53.

Butler, P. D., Ly, D. P., Longaker, M. T. & Yang, G. P. 2008. Use of organotypic coculture to study keloid biology. *The American Journal of Surgery,* 195**,** 144-148.

Cannon, B. & Nedergaard, J. 2004. Brown adipose tissue: function and physiological significance. *Physiological reviews,* 84**,** 277-359.

Cao, Z., Umek, R. M. & Mcknight, S. L. 1991. Regulated expression of three C/EBP isoforms during adipose conversion of 3T3-L1 cells. *Genes & Development,* 5**,** 1538-1552.

Cawthorn, W. P., Scheller, E. L. & Macdougald, O. A. 2012. Adipose tissue stem cells meet preadipocyte commitment: going back to the future. *Journal of Lipid Research,* 53**,** 227-246.

Chen, Y., Siegel, F., Kipschull, S., Haas, B., Fröhlich, H., Meister, G. & Pfeifer, A. 2013. miR-155 regulates differentiation of brown and beige adipocytes via a bistable circuit. *Nature Communications,* 4**,** 1769.

Chevallet, M., Diemer, H., Van Dorssealer, A., Villiers, C. & Rabilloud, T. 2007. Toward a better analysis of secreted proteins: the example of the myeloid cells secretome. *Proteomics,* 7**,** 1757-70.

Chiu, L. L., Sun, C. H., Yeh, A. T., Torkian, B., Karamzadeh, A., Tromberg, B. & Wong, B. J. 2005. Photodynamic therapy on keloid fibroblasts in tissue-engineered keratinocyte-fibroblast co-culture. *Lasers in Surgery and Medicine: The Official Journal of the American Society for Laser Medicine and Surgery,* 37**,** 231-244.

Chou, Y. T., Wang, H., Chen, Y., Danielpour, D. & Yang, Y. C. 2006. Cited2 modulates TGF-beta-mediated upregulation of MMP9. *Oncogene,* 25**,** 5547-60.

Choy, L. & Derynck, R. 2003. Transforming growth factor-β inhibits adipocyte differentiation by Smad3 interacting with CCAAT/enhancer-binding protein (C/EBP) and repressing C/EBP transactivation function. *Journal of Biological Chemistry,* 278**,** 9609-9619.

Christy, R. J., Kaestner, K. H., Geiman, D. E. & Lane, M. D. 1991. CCAAT/enhancer binding protein gene promoter: binding of nuclear factors during differentiation of 3T3-L1 preadipocytes. *Proceedings of the National Academy of Sciences,* 88**,** 2593-2597.

Clarke, S. L., Robinson, C. E. & Gimble, J. M. 1997. CAAT/enhancer binding proteins directly modulate transcription from the peroxisome proliferator-activated receptor

γ2 promoter. *Biochemical and Biophysical Research Communications,* 240**,** 99-103.

Cleveland, E. C., Albano, N. J. & Hazen, A. 2015. Roll, spin, wash, or filter? Processing of lipoaspirate for autologous fat grafting: an updated, evidence-based review of the literature. *Plastic and Reconstructive Surgery,* 136**,** 706-713.

Coleman, S. R. 1995. Long-term survival of fat transplants: controlled demonstrations. *Aesthetic Plastic Surgery,* 19**,** 421-425.

Coleman, S. R. & Saboeiro, A. P. 2007. Fat grafting to the breast revisited: safety and efficacy. *Plastic and Reconstructive Surgery,* 119**,** 775-785.

Cosman, B., Crikelair, G., Ju, D., Gaulin, J. & Lattes, R. 1961. The surgical treatment of keloids. *Plastic and Reconstructive Surgery,* 27**,** 335-358.

Coulombe, P. A. 2003. Wound epithelialization: accelerationg the pace of discovery. *Journal of Investigative Dermatology,* 121**,** 219-230.

Cousin, B., Cinti, S., Morroni, M., Raimbault, S., Ricquier, D., Penicaud, L. & Casteilla, L. 1992. Occurrence of brown adipocytes in rat white adipose tissue: molecular and morphological characterization. *Journal of Cell Science,* 103**,** 931-942.

Da Silva Meirelles, L., Chagastelles, P. C. & Nardi, N. B. 2006. Mesenchymal stem cells reside in virtually all post-natal organs and tissues. *Journal of Cell Science,* 119**,** 2204-2213.

Darlington, G. J., Ross, S. E. & Macdougald, O. A. 1998. The role of C/EBP genes in adipocyte differentiation. *Journal of Biological Chemistry,* 273**,** 30057-30060.

Derderian, C. A., Bastidas, N., Lerman, O. Z., Bhatt, K. A., Lin, S.-E., Voss, J., Holmes, J. W., Levine, J. P. & Gurtner, G. C. 2005. Mechanical strain alters gene expression in an in vitro model of hypertrophic scarring. *Annals of Plastic Surgery,* 55**,** 69-75.

Desmoulière, A., Chaponnier, C. & Gabbiani, G. 2005. Tissue repair, contraction, and the myofibroblast. *Wound Repair and Regeneration,* 13**,** 7-12.

Desmouliere, A., Redard, M., Darby, I. & Gabbiani, G. 1995. Apoptosis mediates the decrease in cellularity during the transition between granulation tissue and scar. *The American Journal of Pathology,* 146**,** 56.

Diao, J.-S., Xia, W.-S. & Guo, S.-Z. 2010. Bevacizumab: a potential agent for prevention and treatment of hypertrophic scar. *Burns: Journal of the International Society for Burn Injuries,* 36**,** 1136-1137.

Dobaczewski, M., Bujak, M., Li, N., Gonzalez-Quesada, C., Mendoza, L. H., Wang, X.-F. & Frangogiannis, N. G. 2010. Smad3 signaling critically regulates fibroblast phenotype and function in healing myocardial infarction. *Circulation Research,* 107**,** 418-428.

Dominici, M., Le Blanc, K., Mueller, I., Slaper-Cortenbach, I., Marini, F., Krause, D., Deans, R., Keating, A., Prockop, D. & Horwitz, E. 2006. Minimal criteria for defining multipotent mesenchymal stromal cells. The International Society for Cellular Therapy position statement. *Cytotherapy,* 8**,** 315-317.

Dong, Z., Peng, Z., Chang, Q., Zhan, W., Zeng, Z., Zhang, S. & Lu, F. 2015. The angiogenic and adipogenic modes of adipose tissue after free fat grafting. *Plastic and Reconstructive Surgery,* 135**,** 556e-567e.

Eckl, K.-M., Alef, T., Torres, S. & Hennies, H. C. 2011. Full-thickness human skin models for congenital ichthyosis and related keratinization disorders. *The Journal of Investigative Dermatology,* 131**,** 1938-42.

Eddy, A. A. 2013. The origin of scar-forming kidney myofibroblasts. *Nature Medicine,* 19**,** 964.

Estrem, S. A., Domayer, M., Bardach, J. & Cram, A. E. 1987. Implantation of human keloid into athymic mice. *The Laryngoscope,* 97**,** 1214-1218.

Eto, H., Kato, H., Suga, H., Aoi, N., Doi, K., Kuno, S. & Yoshimura, K. 2012. The fate of adipocytes after nonvascularized fat grafting: evidence of early death and replacement of adipocytes. *Plastic and Reconstructive Surgery,* 129**,** 1081-1092.

Farmer, S. R. 2006. Transcriptional control of adipocyte formation. *Cell Metabolism,* 4**,** 263-273.

Feng, X.-H. & Derynck, R. 2005. Specificity and versatility in TGF-β signaling through Smads. *Annual Review of Cell and Developmental Biology,* 21**,** 659-693.

Fossett, E., Khan, W. S., Longo, U. G. & Smitham, P. J. 2012. Effect of age and gender on cell proliferation and cell surface characterization of synovial fat pad derived mesenchymal stem cells. *Journal of Orthopaedic Research,* 30**,** 1013-1018.

Frank, S., Stallmeyer, B., Kämpfer, H., Kolb, N. & Pfeilschifter, J. 2000. Leptin enhances wound re-epithelialization and constitutes a direct function of leptin in skin repair. *The Journal of Clinical Investigation,* 106**,** 501-509.

Fraser, J. K., Wulur, I., Alfonso, Z. & Hedrick, M. H. 2006. Fat tissue: an underappreciated source of stem cells for biotechnology. *Trends in Biotechnology,* 24**,** 150-154.

Fredman, R., Katz, A. J. & Hultman, C. S. 2017. Fat grafting for burn, traumatic, and surgical scars. *Clinics in Plastic Surgery,* 44**,** 781-791.

Freytag, S. O., Paielli, D. L. & Gilbert, J. D. 1994. Ectopic expression of the CCAAT/enhancer-binding protein alpha promotes the adipogenic program in a variety of mouse fibroblastic cells. *Genes & Development,* 8**,** 1654-1663.

Friedenstein, A., Chailakhyan, R. & Gerasimov, U. 1987. Bone marrow osteogenic stem cells: in vitro cultivation and transplantation in diffusion chambers. *Cell Proliferation,* 20**,** 263-272.

Friedman, J. M. & Halaas, J. L. 1998. Leptin and the regulation of body weight in mammals. *Nature,* 395**,** 763.

Frühbeck, G. 2008. Overview of adipose tissue and its role in obesity and metabolic disorders. *Adipose Tissue Protocols.* Springer.

Fu, S., Luan, J., Xin, M., Wang, Q., Xiao, R. & Gao, Y. 2013. Fate of adipose-derived stromal vascular fraction cells after co-implantation with fat grafts: evidence of cell survival and differentiation in ischemic adipose tissue. *Plastic and Reconstructive Surgery,* 132**,** 363-373.

Fulton Jr, J. E. 1995. Silicone gel sheeting for the prevention and management of evolving hypertrophic and keloid scars. *Dermatologic surgery,* 21**,** 947-951.

Funayama, E., Chodon, T., Oyama, A. & Sugihara, T. 2003. Keratinocytes promote proliferation and inhibit apoptosis of the underlying fibroblasts: an important role in the pathogenesis of keloid. *Journal of Investigative Dermatology,* 121**,** 1326-1331.

Gaestel, M. 2016. MAPK-activated protein kinases (MKs): novel insights and challenges. *Frontiers in Cell and Developmental Biology,* 3**,** 88.

Gauglitz, G. G., Korting, H. C., Pavicic, T., Ruzicka, T. & Jeschke, M. G. 2011. Hypertrophic scarring and keloids: pathomechanisms and current and emerging treatment strategies. *Molecular Medicine,* 17**,** 113.

Ghaffari, A., Kilani, R. T. & Ghahary, A. 2009. Keratinocyte-conditioned media regulate collagen expression in dermal fibroblasts. *Journal of Investigative Dermatology,* 129**,** 340-347.

Ghosh, A. K., Bhattacharyya, S., Lakos, G., Chen, S. J., Mori, Y. & Varga, J. 2004. Disruption of transforming growth factor beta signaling and profibrotic responses in normal skin fibroblasts by peroxisome proliferator-activated receptor gamma. *Arthritis & Rheumatology,* 50**,** 1305-18.

Giese, C., Lubitz, A., Demmler, C. D., Reuschel, J., Bergner, K. & Marx, U. 2010. Immunological substance testing on human lymphatic micro-organoids in vitro. *Journal of Biotechnology,* 148**,** 38-45.

Gimble, J. M., Katz, A. J. & Bunnell, B. A. 2007. Adipose-derived stem cells for regenerative medicine. *Circulation research,* 100**,** 1249-1260.

Gira, A. K., Brown, L. F., Washington, C. V., Cohen, C. & Arbiser, J. L. 2004. Keloids demonstrate high-level epidermal expression of vascular endothelial growth factor. *Journal of the American Academy of Dermatology,* 50**,** 850-853.

Gruber, H., Somayaji, S., Riley, F., Hoelscher, G., Norton, H., Ingram, J. & Hanley Jr, E. 2012. Human adipose-derived mesenchymal stem cells: serial passaging, doubling time and cell senescence. *Biotechnic & Histochemistry,* 87**,** 303-311.

Gupta, R. K., Arany, Z., Seale, P., Mepani, R. J., Ye, L., Conroe, H. M., Roby, Y. A., Kulaga, H., Reed, R. R. & Spiegelman, B. M. 2010. Transcriptional control of preadipocyte determination by Zfp423. *Nature,* 464**,** 619.

Gurtner, G. C., Werner, S., Barrandon, Y. & Longaker, M. T. 2008. Wound repair and regeneration. *Nature,* 453**,** 314.

Hammarstedt, A., Hedjazifar, S., Jenndahl, L., Gogg, S., Grunberg, J., Gustafson, B., Klimcakova, E., Stich, V., Langin, D., Laakso, M., et al. 2013. WISP2 regulates preadipocyte commitment and PPARgamma activation by BMP4. *Proceedings of the National Academy of Sciences of the USA,* 110**,** 2563-8.

Han, H. S., Ju, F. & Geng, S. 2018. In vivo and in vitro effects of PTH1-34 on osteogenic and adipogenic differentiation of human bone marrow-derived mesenchymal stem cells through regulating microRNA-155. *Journal of Cellular Biochemistry,* 119**,** 3220-3235.

Hass, R., Kasper, C., Böhm, S. & Jacobs, R. 2011. Different populations and sources of human mesenchymal stem cells (MSC): a comparison of adult and neonatal tissue-derived MSC. *Cell Communication and Signaling,* 9**,** 12.

Hata, A., Seoane, J., Lagna, G., Montalvo, E., Hemmati-Brivanlou, A. & Massagué, J. 2000. OAZ uses distinct DNA-and protein-binding zinc fingers in separate BMP-Smad and Olf signaling pathways. *Cell,* 100**,** 229-240.

Hecker, L., Jagirdar, R., Jin, T. & Thannickal, V. J. 2011. Reversible differentiation of myofibroblasts by MyoD. *Experimental Cell Research,* 317**,** 1914-21.

Heldin, C.-H., Miyazono, K. & Ten Dijke, P. 1997. TGF-β signalling from cell membrane to nucleus through SMAD proteins. *Nature,* 390**,** 465.

Hillmer, M. & Macleod, S. 2002. Experimental keloid scar models: a review of methodological issues. *Journal of Cutaneous Medicine and Surgery: Incorporating Medical and Surgical Dermatology,* 6**,** 354-359.

Hinz, B. 2007. Formation and function of the myofibroblast during tissue repair. *Journal of Investigative Dermatology,* 127**,** 526-537.

Hinz, B. 2016. The role of myofibroblasts in wound healing. *Current Research in Translational Medicine,* 64**,** 171-177.

Hinz, B., Celetta, G., Tomasek, J. J., Gabbiani, G. & Chaponnier, C. 2001. Alpha-smooth muscle actin expression upregulates fibroblast contractile activity. *Molecular Biology of the Cell,* 12**,** 2730-2741.

Hinz, B., Pittet, P., Smith-Clerc, J., Chaponnier, C. & Meister, J.-J. 2004. Myofibroblast development is characterized by specific cell-cell adherens junctions. *Molecular Biology of the Cell,* 15**,** 4310-4320.

Hoang, D., Orgel, M. I. & Kulber, D. A. 2016. Hand rejuvenation: a comprehensive review of fat grafting. *The Journal of Hand Surgery,* 41**,** 639-644.

Hoerst, K., Van Den Broek, L., Erdmann, G., Klein, O., Von Fritschen, U., Gibbs, S. & Hedtrich, S. 2019. Regenerative potential of adipocytes in hypertrophic scars is mediated by myofibroblast reprogramming. *Journal of Molecular Medicine***,** 1-15.

Hong, K. Y., Yim, S., Kim, H. J., Jin, U. S., Lim, S., Eo, S., Chang, H. & Minn, K. W. 2018. The fate of the adipose-derived stromal cells during angiogenesis and adipogenesis after cell-assisted lipotransfer. *Plastic and Reconstructive Surgery,* 141**,** 365-375.

Horowitz, J. C. & Thannickal, V. J. 2018. Mechanisms for the resolution of organ fibrosis. *Physiology,* 34**,** 43-55.

Hu, B., Wu, Z. & Phan, S. H. 2003. Smad3 mediates transforming growth factor-β–induced α-smooth muscle actin expression. *American Journal of Respiratory Cell and Molecular Biology,* 29**,** 397-404.

Huang, H., Song, T.-J., Li, X., Hu, L., He, Q., Liu, M., Lane, M. D. & Tang, Q.-Q. 2009. BMP signaling pathway is required for commitment of C3H10T1/2 pluripotent stem cells to the adipocyte lineage. *Proceedings of the National Academy of Sciences,* 106**,** 12670-12675.

Huh, D., Matthews, B. D., Mammoto, A., Montoya-Zavala, M., Hsin, H. Y. & Ingber, D. E. 2010. Reconstituting organ-level lung functions on a chip. *Science,* 328**,** 1662-1668.

Ignotz, R. A. & Massague, J. 1985. Type beta transforming growth factor controls the adipogenic differentiation of 3T3 fibroblasts. *Proceedings of the National Academy of Sciences,* 82**,** 8530-8534.

Ito, S., Kai, Y., Masuda, T., Tanaka, F., Matsumoto, T., Kamohara, Y., Hayakawa, H., Ueo, H., Iwaguro, H. & Hedrick, M. H. 2017. Long-term outcome of adipose-derived regenerative cell-enriched autologous fat transplantation for reconstruction after breast-conserving surgery for Japanese women with breast cancer. *Surgery Today,* 47**,** 1500-1511.

Javazon, E. H., Keswani, S. G., Badillo, A. T., Crombleholme, T. M., Zoltick, P. W., Radu, A. P., Kozin, E. D., Beggs, K., Malik, A. A. & Flake, A. W. 2007. Enhanced epithelial gap closure and increased angiogenesis in wounds of diabetic mice treated with adult murine bone marrow stromal progenitor cells. *Wound Repair and Regeneration,* 15**,** 350-359.

Jin, C., Xiao, L., Ge, Z., Zhan, X. & Zhou, H. 2015. Role of adiponectin in adipose tissue wound healing. *Genetics and Molecular Research,* 14**,** 8883-91.

Jin, W., Takagi, T., Kanesashi, S.-N., Kurahashi, T., Nomura, T., Harada, J. & Ishii, S. 2006. Schnurri-2 controls BMP-dependent adipogenesis via interaction with Smad proteins. *Developmental Cell,* 10**,** 461-471.

Junker, J. P., Kratz, C., Tollbäck, A. & Kratz, G. 2008. Mechanical tension stimulates the transdifferentiation of fibroblasts into myofibroblasts in human burn scars. *Burns,* 34**,** 942-946.

Kachgal, S. & Putnam, A. J. 2011. Mesenchymal stem cells from adipose and bone marrow promote angiogenesis via distinct cytokine and protease expression mechanisms. *Angiogenesis,* 14**,** 47-59.

Kakagia, D. & Pallua, N. 2014. Autologous fat grafting: in search of the optimal technique. *Surgical Innovation,* 21**,** 327-336.

Kang, S.-W., Seo, S.-W., Choi, C. Y. & Kim, B.-S. 2008. Porous poly (lactic-co-glycolic acid) microsphere as cell culture substrate and cell transplantation vehicle for adipose tissue engineering. *Tissue Engineering Part C: Methods,* 14**,** 25-34.

Keipert, S. & Jastroch, M. 2014. Brite/beige fat and UCP1—is it thermogenesis? *Biochimica et Biophysica Acta (BBA)-Bioenergetics,* 1837**,** 1075-1082.

Kershaw, E. E. & Flier, J. S. 2004. Adipose tissue as an endocrine organ. *The Journal of Clinical Endocrinology & Metabolism,* 89**,** 2548-2556.

Khoo, Y. T., Ong, C. T., Mukhopadhyay, A., Han, H. C., Do, D. V., Lim, I. J. & Phan, T. T. 2006. Upregulation of secretory connective tissue growth factor (CTGF) in keratinocyte-fibroblast coculture contributes to keloid pathogenesis. *Journal of Cellular Physiology,* 208**,** 336-343.

Kim, E. K., Li, G., Lee, T. J. & Hong, J. P. 2011. The effect of human adipose-derived stem cells on healing of ischemic wounds in a diabetic nude mouse model. *Plastic and Reconstructive Surgery,* 128**,** 387-394.

Kim, E. Y., Kim, W. K., Oh, K. J., Han, B. S., Lee, S. C. & Bae, K. H. 2015. Recent advances in proteomic studies of adipose tissues and adipocytes. *International Journal of Molecular Sciences,* 16**,** 4581-99.

Kim, J., Choi, Y. S., Lim, S., Yea, K., Yoon, J. H., Jun, D. J., Ha, S. H., Kim, J. W., Kim, J. H. & Suh, P. G. 2010. Comparative analysis of the secretory proteome of human adipose stromal vascular fraction cells during adipogenesis. *Proteomics,* 10**,** 394-405.

Kim, J. B. & Spiegelman, B. M. 1996. ADD1/SREBP1 promotes adipocyte differentiation and gene expression linked to fatty acid metabolism. *Genes & Development,* 10**,** 1096-1107.

Kim, W. S., Park, B. S., Sung, J. H., Yang, J. M., Park, S. B., Kwak, S. J. & Park, J. S. 2007. Wound healing effect of adipose-derived stem cells: a critical role of

secretory factors on human dermal fibroblasts. *Journal of Dermatological Science,* 48**,** 15-24.

Kischer, C., Pindur, J., Shetlar, M. & Shetlar, C. 1989. Implants of hypertrophic scars and keloids into the nude (athymic) mouse: viability and morphology. *The Journal of Trauma,* 29**,** 672-677.

Klinger, M., Caviggioli, F., Klinger, F. M., Giannasi, S., Bandi, V., Banzatti, B., Forcellini, D., Maione, L., Catania, B. & Vinci, V. 2013. Autologous fat graft in scar treatment. *Journal of Craniofacial Surgery,* 24**,** 1610-5.

Klinger, M., Marazzi, M., Vigo, D. & Torre, M. 2008. Fat injection for cases of severe burn outcomes: a new perspective of scar remodeling and reduction. *Aesthetic Plast Surg,* 32**,** 465-9.

Koh, Y. J., Koh, B. I., Kim, H., Joo, H. J., Jin, H. K., Jeon, J., Choi, C., Lee, D. H., Chung, J. H. & Cho, C.-H. 2011. Stromal vascular fraction from adipose tissue forms profound vascular network through the dynamic reassembly of blood endothelial cells. *Arteriosclerosis, Thrombosis, and Vascular Biology,* 31**,** 1141-1150.

Kølle, S.-F. T., Fischer-Nielsen, A., Mathiasen, A. B., Elberg, J. J., Oliveri, R. S., Glovinski, P. V., Kastrup, J., Kirchhoff, M., Rasmussen, B. S. & Talman, M.-L. M. 2013. Enrichment of autologous fat grafts with ex-vivo expanded adipose tissue-derived stem cells for graft survival: a randomised placebo-controlled trial. *The Lancet,* 382**,** 1113-1120.

Krenning, G., Zeisberg, E. M. & Kalluri, R. 2010. The origin of fibroblasts and mechanism of cardiac fibrosis. *Journal of Cellular Physiology,* 225**,** 631-637.

Kubota, N., Terauchi, Y., Miki, H., Tamemoto, H., Yamauchi, T., Komeda, K., Satoh, S., Nakano, R., Ishii, C. & Sugiyama, T. 1999. PPARγ mediates high-fat diet–induced adipocyte hypertrophy and insulin resistance. *Molecular Cell,* 4**,** 597-609.

Küchler, S., Henkes, D., Eckl, K.-M., Ackermann, K., Plendl, J., Korting, H.-C., Hennies, H.-C. & Schäfer-Korting, M. 2011. Hallmarks of atopic skin mimicked in vitro by means of a skin disease model based on FLG knock-down. *Alternatives to Laboratory Animals-ATLA,* 39**,** 471.

Lakshmi, S. P., Reddy, A. T. & Reddy, R. C. 2017. Transforming growth factor β suppresses peroxisome proliferator-activated receptor γ expression via both SMAD binding and novel TGF-β inhibitory elements. *Biochemical Journal,* 474**,** 1531-1546.

Lam, M. T., Nauta, A., Meyer, N. P., Wu, J. C. & Longaker, M. T. 2012. Effective delivery of stem cells using an extracellular matrix patch results in increased cell survival and proliferation and reduced scarring in skin wound healing. *Tissue Engineering Part A,* 19**,** 738-747.

Lecka-Czernik, B., Moerman, E. J., Grant, D. F., Lehmann, J. R. M., Manolagas, S. C. & Jilka, R. L. 2002. Divergent effects of selective peroxisome proliferator-activated receptor-γ2 ligands on adipocyte versus osteoblast differentiation. *Endocrinology,* 143**,** 2376-2384.

Lee, H. C., An, S. G., Lee, H. W., Park, J.-S., Cha, K. S., Hong, T. J., Park, J. H., Lee, S. Y., Kim, S.-P. & Kim, Y. D. 2012. Safety and effect of adipose tissue-derived stem cell implantation in patients with critical limb ischemia. *Circulation Journal***,** 1204091686-1204091686.

Lee, J. Y.-Y., Yang, C.-C., Chao, S.-C. & Wong, T.-W. 2004. Histopathological differential diagnosis of keloid and hypertrophic scar. *The American Journal of Dermatopathology,* 26**,** 379-384.

Lee, S., Jin, S.-P., Kim, Y. K., Sung, G. Y., Chung, J. H. & Sung, J. H. 2017. Construction of 3D multicellular microfluidic chip for an in vitro skin model. *Biomedical Microdevices,* 19**,** 22.

Lee, S. J., Yang, E. K. & Kim, S. G. 2006. Peroxisome proliferator-activated receptor-γ and retinoic acid X receptor α represses the TGFβ1 gene via PTEN-mediated p70 ribosomal S6 kinase-1 inhibition: role for Zf9 dephosphorylation. *Molecular Pharmacology,* 70**,** 415-425.

Levenson, S., Geever, E., Crowley, L., Oates Iii, J., Berard, C. & Rosen, H. 1965. Healing of rat skin wounds. *Annals of Surgery,* 161**,** 293.

Leventhal, D., Furr, M. & Reiter, D. 2006. Treatment of keloids and hypertrophic scars: a meta-analysis and review of the literature. *Archives of Facial Plastic Surgery,* 8**,** 362-368.

Li, D., Yea, S., Li, S., Chen, Z., Narla, G., Banck, M., Laborda, J., Tan, S., Friedman, J. M. & Friedman, S. L. 2005. Krüppel-like factor-6 promotes preadipocyte differentiation through histone deacetylase 3-dependent repression of DLK1. *Journal of Biological Chemistry,* 280**,** 26941-26952.

Li, J., Zhang, Y. P. & Kirsner, R. S. 2003. Angiogenesis in wound repair: angiogenic growth factors and the extracellular matrix. *Microscopy Research and Technique,* 60**,** 107-114.

Li, Y., Zhang, W., Gao, J., Liu, J., Wang, H., Li, J., Yang, X., He, T., Guan, H., Zheng, Z., et al. 2016. Adipose tissue-derived stem cells suppress hypertrophic scar fibrosis via the p38/MAPK signaling pathway. *Stem Cell Research & Therapy,* 7**,** 102.

Lim, C. P., Phan, T. T., Lim, I. J. & Cao, X. 2009. Cytokine profiling and Stat3 phosphorylation in epithelial–mesenchymal interactions between keloid keratinocytes and fibroblasts. *Journal of Investigative Dermatology,* 129**,** 851-861.

Lin, F.-T. & Lane, M. D. 1994. CCAAT/enhancer binding protein alpha is sufficient to initiate the 3T3-L1 adipocyte differentiation program. *Proceedings of the National Academy of Sciences,* 91**,** 8757-8761.

Lin, S.-D., Wang, K.-H. & Kao, A.-P. 2008. Engineered adipose tissue of predefined shape and dimensions from human adipose-derived mesenchymal stem cells. *Tissue Engineering Part A,* 14**,** 571-581.

Liu, Y., Kongsuphol, P., Chiam, S. Y., Zhang, Q. X., Gourikutty, S. B. N., Saha, S., Biswas, S. K. & Ramadan, Q. 2019. Adipose-on-a-chip: a dynamic microphysiological in vitro model of the human adipose for immune-metabolic analysis in type II diabetes. *Lab on a Chip,* 19**,** 241-253.

Lo, K. A. & Sun, L. 2013. Turning WAT into BAT: a review on regulators controlling the browning of white adipocytes. *Bioscience Reports,* 33**,** e00065.

Longaker, M. T., Aston, S. J., Baker, D. C. & Rohrich, R. J. 2014. Fat transfer in 2014: what we do not know. *Plastic and Reconstructive Surgery,* 133**,** 1305-1307.

Loskill, P., Sezhian, T., Tharp, K. M., Lee-Montiel, F. T., Jeeawoody, S., Reese, W. M., Zushin, P.-J. H., Stahl, A. & Healy, K. E. 2017. WAT-on-a-chip: a physiologically relevant microfluidic system incorporating white adipose tissue. *Lab on a Chip,* 17**,** 1645-1654.

Marshall, C. D., Hu, M. S., Leavitt, T., Barnes, L. A., Lorenz, H. P. & Longaker, M. T. 2018. Cutaneous scarring: Basic science, current treatments, and future directions. *Advances in Wound Care,* 7**,** 29-45.

Massa, M., Gasparini, S., Baldelli, I., Scarabelli, L., Santi, P., Quarto, R. & Repaci, E. 2015. Interaction between breast cancer cells and adipose tissue cells derived from fat grafting. *Aesthetic Surgery Journal,* 36**,** 358-363.

Mauney, J. R., Nguyen, T., Gillen, K., Kirker-Head, C., Gimble, J. M. & Kaplan, D. L. 2007. Engineering adipose-like tissue in vitro and in vivo utilizing human bone marrow and adipose-derived mesenchymal stem cells with silk fibroin 3D scaffolds. *Biomaterials,* 28**,** 5280-5290.

Mcvicker, B. L. & Bennett, R. G. 2017. Novel Anti-fibrotic Therapies. *Frontiers in Pharmacology,* 8**,** 318.

Mokos, Z. B., Jovic, A., Grgurevic, L., Dumic-Cule, I., Kostovic, K., Ceovic, R. & Marinovic, B. 2017. Current Therapeutic Approach to Hypertrophic Scars. *Frontiers in Medicine (Lausanne),* 4**,** 83.

Momtazi, M., Kwan, P., Ding, J., Anderson, C. C., Honardoust, D., Goekjian, S. & Tredget, E. E. 2013. A nude mouse model of hypertrophic scar shows morphologic and histologic characteristics of human hypertrophic scar. *Wound Repair and Regeneration,* 21**,** 77-87.

Monaco, J. L. & Lawrence, W. T. 2003. Acute wound healing: an overview. *Clinics in Plastic Surgery,* 30**,** 1-12.

Munger, J. S., Harpel, J. G., Gleizes, P.-E., Mazzieri, R., Nunes, I. & Rifkin, D. B. 1997. Latent transforming growth factor-β: structural features and mechanisms of activation. *Kidney International,* 51**,** 1376-1382.

Nedergaard, J., Bengtsson, T. & Cannon, B. 2007. Unexpected evidence for active brown adipose tissue in adult humans. *American Journal of Physiology-Endocrinology and Metabolism,* 293**,** E444-E452.

Negenborn, V. L., Groen, J.-W., Smit, J. M., Niessen, F. B. & Mullender, M. G. 2016. The use of autologous fat grafting for treatment of scar tissue and scar-related conditions: a systematic review. *Plastic and Reconstructive Surgery,* 137**,** 31e-43e.

Niechajev, I. & Sevćuk, O. 1994. Long-term results of fat transplantation: clinical and histologic studies. *Plastic and Reconstructive Surgery,* 94**,** 496-506.

O'Brien, L., & Jones, D. J. (2013). Silicone gel sheeting for preventing and treating hypertrophic and keloid scars. Cochrane database of systematic reviews, (9):CD003826.

Oishi, Y., Manabe, I., Tobe, K., Ohsugi, M., Kubota, T., Fujiu, K., Maemura, K., Kubota, N., Kadowaki, T. & Nagai, R. 2008. SUMOylation of Krüppel-like transcription factor 5 acts as a molecular switch in transcriptional programs of lipid metabolism involving PPAR-δ. *Nature Medicine,* 14**,** 656.

Ojima, K., Oe, M., Nakajima, I., Muroya, S. & Nishimura, T. 2016. Dynamics of protein secretion during adipocyte differentiation. *FEBS Open Bio,* 6**,** 816-26.

Pannu, J., Nakerakanti, S., Smith, E., Ten Dijke, P. & Trojanowska, M. 2007. Transforming growth factor-β receptor type I-dependent fibrogenic gene program is mediated via activation of Smad1 and ERK1/2 pathways. *Journal of Biological Chemistry,* 282**,** 10405-10413.

Park, H.-Y., Kwon, H. M., Lim, H. J., Hong, B. K., Lee, J. Y., Park, B. E., Jang, Y. S., Cho, S. Y. & Kim, H.-S. 2001. Potential role of leptin in angiogenesis: leptin induces endothelial cell proliferation and expression of matrix metalloproteinases in vivo and in vitro. *Experimental & Molecular Medicine,* 33**,** 95.

Parvizi, M. & Harmsen, M. C. 2015. Therapeutic prospect of adipose-derived stromal cells for the treatment of abdominal aortic aneurysm. *Stem Cells and Development,* 24**,** 1493-1505.

Pegorier, S., Campbell, G. A., Kay, A. B. & Lloyd, C. M. 2010. Bone morphogenetic protein (BMP)-4 and BMP-7 regulate differentially transforming growth factor (TGF)-beta1 in normal human lung fibroblasts (NHLF). *Respiratory Research,* 11**,** 85.

Peltoniemi, H. H., Salmi, A., Miettinen, S., Mannerström, B., Saariniemi, K., Mikkonen, R., Kuokkanen, H. & Herold, C. 2013. Stem cell enrichment does not warrant a higher graft survival in lipofilling of the breast: a prospective comparative study. *Journal of Plastic, Reconstructive & Aesthetic Surgery,* 66**,** 1494-1503.

Phan, T.-T., Sun, L., Bay, B.-H., Chan, S.-Y. & Lee, S.-T. 2003. Dietary compounds inhibit proliferation and contraction of keloid and hypertrophic scar-derived fibroblasts in vitro: therapeutic implication for excessive scarring. *Journal of Trauma and Acute Care Surgery,* 54**,** 1212-1224.

Picinich, S. C., Mishra, P. J., Mishra, P. J., Glod, J. & Banerjee, D. 2007. The therapeutic potential of mesenchymal stem cells: Cell-& tissue-based therapy. *Expert Opinion on Biological Therapy,* 7**,** 965-973.

Plikus, M. V., Guerrero-Juarez, C. F., Ito, M., Li, Y. R., Dedhia, P. H., Zheng, Y., Shao, M., Gay, D. L., Ramos, R., Hsi, T. C., et al. 2017. Regeneration of fat cells from myofibroblasts during wound healing. *Science,* 355**,** 748-752.

Powell, D., Mifflin, R., Valentich, J., Crowe, S., Saada, J. & West, A. 1999. Myofibroblasts. I. Paracrine cells important in health and disease. *American Journal of Physiology-Cell Physiology,* 277**,** C1-C19.

Prockop, D. J. 1997. Marrow stromal cells as stem cells for nonhematopoietic tissues. *Science,* 276**,** 71-74.

Pu, L. L. 2016. Mechanisms of fat graft survival. *Annals of plastic surgery,* 77**,** S84-S86.

Rabello, F. B., Souza, C. D. & Farina Júnior, J. A. 2014. Update on hypertrophic scar treatment. *Clinics,* 69**,** 565-573.

Rahimi, R. A. & Leof, E. B. 2007. TGF-β signaling: A tale of two responses. *Journal of Cellular Biochemistry,* 102**,** 593-608.

Raja, S. K., Garcia, M. S. & Isseroff, R. R. 2007. Wound re-epithelialization: modulating keratinocyte migration in wound healing. *Frontiers in Bioscience,* 12**,** 2849-2868.

Rajkumar, V. S., Howell, K., Csiszar, K., Denton, C. P., Black, C. M. & Abraham, D. J. 2005. Shared expression of phenotypic markers in systemic sclerosis indicates a convergence of pericytes and fibroblasts to a myofibroblast lineage in fibrosis. *Arthritis Research & Therapy,* 7**,** R1113.

Ramalho-Santos, M. & Willenbring, H. 2007. On the origin of the term “stem cell”. *Cell Stem Cell,* 1**,** 35-38.

Ramos, M. L. C., Gragnani, A. & Ferreira, L. M. 2008. Is there an ideal animal model to study hypertrophic scarring? *Journal of Burn Care & Research,* 29**,** 363-368.

Ren, H.-T., Hu, H., Li, Y., Jiang, H.-F., Hu, X.-L. & Han, C.-M. 2013. Endostatin inhibits hypertrophic scarring in a rabbit ear model. *Journal of Zhejiang University SCIENCE B,* 14**,** 224-230.

Rigotti, G., Marchi, A., Galie, M., Baroni, G., Benati, D., Krampera, M., Pasini, A. & Sbarbati, A. 2007. Clinical treatment of radiotherapy tissue damage by lipoaspirate transplant: a healing process mediated by adipose-derived adult stem cells. *Plastic and Reconstructive Surgery,* 119**,** 1409-1422.

Ring, B. D., Scully, S., Davis, C. R., Baker, M. B., Cullen, M. J., Pelleymounter, M. A. & Danilenko, D. M. 2000. Systemically and topically administered leptin both accelerate wound healing in diabetic ob/ob mice. *Endocrinology,* 141**,** 446-449.

Rockwell, W. B., Cohen, I. K. & Ehrlich, H. P. 1989. Keloids and hypertrophic scars: a comprehensive review. *Plastic and Reconstructive Surgery,* 84**,** 827-837.

Rohrich, R. J. & Pessa, J. E. 2007. The fat compartments of the face: anatomy and clinical implications for cosmetic surgery. *Plastic and Reconstructive Surgery,* 119**,** 2219-2227.

Rønnov-Jessen, L. & Petersen, O. W. 1993. Induction of alpha-smooth muscle actin by transforming growth factor-beta 1 in quiescent human breast gland fibroblasts. Implications for myofibroblast generation in breast neoplasia. *Laboratory Investigation; a Journal of Technical Methods and Pathology,* 68**,** 696-707.

Rosen, E. D., Hsu, C.-H., Wang, X., Sakai, S., Freeman, M. W., Gonzalez, F. J. & Spiegelman, B. M. 2002. C/EBPα induces adipogenesis through PPARγ: a unified pathway. *Genes & Development,* 16**,** 22-26.

Rosen, E. D., Sarraf, P., Troy, A. E., Bradwin, G., Moore, K., Milstone, D. S., Spiegelman, B. M. & Mortensen, R. M. 1999. PPARγ is required for the differentiation of adipose tissue in vivo and in vitro. *Molecular Cell,* 4**,** 611-617.

Rosen, E. D. & Spiegelman, B. M. 2006. Adipocytes as regulators of energy balance and glucose homeostasis. *Nature,* 444**,** 847-53.

Rosen, E. D. & Spiegelman, B. M. 2014. What we talk about when we talk about fat. *Cell,* 156**,** 20-44.

Rosenow, A., Arrey, T. N., Bouwman, F. G., Noben, J.-P., Wabitsch, M., Mariman, E. C., Karas, M. & Renes, J. 2010. Identification of novel human adipocyte secreted proteins by using SGBS cells. *Journal of Proteome Research,* 9**,** 5389-5401.

Ross, S. E., Hemati, N., Longo, K. A., Bennett, C. N., Lucas, P. C., Erickson, R. L. & Macdougald, O. A. 2000. Inhibition of adipogenesis by Wnt signaling. *Science,* 289**,** 950-953.

Salathia, N. S., Shi, J., Zhang, J. & Glynne, R. J. 2013. An in vivo screen of secreted proteins identifies adiponectin as a regulator of murine cutaneous wound healing. *Journal of Investigative Dermatology,* 133**,** 812-821.

Sarrazy, V., Billet, F., Micallef, L., Coulomb, B. & Desmouliere, A. 2011. Mechanisms of pathological scarring: role of myofibroblasts and current developments. *Wound Repair and Regeneration,* 19 Suppl 1**,** s10-5.

Schaffler, A. & Buchler, C. 2007. Concise review: adipose tissue-derived stromal cells--basic and clinical implications for novel cell-based therapies. *Stem Cells,* 25**,** 818-27.

Scherer, P. E. 2006. Adipose tissue: from lipid storage compartment to endocrine organ. *Diabetes,* 55**,** 1537-1545.

Schmidt, B. A. & Horsley, V. 2013. Intradermal adipocytes mediate fibroblast recruitment during skin wound healing. *Development,* 140**,** 1517-27.

Schnabl, B., Kweon, Y. O., Frederick, J. P., Wang, X. F., Rippe, R. A. & Brenner, D. A. 2001. The role of Smad3 in mediating mouse hepatic stellate cell activation. *Hepatology,* 34**,** 89-100.

Schreiber, I., Dorpholz, G., Ott, C. E., Kragesteen, B., Schanze, N., Lee, C. T., Kohrle, J., Mundlos, S., Ruschke, K. & Knaus, P. 2017. BMPs as new insulin sensitizers: enhanced glucose uptake in mature 3T3-L1 adipocytes via PPARgamma and GLUT4 upregulation. *Scientific Reports,* 7**,** 17192.

Schűrch, W., Seemayer, T., Hinz, B. & Gabbiani, G. 2006. Myofibroblast. *Histology for Pathologist***,** 123-156.

Seo, B. F., Lee, J. Y. & Jung, S.-N. 2013. Models of abnormal scarring. *BioMed Research International,* 2013.

Seok, J., Warren, H. S., Cuenca, A. G., Mindrinos, M. N., Baker, H. V., Xu, W., Richards, D. R., Mcdonald-Smith, G. P., Gao, H. & Hennessy, L. 2013. Genomic responses in mouse models poorly mimic human inflammatory diseases. *Proceedings of the National Academy of Sciences,* 110**,** 3507-3512.

Serini, G. & Gabbiani, G. 1999. Mechanisms of myofibroblast activity and phenotypic modulation. *Experimental Cell Research,* 250**,** 273-283.

Sethi, J. K. & Vidal-Puig, A. J. 2007. Thematic review series: adipocyte biology. Adipose tissue function and plasticity orchestrate nutritional adaptation. *Journal of Lipid Research,* 48**,** 1253-1262.

Shanti, R. M., Janjanin, S., Li, W.-J., Nesti, L. J., Mueller, M. B., Tzeng, M. B. & Tuan, R. S. 2008. In vitro adipose tissue engineering using an electrospun nanofibrous scaffold. *Annals of Plastic Surgery,* 61**,** 566-571.

Shetlar, M., Shetlar, C., Hendricks, L. & Kischer, C. 1985. The use of athymic nude mice for the study of human keloids. *Proceedings of the Society for Experimental Biology and Medicine,* 179**,** 549-552.

Shi, Y. & Massagué, J. 2003. Mechanisms of TGF-β signaling from cell membrane to the nucleus. *Cell,* 113**,** 685-700.

Shibata, S., Tada, Y., Asano, Y., Hau, C. S., Kato, T., Saeki, H., Yamauchi, T., Kubota, N., Kadowaki, T. & Sato, S. 2012. Adiponectin regulates cutaneous wound healing by promoting keratinocyte proliferation and migration via the ERK signaling pathway. *The Journal of Immunology,* 189**,** 3231-3241.

Shlyonsky, V., Soussia, I. B., Naeije, R. & Mies, F. 2011. Opposing effects of bone morphogenetic protein-2 and endothelin-1 on lung fibroblast chloride currents. *American Journal of Respiratory Cell and Molecular Biology,* 45**,** 1154-60.

Siersbæk, R., Nielsen, R. & Mandrup, S. 2012. Transcriptional networks and chromatin remodeling controlling adipogenesis. *Trends in Endocrinology & Metabolism,* 23**,** 56-64.

Simon, G. A. & Maibach, H. I. 2000. The pig as an experimental animal model of percutaneous permeation in man: qualitative and quantitative observations–an overview. *Skin Pharmacology and Physiology,* 13**,** 229-234.

Simonacci, F., Bertozzi, N., Grieco, M. P., Grignaffini, E. & Raposio, E. 2017. Procedure, applications, and outcomes of autologous fat grafting. *Annals of Medicine and Surgery,* 20**,** 49-60.

Singer, A. 1999. Clark RA. Cutaneous wound healing*. The New England Journal of Medicine,* 341**,** 738-746.

Skalli, O., Schürch, W., Seemayer, T., Lagace, R., Montandon, D., Pittet, B. & Gabbiani, G. 1989. Myofibroblasts from diverse pathologic settings are heterogeneous in their content of actin isoforms and intermediate filament proteins. *Laboratory Investigation; a Journal of Technical Methods and Pathology,* 60**,** 275-285.

Slemp, A. E. & Kirschner, R. E. 2006. Keloids and scars: a review of keloids and scars, their pathogenesis, risk factors, and management. *Current Opinion in Pediatrics,* 18**,** 396-402.

Sottile, V. & Seuwen, K. 2000. Bone morphogenetic protein-2 stimulates adipogenic differentiation of mesenchymal precursor cells in synergy with BRL 49653 (rosiglitazone). *FEBS letters,* 475**,** 201-204.

Spiekman, M., Przybyt, E., Plantinga, J. A., Gibbs, S., Van Der Lei, B. & Harmsen, M. C. 2014. Adipose tissue-derived stromal cells inhibit TGF-beta1-induced differentiation of human dermal fibroblasts and keloid scar-derived fibroblasts in a paracrine fashion. *Plastic and Reconstructive Surgery,* 134**,** 699-712.

Stambe, C., Atkins, R. C., Tesch, G. H., Masaki, T., Schreiner, G. F. & Nikolic-Paterson, D. J. 2004. The role of p38α mitogen-activated protein kinase activation in renal fibrosis. *Journal of the American Society of Nephrology,* 15**,** 370-379.

Summerfield, A., Meurens, F. & Ricklin, M. E. 2015. The immunology of the porcine skin and its value as a model for human skin. *Molecular Immunology,* 66**,** 14-21.

Sund, B. & Arrow, A. K. 2000. *New Developments in Wound Care*, Clinica reports.

Suzuki, M., Satoh, A., Ide, H. & Tamura, K. 2005. Nerve-dependent and-independent events in blastema formation during Xenopus froglet limb regeneration. *Developmental Biology,* 286**,** 361-375.

Takada, I., Suzawa, M., Matsumoto, K. & Kato, S. 2007. Suppression of PPAR transactivation switches cell fate of bone marrow stem cells from adipocytes into osteoblasts. *Annals of the New York Academy of Sciences,* 1116**,** 182-195.

Tang, Q.-Q., Otto, T. C. & Lane, M. D. 2004. Commitment of C3H10T1/2 pluripotent stem cells to the adipocyte lineage. *Proceedings of the National Academy of Sciences,* 101**,** 9607-9611.

Tanikawa, D. Y., Aguena, M., Bueno, D. F., Passos-Bueno, M. R. & Alonso, N. 2013. Fat grafts supplemented with adipose-derived stromal cells in the rehabilitation of patients with craniofacial microsomia. *Plastic and Reconstructive Surgery,* 132**,** 141-152.

Ten Dijke, P., Goumans, M. J., Itoh, F. & Itoh, S. 2002. Regulation of cell proliferation by Smad proteins. *Journal of Cellular Physiology,* 191**,** 1-16.

Ten Dijke, P. & Hill, C. S. 2004. New insights into TGF-β–Smad signalling. *Trends in Biochemical Sciences,* 29**,** 265-273.

Thomou, T., Mori, M. A., Dreyfuss, J. M., Konishi, M., Sakaguchi, M., Wolfrum, C., Rao, T. N., Winnay, J. N., Garcia-Martin, R. & Grinspoon, S. K. 2017. Adipose-derived circulating miRNAs regulate gene expression in other tissues. *Nature,* 542**,** 450.

Tien, E. S., Davis, J. W. & Vanden Heuvel, J. P. 2004. Identification of the CREB-binding protein/p300-interacting protein CITED2 as a peroxisome proliferator-activated receptor alpha coregulator. *Journal of Biological Chemistry,* 279**,** 24053-63.

Tiryaki, T., Findikli, N. & Tiryaki, D. 2011. Staged stem cell-enriched tissue (SET) injections for soft tissue augmentation in hostile recipient areas: a preliminary report. *Aesthetic Plastic Surgery,* 35**,** 965-971.

Todorovic, V., Jurukovski, V., Chen, Y., Fontana, L., Dabovic, B. & Rifkin, D. 2005. Latent TGF-β binding proteins. *The International Journal of Biochemistry & Cell Biology,* 37**,** 38-41.

Tomasek, J. J., Gabbiani, G., Hinz, B., Chaponnier, C. & Brown, R. A. 2002. Myofibroblasts and mechano-regulation of connective tissue remodelling. *Nature Reviews Molecular Cell Biology,* 3**,** 349.

Tontonoz, P., Hu, E., Graves, R. A., Budavari, A. I. & Spiegelman, B. M. 1994a. mPPAR gamma 2: tissue-specific regulator of an adipocyte enhancer. *Genes & Development,* 8**,** 1224-1234.

Tontonoz, P., Hu, E. & Spiegelman, B. M. 1994b. Stimulation of adipogenesis in fibroblasts by PPARγ2, a lipid-activated transcription factor. *Cell,* 79**,** 1147-1156.

Trayhurn, P. & Beattie, J. H. 2001. Physiological role of adipose tissue: white adipose tissue as an endocrine and secretory organ. *Proceedings of the Nutrition Society,* 60**,** 329-339.

Treindl, F., Ruprecht, B., Beiter, Y., Schultz, S., Döttinger, A., Staebler, A., Joos, T. O., Kling, S., Poetz, O. & Fehm, T. 2016. A bead-based western for high-throughput cellular signal transduction analyses. *Nature Communications,* 7**,** 12852.

Tremolada, C., Palmieri, G. & Ricordi, C. 2010. Adipocyte transplantation and stem cells: plastic surgery meets regenerative medicine. *Cell Transplantation,* 19**,** 1217-1223.

Tseng, Y.-H., Kokkotou, E., Schulz, T. J., Huang, T. L., Winnay, J. N., Taniguchi, C. M., Tran, T. T., Suzuki, R., Espinoza, D. O. & Yamamoto, Y. 2008. New role of bone morphogenetic protein 7 in brown adipogenesis and energy expenditure. *Nature,* 454**,** 1000.

Uemura, M., Swenson, E. S., Gaça, M. D., Giordano, F. J., Reiss, M. & Wells, R. G. 2005. Smad2 and Smad3 play different roles in rat hepatic stellate cell function and α-smooth muscle actin organization. *Molecular Biology of the Cell,* 16**,** 4214-4224.

Uysal, C. A., Tobita, M., Hyakusoku, H. & Mizuno, H. 2014. The effect of bone-marrow-derived stem cells and adipose-derived stem cells on wound contraction and epithelization. *Advances in Wound Care,* 3**,** 405-413.

Vallée, A., Lecarpentier, Y., Guillevin, R. & Vallée, J.-N. 2017. Interactions between TGF-β1, canonical WNT/β-catenin pathway and PPAR γ in radiation-induced fibrosis. *Oncotarget,* 8**,** 90579.

Van Den Broek, L. J., Bergers, L. I., Reijnders, C. M. & Gibbs, S. 2017. Progress and future prospectives in skin-on-chip development with emphasis on the use of different cell types and technical challenges. *Stem Cell Reviews and Reports,* 13**,** 418-429.

Van Den Broek, L. J., Limandjaja, G. C., Niessen, F. B. & Gibbs, S. 2014. Human hypertrophic and keloid scar models: principles, limitations and future challenges from a tissue engineering perspective. *Experimental Dermatology,* 23**,** 382-386.

Van Dongen, J., Harmsen, M., Van Der Lei, B. & Stevens, H. 2018. Augmentation of Dermal Wound Healing by Adipose Tissue-Derived Stromal Cells (ASC). *Bioengineering,* 5**,** 91.

Vaughan, M. B., Howard, E. W. & Tomasek, J. J. 2000. Transforming growth factor-β1 promotes the morphological and functional differentiation of the myofibroblast. *Experimental Cell Research,* 257**,** 180-189.

Verhoekx, J. S., Mudera, V., Walbeehm, E. T. & Hovius, S. E. 2013. Adipose-derived stem cells inhibit the contractile myofibroblast in Dupuytren's disease. *Plastic and Reconstructive Surgery,* 132**,** 1139-48.

Villarroya, F., Cereijo, R., Villarroya, J. & Giralt, M. 2017. Brown adipose tissue as a secretory organ. *Nature Reviews Endocrinology,* 13**,** 26.

Von Heimburg, D., Hemmrich, K., Zachariah, S., Staiger, H. & Pallua, N. 2005. Oxygen consumption in undifferentiated versus differentiated adipogenic mesenchymal precursor cells. *Respiratory Physiology & Neurobiology,* 146**,** 107-116.

Wang, N.-D., Finegold, M. J., Bradley, A., Ou, C. N., Abdelsayed, S. V., Wilde, M. D., Taylor, L. R., Wilson, D. R. & Darlington, G. J. 1995. Impaired energy homeostasis in C/EBP alpha knockout mice. *Science,* 269**,** 1108-1112.

Wei, J., Ghosh, A. K., Sargent, J. L., Komura, K., Wu, M., Huang, Q. Q., Jain, M., Whitfield, M. L., Feghali-Bostwick, C. & Varga, J. 2010. PPARgamma downregulation by TGFss in fibroblast and impaired expression and function in systemic sclerosis: a novel mechanism for progressive fibrogenesis. *PLoS One,* 5**,** e13778.

Weissman, I. L. 2000. Stem cells: units of development, units of regeneration, and units in evolution. *Cell,* 100**,** 157-168.

Werner, S. & Grose, R. 2003. Regulation of wound healing by growth factors and cytokines. *Physiological Reviews,* 83**,** 835-870.

Wettlaufer, S. H., Scott, J. P., Mceachin, R. C., Peters-Golden, M. & Huang, S. K. 2016. Reversal of the Transcriptome by Prostaglandin E2 during Myofibroblast Dedifferentiation. *American Journal of Respiratory Cell and Molecular Biology,* 54**,** 114-27.

Wheeland, R. 1996. Keloids and hypertrphic scars. *Cutaneous Medicine and Surgery***,** 900-5.

White, E. S., Atrasz, R. G., Hu, B., Phan, S. H., Stambolic, V., Mak, T. W., Hogaboam, C. M., Flaherty, K. R., Martinez, F. J. & Kontos, C. D. 2006. Negative regulation of myofibroblast differentiation by PTEN (Phosphatase and Tensin Homolog Deleted on chromosome 10). *American Journal of Respiratory and Critical Care Medicine,* 173**,** 112-121.

Wilgus, T. A., Ferreira, A. M., Oberyszyn, T. M., Bergdall, V. K. & Dipietro, L. A. 2008. Regulation of scar formation by vascular endothelial growth factor. *Laboratory Investigation,* 88**,** 579.

Wu, J., Boström, P., Sparks, L. M., Ye, L., Choi, J. H., Giang, A.-H., Khandekar, M., Virtanen, K. A., Nuutila, P. & Schaart, G. 2012. Beige adipocytes are a distinct type of thermogenic fat cell in mouse and human. *Cell,* 150**,** 366-376.

Wu, M., Melichian, D. S., Chang, E., Warner-Blankenship, M., Ghosh, A. K. & Varga, J. 2009. Rosiglitazone abrogates bleomycin-induced scleroderma and blocks profibrotic responses through peroxisome proliferator-activated receptor-γ. *The American Journal of Pathology,* 174**,** 519-533.

Wu, Z., Bucher, N. & Farmer, S. R. 1996. Induction of peroxisome proliferator-activated receptor gamma during the conversion of 3T3 fibroblasts into adipocytes is mediated by C/EBPbeta, C/EBPdelta, and glucocorticoids. *Molecular and Cellular Biology,* 16**,** 4128-4136.

Wu, Z., Rosen, E. D., Brun, R., Hauser, S., Adelmant, G., Troy, A. E., Mckeon, C., Darlington, G. J. & Spiegelman, B. M. 1999. Cross-regulation of C/EBPα and PPARγ controls the transcriptional pathway of adipogenesis and insulin sensitivity. *Molecular Cell,* 3**,** 151-158.

Wu, Z., Xie, Y., Bucher, N. & Farmer, S. R. 1995. Conditional ectopic expression of C/EBP beta in NIH-3T3 cells induces PPAR gamma and stimulates adipogenesis. *Genes & Development,* 9**,** 2350-2363.

Wynn, T. A. 2008. Cellular and molecular mechanisms of fibrosis. *The Journal of Pathology: A Journal of the Pathological Society of Great Britain and Ireland,* 214**,** 199-210.

Yang, D. Y., Li, S. R., Wu, J. L., Chen, Y. Q., Li, G., Bi, S. & Dai, X. 2007a. Establishment of a hypertrophic scar model by transplanting full-thickness human skin grafts onto the backs of nude mice. *Plastic and Reconstructive Surgery,* 119**,** 104-109.

Yang, Z., Mu, Z., Dabovic, B., Jurukovski, V., Yu, D., Sung, J., Xiong, X. & Munger, J. S. 2007b. Absence of integrin-mediated TGFβ1 activation in vivo recapitulates the phenotype of TGFβ1-null mice. *The Journal of Cell Biology,* 176**,** 787-793.

Yeh, W.-C., Cao, Z., Classon, M. & Mcknight, S. L. 1995. Cascade regulation of terminal adipocyte differentiation by three members of the C/EBP family of leucine zipper proteins. *Genes & Development,* 9**,** 168-181.

Ying, W., Riopel, M., Bandyopadhyay, G., Dong, Y., Birmingham, A., Seo, J. B., Ofrecio, J. M., Wollam, J., Hernandez-Carretero, A. & Fu, W. 2017. Adipose tissue macrophage-derived exosomal miRNAs can modulate in vivo and in vitro insulin sensitivity. *Cell,* 171**,** 372-384. e12.

Zeisberg, E. M., Tarnavski, O., Zeisberg, M., Dorfman, A. L., Mcmullen, J. R., Gustafsson, E., Chandraker, A., Yuan, X., Pu, W. T. & Roberts, A. B. 2007. Endothelial-to-mesenchymal transition contributes to cardiac fibrosis. *Nature Medicine,* 13**,** 952.

Zhang, C., Niu, C., Yang, K. & Shaker, A. 2018. Human esophageal myofibroblast secretion of bone morphogenetic proteins and GREMLIN1 and paracrine regulation of squamous epithelial growth. *Scientific Reports,* 8**,** 12354.

Zhang, G.-Y., Cheng, T., Zheng, M.-H., Yi, C.-G., Pan, H., Li, Z.-J., Chen, X.-L., Yu, Q., Jiang, L.-F. & Zhou, F.-Y. 2009. Activation of peroxisome proliferator-activated receptor-γ inhibits transforming growth factor-β1 induction of connective tissue growth factor and extracellular matrix in hypertrophic scar fibroblasts in vitro. *Archives of Dermatological Research,* 301**,** 515-522.

Zhang, H., Kumar, S., Barnett, A. & Eggo, M. 2000. Ceiling culture of mature human adipocytes: use in studies of adipocyte functions. *Journal of Endocrinology,* 164**,** 119-128.

Zhang, Q., Liu, L. N., Yong, Q., Deng, J. C. & Cao, W. G. 2015. Intralesional injection of adipose-derived stem cells reduces hypertrophic scarring in a rabbit ear model. *Stem Cell Research & Therapy,* 6**,** 145.

Zhang, Y., Proenca, R., Maffei, M., Barone, M., Leopold, L. & Friedman, J. M. 1994. Positional cloning of the mouse obese gene and its human homologue. *Nature,* 372**,** 425.

Zhao, J., Shi, W., Wang, Y.-L., Chen, H., Bringas Jr, P., Datto, M. B., Frederick, J. P., Wang, X.-F. & Warburton, D. 2002. Smad3 deficiency attenuates bleomycin-induced pulmonary fibrosis in mice. *American Journal of Physiology-Lung Cellular and Molecular Physiology,* 282**,** L585-L593.

Zhong, J., Krawczyk, S. A., Chaerkady, R., Huang, H., Goel, R., Bader, J. S., Wong, G. W., Corkey, B. E. & Pandey, A. 2010. Temporal profiling of the secretome during adipogenesis in humans. *Journal of Proteome Research,* 9**,** 5228-5238.

Zhu, K. Q., Engrav, L. H., Gibran, N. S., Cole, J. K., Matsumura, H., Piepkorn, M., Isik, F. F., Carrougher, G. J., Muangman, P. M. & Yunusov, M. Y. 2003. The female, red Duroc pig as an animal model of hypertrophic scarring and the potential role of the cones of skin. *Burns,* 29**,** 649-664.

Zuk, P. A., Zhu, M., Ashjian, P., De Ugarte, D. A., Huang, J. I., Mizuno, H., Alfonso, Z. C., Fraser, J. K., Benhaim, P. & Hedrick, M. H. 2002. Human adipose tissue is a source of multipotent stem cells. *Molecular Biology of the Cell,* 13**,** 4279-95.

Zuk, P. A., Zhu, M., Mizuno, H., Huang, J., Futrell, J. W., Katz, A. J., Benhaim, P., Lorenz, H. P. & Hedrick, M. H. 2001. Multilineage cells from human adipose tissue: implications for cell-based therapies. *Tissue Engineering,* 7**,** 211-228.

Zvonic, S., Lefevre, M., Kilroy, G., Floyd, Z. E., Delany, J. P., Kheterpal, I., Gravois, A., Dow, R., White, A. & Wu, X. 2007. Secretome of Primary Cultures of Human

Adipose-derived Stem Cells Modulation of Serpins by Adipogenesis. *Molecular & Cellular Proteomics,* 6**,** 18-28.

LIST OF FIGURES

PUBLICATIONS AND CONTRIBUTIONS

ORIGINAL ARTICLES

Hoerst K., van den Broek L., Erdmann G., Klein O., von Fritschen U., Gibbs S., Hedtrich S., *Regenerative potential of adipocytes in hypertrophic scars is mediated by myofibroblast reprogramming,* J Mol Med, 2019

CONFERENCE PROCEEDINGS

Hörst, K., v. Fritschen, U., Gibbs, S., Knaus P., Hedtrich, S., *Regenerative potential of adipocytes on scarring,* On-site visit - Proposal for an Einstein Center for Regenerative Therapies, Berlin, September 2018

Hörst, K., van den Broek, Gibbs, S., v. Fritschen, U., Hedtrich, S. *Regenerative Potential of Adipose Tissue – The Role of BMPs in Myofibroblast Reprogramming,* 3rd German Pharm-Tox Summit, Göttingen, February 2018

Hörst, K., van den Broek, Gibbs, S., v. Fritschen, U., Hedtrich, S. *Regenerative potential of adipocytes – Potential treatment for hypertrophic scars?* Ernst Klenk Symposium in Molecular Medicine: Tissue regeneration, wound healing and fibrosis: Translating basic concepts into regenerative therapy, Köln, October 2017

Hörst, K., van den Broek, Gibbs, S., v. Fritschen, U., Hedtrich, S. *Regenerative Potential of Adipocytes on Hypertrophic Scar Tissue?* Annual Meeting of the German Pharmaceutical Society *(*DPhG), Saarbrücken, September 2017

Hörst, K., v. Fritschen, U., Hedtrich, S. *Intercellular crosstalk of adipocytes and (myo-) fibroblasts and its potential relevance for tissue regeneration* 10th Scientific Symposium - Shaping future pharmaceutical research: Junior scientists present (DPhG), Berlin, July 2016

TALKS

Hörst, K., van den Broek, Gibbs, S., v. Fritschen, U., Hedtrich, S. *Co-Cultivation of myofibroblasts and adipocytes provides new insights into hypertrophic scar regeneration,* European Congress for Alternatives to Animal Testing (EUSAAT), Linz, September 2018

Hörst, K., van den Broek, Gibbs, S., v. Fritschen, U., Hedtrich, S. *Myofibroblast reprogramming in hypertrophic scars is mediated by adipocytes via BMPs,* 12th Scientific

Symposium - Shaping future pharmaceutical research: Junior scientists present, Berlin, July 2018

Hörst, K. (invited speaker), *Regenerative Potential of Adipose Tissue*, 16th International BEAULI™ Symposium, Berlin, June 2018

Hörst, K., van den Broek, Gibbs, S., v. Fritschen, U., Hedtrich, S. *Regenerative Potential of Adipose Tissue – The Role of BMPs in Myofibroblast Reprogramming,* ScarCon ETRS congress, Amsterdam, Jun 2018

Hörst, K., van den Broek, Gibbs, S., v. Fritschen, U., Hedtrich, S*. Regeneratives Potenzial von Adipozyten durch Reprogrammierung von Myofibroblasten*, Arbeitsgemeinschaft Dermatologischer Forschung (ADF), Round Table, Zeuthen, December 2017

AWARDS

Best oral presentation, 3rd place, European Congress for Alternatives to Animal Testing (EUSAAT), Linz, September 2018

YSTA, Young Scientist Travel Award, European Congress for Alternatives to Animal Testing (EUSAAT), Linz, September 2018

ECRT Grant 2018, Einstein Center for Regenerative Therapies (ECRT), Berlin, 2018

Travel Grant by Women's Representative (Frauenförderung des Fachbereichs BCP) of Freie Universität Berlin for the Annual Meeting of the German Pharmaceutical Society (DPhG), Saarbrücken, September 2017

Einstein Kickbox Seed Grant 2017, Einstein Center for Regenerative Therapies (ECRT), Berlin, 2017

ACKNOWLEDGMENT

Throughout the realization of this doctoral project, I have received a great deal of support and assistance. I would first like to thank my supervisor, Prof. Dr. Sarah Hedtrich. Thank you very much for providing me this interesting, interdisciplinary project and your ongoing trust in me. You were always there for any scientific but also personal advice.

I would also like to thank Prof. Dr. Matthias Melzig for taking time and effort to evaluate this thesis as a second reviewer.

A special thanks goes to Prof. Dr. Susan Gibbs who invited me to perform experiments in her lab in Amsterdam. Not only the experiments I have run there were of great importance for this project but also her scientific experience and personal advice has had a major impact on my development as a doctoral candidate. Her group at VUmc made my stays in Amsterdam very special: Maria who had answers to every question and Judith and Elisabetta who introduced me into the Dutch way of life. Especially I will always remember the discussions with Sander on a Monday morning after a formula 1 grand prix about the best German (or Dutch) driver.

Dr. Uwe von Fritschen gave me valuable insights into the daily life of a plastic surgeon – not only in the OR but especially by inviting me to the BEAULI workshop, thanks for this opportunity!

Thanks to the Einstein Center for Regenerative Therapies (ECRT) in Berlin that supported this project financially and scientifically.

Since the everyday life of a doctoral candidate can be very frustrating and challenging from time to time, a supporting work environment makes a major difference. Especially the people from the “Kieztour” group have made this difference. Thanks for the ongoing advice, coffee breaks and after work beers to Dr. Gerrit Müller, Dr. Leonie Verheyen, Dr. Guy Yealland, Dr. Kay Strüver and Dr. Stefan Hönzke. A special thanks goes to Anna Löwa who was still there when the others successfully had left the institute and supported me with scientific and personal advice in any possible way.

Without Petra Schmidt I would still struggle with the order procedure. Your support and humour helped me through a lot of demanding days.

Of course, also my family, especially my parents, my grandma and my brother, deserve words of thank for their ongoing and unconditional support and help, thank you!

STATEMENT OF AUTHORSHIP

Hiermit versichere ich, Katharina Hörst, die vorliegende Arbeit selbstständig verfasst zu haben. Alle verwendeten Hilfsmittel und Hilfen habe ich angegeben. Die Arbeit wurde weder in einem früheren Promotionsverfahren angenommen noch als ungenügend beurteilt.

Berlin, 04.06.2019

_____

Katharina Hörst

CURRICULUM VITAE

Due to data protection reasons, the CV has been removed.

APPENDIX

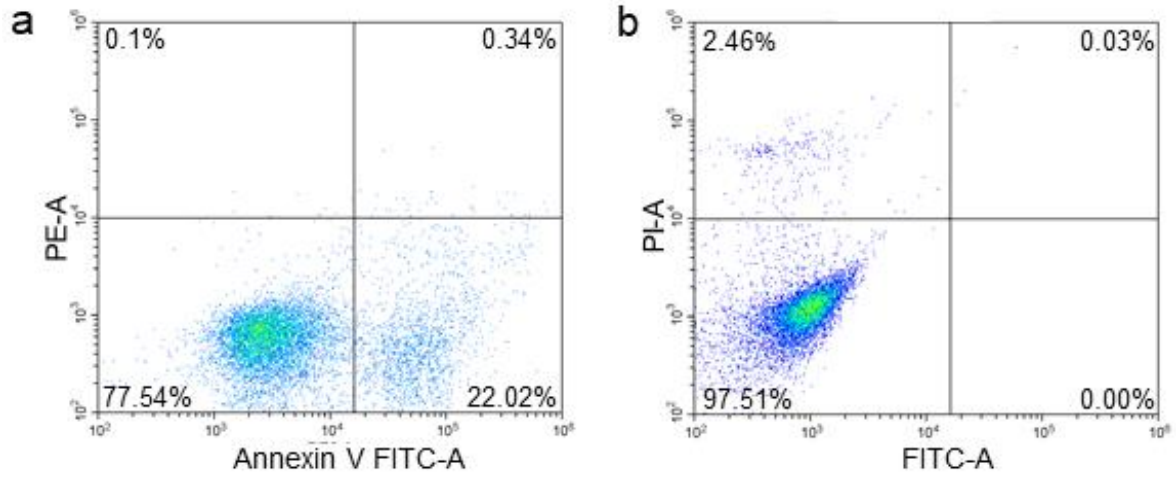

Fig. 30: Annexin V/PI staining of the DMSO-treated samples according to Fig. 17.
DMSO-treated myofibrbolasts were either stained with Annexin V (a) or incubated with PI (b) and subjected to flow cytometry.

Table 4: List of proteins found in mass spectrometry including their score and peptide number. Proteins associated with GO term 0042060 (wound healing) are marked with [1]. Proteins associated with GO term 0031099 (regeneration) are indicated by [2].

Accession Number	Name	Score A	Score B	Score C	Match A	Match B	Match C
CO1A2[1]	Collagen alpha-2(I) chain	5230.7	7298.0	3113.9	53	46	51
FN1[1]	Fibronectin	2976.7	8833.9	7528.1	32	50	60
CO1A1[1]	Collagen alpha-1(I) chain	2609.2	4921.0	1082.8	38	44	49
CO3A1[1]	Collagen alpha-1(III) chain	1253.0	2798.8	129.4	26	30	38
PGBM	Basement membrane-specific heparan sulfate proteoglycan core protein	329.6	509.6	551.1	11	34	41
CO4A2	Collagen alpha-2(IV) chain	528.5	358.5	142.6	18	15	25
NID1	Nidogen-1	959.4	260.7	574.4	16	17	19
VIME	Vimentin	269.2	1214.8	1390.3	11	16	23
TENA[2]	Tenascin	237.2	133.2	354.8	5	12	31
TSP1[1]	Thrombospondin-1	888.7	987.2	1298.8	14	12	22
A2MG[1]	Alpha-2-macroglobulin	763.6	498.9	768.1	17	13	15
CO6A1	Collagen alpha-1(VI) chain	502.5	1570.0	503.9	8	13	23
TSP2	Thrombospondin-2	361.8	448.8	591.7	11	15	16
CO3[1]	Complement C3	967.4	543.9	886.3	12	14	13
GELS[1,2]	Gelsolin	404.9	443.4	514.8	10	12	10

COMP	Cartilage oligomeric matrix protein	1159.0	629.8	976.6	12	9	10
ACTN4[1]	Alpha-actinin-4	68.3	602.0	873.0	4	12	14
CO5A1[1]	Collagen alpha-1(V) chain	311.6	686.0	252.4	7	11	11
LDHA	L-lactate dehydrogenase A chain	735.7	1174.8	2016.5	11	8	9
BGH3	Transforming growth factor-beta-induced protein ig-h3	84.7	1227.3	671.7	4	10	13
PTX3	Pentraxin-related protein PTX3	329.0	1084.8	721.0	5	8	14
VINC[1]	Vinculin	221.6	371.7	690.6	8	4	14
PAI1[1]	Plasminogen activator inhibitor 1	198.0	786.8	142.2	3	10	12
LAMA4	Laminin subunit alpha-4	199.5	227.5	168.0	5	7	12
ENOA	Alpha-enolase	776.6	975.5	1032.3	8	5	10
C1R	Complement C1r subcomponent	373.9	93.3	79.1	6	7	7
LAMB1	Laminin subunit beta-1		107.8	56.6		7	11
C1S	Complement C1s subcomponent	21.5	357.4	234.9	1	9	7
LG3BP	Galectin-3-binding protein	71.3	135.9	107.5	4	6	7
DPYL2	Dihydropyrimidinase-related protein 2	128.8	267.9	112.0	6	5	6
FBLN1[1]	Fibulin-1		188.6	161.6		8	9
LAMC1	Laminin subunit gamma-1	19.0	96.7	146.2	1	7	8
LUM	Lumican	759.4	373.3	411.9	4	7	5
PGK1	Phosphoglycerate kinase 1	142.1	535.4	623.9	4	4	8
NID2	Nidogen-2	130.9	46.1	67.0	5	5	6
SPRC[1]	SPARC	214.0	903.1	499.9	6	5	5
CALU[1,2]	Calumenin		293.0	293.4		10	6
FSTL1	Follistatin-related protein 1	277.2	527.7	423.2	6	4	5
ALDOA[1]	Fructose-bisphosphate aldolase A	203.2	503.2	382.1	7	4	4
PDIA3	Protein disulfide-isomerase A3	77.6	317.5	126.6	5	7	2
TPM4	Tropomyosin alpha-4 chain	213.7	220.4	303.3	5	4	5
TKT	Transketolase	195.9	475.3	492.7	5	4	5
G3P	Glyceraldehyde-3-phosphate dehydrogenase	449.6	1014.1	589.4	6	3	5
CALR	Calreticulin	103.6	725.4	485.9	3	6	4
TAGL	Transgelin	39.9	280.9	249.9	3	3	7
LDHB	L-lactate dehydrogenase B chain	127.2	192.2	109.1	4	5	3
PPIA[1]	Peptidyl-prolyl cis-trans isomerase A	201.9	690.0	570.8	2	4	5
SPON1	Spondin-1	73.4	93.4	84.5	2	5	4

COF1[1]	Cofilin-1	169.2	360.8	375.4	4	4	3
PGAM1	Phosphoglycerate mutase 1	109.5	152.0	133.8	4	4	3
MOES	Moesin	89.2	335.7	259.1	4	2	5
IBP7	Insulin-like growth factor-binding protein 7	42.8	225.0	195.6	1	4	5
PRDX1	Peroxiredoxin-1	51.5	136.9	100.4	4	2	4
PROF1[1]	Profilin-1	200.1	335.3	302.5	4	3	3
APOE[2]	Apolipoprotein E	117.1	476.2		3	7	
CYTC	Cystatin-C		273.1	240.6		4	6
GSTP1	Glutathione S-transferase P	128.5	286.3	233.6	3	3	3
ISLR	Immunoglobulin superfamily containing leucine-rich repeat protein	62.8	120.4	82.3	3	3	3
FABP4	Fatty acid-binding protein, adipocyte	111.2	559.8		5	1	
SPTN1	Spectrin alpha chain, non-erythrocytic 1		99.5	55.9		2	7
FBLN2	Fibulin-2	17.6	119.6	279.0	1	4	3
PGS1	Biglycan	22.9	146.3	13.2	1	4	3
KPYM[1,2]	Pyruvate kinase PKM	70.7	724.5	326.6	3	2	3
FAS	Fatty acid synthase	190.4	1189.3	30.9	4	5	4
COTL1	Coactosin-like protein	37.7	229.3	258.7	3	2	2
HSPB1[1]	Heat shock protein beta-1	54.3	214.2	152.8	3	1	3
CFAD[1]	Complement factor D	114.8	39.1		3	3	
FBLN5	Fibulin-5		30.5	28.0		3	4
CSTN1	Calsyntenin-1		33.8	91.9		2	3
PSA7	Proteasome subunit alpha type-7	87.0	112.0	91.5	1	1	3
TIMP1[1]	Metalloproteinase inhibitor 1	29.0	169.7	285.6	1	2	2
RLA2	60S acidic ribosomal protein P2	92.2	164.7	124.3	1	1	3
PRG4	Proteoglycan 4	49.7	15.8		2	2	
B2MG	Beta-2-microglobulin		94.1	26.2		2	3
MDHC	Malate dehydrogenase, cytoplasmic	27.1	124.7	90.9	1	1	2
ZYX	Zyxin		24.6	24.8		1	2
SODM	Superoxide dismutase [Mn], mitochondrial	25.0	25.6	37.3	1	2	1
RL10A	60S ribosomal protein L10a	21.9	26.8	29.3	1	1	1
P4HA1	Prolyl 4-hydroxylase subunit alpha-1		79.2	38.4		2	1
CATB	Cathepsin B		44.8	45.3		1	2
PLEC	Plectin		36.1	33.8		1	2
6PGL	6-phosphogluconolactonase	81.4		78.1	1		1

HNRPF	Heterogeneous nuclear ribonucleoprotein F	34.0		68.1	1		1
IBP6	Insulin-like growth factor-binding protein 6		34.0	34.1		1	1
NPM	Nucleophosmin		76.7	23.7		1	1
MDHM	Malate dehydrogenase, mitochondrial		53.9	32.8		1	1
THIO	Thioredoxin		64.0	67.1		1	1
FABP5	Fatty acid-binding protein, epidermal		64.8	24.0		1	1
IF5A1	Eukaryotic translation initiation factor 5A-1		295.3	135.7		1	1
PSB3	Proteasome subunit beta type-3		26.0	28.5		1	1

Table 5: List of proteins found in mass spectrometry including their score and peptide number. Proteins associated with GO term 0042060 (wound healing) are marked with [1]. Proteins associated with GO term 0001525 (angiogenesis) are indicated by [2].

Accession Number	Name	Score A	Score B	Score C	Match A	Match B	Match C
CO1A2[1]	Collagen alpha-2(I) chain	15138.2	16141.3	2815.1	60	39	47
FINC[1,2]	Fibronectin	30778.9	9138.0	8616.9	80	57	63
CO1A1[1]	Collagen alpha-1(I) chain	13013.0	16359.8	3111.8	58	27	44
CO3A1[1]	Collagen alpha-1(III) chain	4838.0	4097.7	474.9	39	12	29
PGBM[2]	Basement membrane-specific heparan sulfate proteoglycan core protein	4340.2	1144.4	614.6	52	36	35
CO4A2[2]	Collagen alpha-2(IV) chain	729.0	191.3	25.3	12	11	10
TSP1[2]	Thrombospondin-1	3429.5	1572.3	335.7	39	8	11
CO6A1	Collagen alpha-1(VI) chain	2181.9	1167.1	391.6	22	18	15
TSP2	Thrombospondin-2	1173.9	1075.0	68.0	11	3	9
CO5A1[1]	Collagen alpha-1(V) chain	2111.3	886.6	309.6	34	8	22
CO6A3	Collagen alpha-3(VI) chain	487.2	19.2	44.1	6	6	6
LDHA	L-lactate dehydrogenase A chain	1608.0	1179.1	779.6	12	11	20
PTX3	Pentraxin-related protein PTX3	1049.9	2101.2	481.3	10	12	8
ANXA2[2]	Annexin A2	2856.6	1170.3	353.2	18	12	12
MMP2[2]	72 kDa type IV collagenase	509.0	160.1	42.2	6	4	9
PAI1[2]	Plasminogen activator inhibitor 1	513.0	32.2	323.8	8	4	12
CO6A2	Collagen alpha-2(VI) chain	853.2	237.2	75.6	12	6	8
CO5A2	Collagen alpha-2(V) chain	2177.8	1501.2	260.8	12	9	11

GDN[1]	Glia-derived nexin	338.5		30.0	12		5
C1S	Complement C1s subcomponent	348.2	486.1	136.5	8	7	9
FBLN1[1]	Fibulin-1		792.8	152.5	100.3	11	5
LAMC1	Laminin subunit gamma-1	744.1	177.0	190.7	8	13	9
LUM	Lumican		201.3		51.0	3	
SPRC[1]	SPARC		269.7	152.5	50.6	8	5
CALU	Calumenin		772.8	131.4	118.8	12	13
FSTL1	Follistatin-related protein 1	1707.4	1652.3	394.4	7	4	4
PDIA3	Protein disulfide-isomerase A3	560.8	38.5	57.7	13	5	9
CALR	Calreticulin	1519.1	132.4	106.0	8	5	5
TAGL	Transgelin		394.4	24.7	29.0	6	4
SVEP1	Sushi, von Willebrand factor type A, EGF and pentraxin domain-containing protein 1	1101.8		27.4	14		9
FBLN3	EGF-containing fibulin-like extracellular matrix protein 1	1392.2	440.0	98.9	5	5	6
IBP7	Insulin-like growth factor-binding protein 7	812.2	227.0	67.4	5	5	3
CYTC	Cystatin-C		228.7	101.8	165.9	3	4
ISLR	Immunoglobulin superfamily containing leucine-rich repeat protein	533.9	684.1	27.0	4	4	5
FBN1	Fibrillin-1		222.2	573.5	61.8	3	5
QSOX1	Sulfhydryl oxidase 1	595.1	519.3	60.7	9	6	7
LEG1	Galectin-1		736.5	38.6	34.2	4	3
CFAD	Complement factor D	156.4	45.5		4	1	
TIMP1[1]	Metalloproteinase inhibitor 1	316.6	298.4	82.7	2	2	2
CLUS	Clusterin		31.7	27.0	68.8	4	2
TIMP2	Metalloproteinase inhibitor 2	42.9	178.8	166.6	3	2	2

Table 6: List of proteins analyzed in DigiWest® profiling including expression levels and antibody information.

Analyte	Log2 Ratio CM vs. Ctrl			Supplier
	Group 1	Group 2	Group 3	
14-3-3 epsilon	0,588	0,187	0,285	Cell Signaling Technology
14-3-3 sigma	0,879	0,116	0,368	R&D
4E-BP1	0,233	-0,234	-0,105	Abcam
4E-BP1 - phospho	0,653	0,353	0,082	Cell Signaling Technology
Adam9	0,990	0,884	1,107	Cell Signaling Technology
Bax	0,651	0,146	0,445	Cell Signaling Technology
Bcl2	0,676	-0,516	0,000	Cell Signaling Technology
beta-Catenin	-0,127	0,317	0,103	Cell Signaling Technology
beta-Catenin - phospho	-0,026	0,639	0,107	Cell Signaling Technology
beta-Catenin (non-p-S33/37/T41; active)	-0,233	0,810	0,136	Cell Signaling Technology
Bip	-0,067	1,448	1,228	Cell Signaling Technology
BMP4	1,576	1,554	0,232	Abcam
Brachyury	0,369	1,626	1,058	Thermo Fisher Scientific
C/EBP-β	0,203	0,498	0,780	Cell Signaling Technology
Caveolin-1	-0,247	-0,116	-0,106	Cell Signaling Technology
CBP	0,000	0,189	0,748	Cell Signaling Technology
CITED2	0,000	0,345	0,121	Abcam
c-Jun	-0,122	-0,031	-0,284	Cell Signaling Technology
c-Jun - phospho	0,000	0,986	0,112	Cell Signaling Technology
c-myc [61kDa]	-1,836	0,076	-0,176	Cell Signaling Technology
c-myc - phospho	0,000	0,000	0,089	Abcam
CREB	-0,848	0,796	0,200	Cell Signaling Technology
CREB - phospho	-0,666	0,118	-1,026	Cell Signaling Technology
DKK1 [35kDa]	-0,583	0,420	0,267	Biorbyt
E2F-4	-0,008	-0,338	-0,149	Biorbyt
Erk1/2 (MAPK p44/42) [42kDa]	0,566	0,129	0,453	Cell Signaling Technology
Erk1/2 (MAPK p44/42) [47kDa]	0,173	-1,157	0,440	Cell Signaling Technology
Erk1/2 (MAPK p44/42) - phospho [42kDa]	-1,118	-1,647	-1,409	Cell Signaling Technology
Erk1/2 (MAPK p44/42) - phospho [48kDa]	-0,667	-1,561	-1,588	Cell Signaling Technology
FABP4	-1,208	1,091	0,000	Cell Signaling Technology
FAK	0,099	0,282	0,118	Cell Signaling Technology
FAK - phospho	-0,102	0,077	-0,036	Cell Signaling Technology
FAK1	-0,059	0,693	0,017	Abcam
FKBP12	0,592	-0,525	-0,287	Abcam
FRA1 - phospho	-0,749	-0,760	-1,827	Cell Signaling Technology
GDF3	1,093	-0,060	-0,011	Abcam
GDF8 (Myostatin)	-0,774	0,669	0,076	Abcam
Ha-ras	-0,357	0,653	-0,414	Millipore

HNF-4 alpha	0,069	-0,203	-0,047	biorbyt
HNF-4 alpha - phospho	-0,630	-0,963	0,141	biorbyt
HSP70	0,365	0,016	-0,046	Cell Signaling Technology
JNK/SAPK [46kDa]	0,634	0,032	-0,186	Cell Signaling Technology
JNK/SAPK [54kDa]	0,441	-0,372	0,021	Cell Signaling Technology
JNK/SAPK 1/2/3 - phospho	0,000	-0,064	-0,213	Abcam
LEF1	0,000	0,000	-0,496	Cell Signaling Technology
Lipoprotein lipase	0,066	0,000	0,000	Abcam
MAPK/CDK substrates	-0,538	0,156	-0,444	Cell Signaling Technology
Notch 1	0,246	0,926	0,406	Cell Signaling Technology
p38 MAPK	0,739	0,137	-0,352	Cell Signaling Technology
p70 S6 kinase	0,335	0,130	-0,009	Cell Signaling Technology
p70 S6 kinase - phospho	-0,322	0,278	-0,614	Cell Signaling Technology
PAI-1	0,573	0,813	1,604	Cell Signaling Technology
PARP [116kDa]	-0,229	0,974	0,227	Cell Signaling Technology
PARP [89kDa]	0,000	0,299	0,000	Cell Signaling Technology
Paxillin [60kDa]	-0,290	0,277	-0,046	Abcam
p- Smad 2/3	0,578	0,272	0,748	Cell Signaling Technology
PP2A C - phospho	-1,170	0,126	-0,258	R&D
PP2A C	0,381	-0,041	-0,027	Cell Signaling Technology
PPAR gamma	-0,240	-0,166	-0,142	biorbyt
Ras	-0,283	0,376	-0,309	Cell Signaling Technology
SFRP2	0,000	0,333	0,465	Abcam
Smad1	0,197	0,627	0,396	Cell Signaling Technology
Smad2/3	0,176	0,285	0,383	Cell Signaling Technology
Smad4	0,475	0,662	0,746	Cell Signaling Technology
Smad5	0,797	-0,192	-0,842	Cell Signaling Technology
Src	0,024	0,408	0,294	Cell Signaling Technology
Src - phospho	-0,253	0,289	-0,129	Cell Signaling Technology
Src family - phospho	-0,856	0,615	0,108	Cell Signaling Technology
TACE	-1,433	-0,652	-0,377	Cell Signaling Technology
TAK1	0,434	0,371	-0,559	Cell Signaling Technology
Vimentin	-0,130	0,214	-0,132	Cell Signaling Technology
Vimentin - phospho	0,031	0,634	-0,353	Cell Signaling Technology
14-3-3 zeta delta	-0,550	-0,076	0,363	Cell Signaling Technology
Vimentin - phospho	-0,387	-0,159	-0,439	Cell Signaling Technology